Orbivirus non-structural protein NS2: Its role in virus replication

Nigel John Horscroft

Thesis submitted for the degree of Doctor of Philosophy
at the University of Oxford

Wadham College

Michaelmas 1997

TABLE OF CONTENTS

Orbivirus non-structural protein NS2: Its role in virus replication

Nigel John Horscroft
Wadham College, Oxford

Thesis for Doctor of Philosophy
Michaelmas 1997

ABSTRACT

Bluetongue virus (BTV) is an economically important arthropod-borne virus that causes Bluetongue disease in sheep and other ruminants. BTV is the prototypical orbivirus and is a member of the *Reoviridae* family. Other arthropod-borne orbiviruses include African horse-sickness virus (AHSV) and epizootic haemorraghic disease virus (EHDV). The virus contains 10 dsRNA segments that encode for both structural and non-structural proteins. The structural proteins of orbiviruses and other members of the *Reoviridae,* such as reoviruses and rotaviruses, are arranged in a very similar layered arrangement. The roles of the non-structural proteins are largely unknown. This thesis describes the functional characterisation of one of these non-structural proteins, NS2.

The NS2 protein of BTV-10 was purified to a high degree of homogeneity from insect cells. This purified protein was used in crystal screening experiments and in circular dichroism (CD) experiments. Although a wide range of conditions were tried for crystallography, no crystals were obtained. This may be due to sequence or conformational heterogeneity. Size-exclusion chromatography was used to show that purified NS2 exists in large multimers, supporting the conclusion that conformational heterogeneity was responsible for the lack of crystal formation. CD revealed that NS2 has a high α-helical content.

NS2 is a ssRNA-binding protein. To identify the nucleotides within the viral RNA segments that are important for recognition by NS2, gel-shift and uv-crosslinking experiments with various labelled synthetic RNA probes and *in vitro* transcripts were performed. Initial gel shift analysis with short synthetic RNAs indicated that NS2 bound a sequence corresponding to the conserved 5' terminus of rotavirus genomic RNA. Similar sequences, called the NS2 target sequence or NTS, were identified in all 10 BTV segments. A number of truncations and deletions of BTV segments M4 and S10 were created to investigate the role of this aptamer in NS2 binding. The results indicate that the NTS is required for the binding of NS2 to each BTV viral RNA segment. These results were confirmed by using short synthetic RNA probes corresponding to the aptamer identified in segments M4 and S10 and by showing that the aptamer could confer NS2 binding to non-BTV RNA.

Further biochemical analysis of NS2 revealed previously undescribed features of the protein. Chemical crosslinking and co-immunoprecipitation studies showed that NS2 can interact with VP1 the viral RNA polymerase. The inclusion of NS2 in *in vitro* transcription-translation and translation reactions demonstrated a specific shut-down of BTV protein synthesis, suggesting a role for the protein in a switch from viral RNA translation to RNA packaging. This translation inhibition is dependant on the concentration of NS2 present and may be related to the formation of viral inclusion bodies. NS2 was also found to bind nucleotide triphosphates and to have phosphohydrolase activity. Kinase inhibitors were used to identify casein kinase II as the cellular kinase that phosphorylates NS2 *in vivo*.

ACKNOWLEDGEMENTS

I would like to thank Professor Polly Roy for her supervision and funding during my research in her laboratory, and Professor Keith Dyke, my College supervisor. I would also like to thank everyone at the NERC Institute of Virology and Environmental Microbiology, especially those who are in, or have passed through Polly's lab.

I am especially appreciative of the assistance I have received from outside of the lab; Chris Hatton for photography, Pauline Henbest for polyclonal antibodies, Dr Bridget Lewis for computing support, the office staff for all of their help and all of the others who have provided answers for various questions. The staff, post-docs and students of other departments have also been extremely helpful; the Oxford Centre for Molecular Sciences for help with circular dichroism, the Laboratory for Molecular Biophysics for crystallography, the Oxford Molecular Biology Data Centre for computing assistance and members of the Molbiol mailing list. Also Hans van der Zandt of EMBL, Germany for discussions on the purification of NS2 and Dr Didier Poncet and Dr Jean Cohen of INRA, France for the gift of synthetic RNAs, rotavirus proteins and assistance with the intial RNA-binding work.

My mother and my wife have both been a great source of support over the years and I would like to thank them greatly for their love and patience.

ABBREVIATIONS

A3	N-(2-aminoethyl)-5-chloronaphthalene-1-sulfonamide
aa	amino acid(s)
AcNPV	*Autographa californica* nuclear polyhedrosis virus
AHSV	African horsesickness virus
APS	ammonium persulphate
ATP	adenosine triphosphate
BHK	baby hamster kidney (cells)
BLV	bovine leukaemia virus
bp	base pair(s)
BSA	bovine serum albumin
BT	Bluetongue
BTV	Bluetongue virus
BTV-10	Bluetongue virus serotype 10
cDNA	complementary DNA
Ci	Curie
CIP	calf intestinal phosphatase
CLP	core-like particles
cpm	counts per minute
CTP	cytidine triphosphate
DTT	dithiothreitol
DNA	deoxyribonucleic acid
dNTP	deoxynucleoside triphosphate
dsRNA	double stranded ribonucleic acid(s)
EDTA	ethylenediamine-tetra-acetic-acid
EHDV	epizootic haemorrhagic disease virus
FCS	foetal calf serum
Fig.	figure(s)
GST	glutathione-S-transferase
GTP	guanosine triphosphate
h	hour(s)
H7	1-(5-isoquinolinesulfonyl)-2-methylpiperazine
H8	N-(2-(methylamino)ethyl)-5-isoquinolinesulfonamide
HEPES	N-2-hydroxy-ethylpiperazine-N'-2-ethanesulphuric acid
HPLC	high pressure liquid chromatography
kDa	kiloDalton(s)
LB	Luria broth
µCi	micro Curie
MAb	monoclonal antibody
mg	milligram(s)
min	minute(s)
µl	microlitre(s)
ml	millilitre(s)
MOI	multiplicity of infection
mRNA	messenger RNA
MW	molecular weight
nm	nanometre(s)

NP-40	Nonidet P-40
NTP	nucleoside triphosphate
NS	non-structural protein
OD	optical density
ORF	open reading frame
PAGE	polyacrylamide gel electrophoresis
PBS	phosphate buffered saline
PEG	polyethylene glycol
pfu	plaque forming unit
p.i.	post-infection
PCR	polymerise chain reaction
RNA	ribonucleic acid
Rnase	ribonuclease
R.T.	room temperature
SDS	sodium dodecyl sulphate
sec	second(s)
Sf	*Spodoptera frugiperda*
ssRNA	single-stranded ribonucleic acid
TBE	Tris-borate EDTA buffer
TE	Tris-HCl EDTA buffer
TEMED	NNN'N''-tetramethylethylenediamine
TTP	thymidine triphosphate
U	uracil
UTP	uridine triphosphate
UV	ultraviolet
VP1, VP2, etc	viral protein 1, viral protein 2, etc.
v/v	volume per volume
wt	wild type
w/v	weight per volume
w/w	weight per weight

Chapter 1

INTRODUCTION

Bluetongue is a disease of major economic importance to the livestock industry. It is an arthropod-borne viral disease affecting mainly sheep, although cattle, goats and wild ruminants may also become infected. Mortality rates as high as 75% have been reported (Gorman, 1990). In countries were Bluetongue is endemic, international restrictions on the movement of livestock have been imposed to prevent severe losses to the livestock industry.

1.1 HISTORY

Research on Bluetongue dates back to the late 19th century and earlier studies leading up to the current molecular approaches have been reviewed (Gorman, 1990, Parsonson, 1991).

Bluetongue virus is believed to have originated in Africa and the disease was initially recognised with the introduction of Merino and other susceptible European breeds of sheep into southern Africa in the 17th and 18th century. The disease was first reported in sheep in the scientific literature by Hutcheon in 1881 in South Africa where it was described as a febrile disease with a morbidity of 30% and a high mortality rate. It was initially named epizootic catarrh. Hutcheon suggested that the causative agent was an insect-transmitted plasmodium and the disease was subsequently renamed malarial catarrhal fever. Theiler demonstrated that the infectious agent was filterable by passing serum and blood from infected sheep through filters (Theiler, 1908). Research in South Africa showed that transmission could only occur by inoculation with infected blood or tissue suspensions and not orally or by contact. In 1905 Spreull showed that goats and calves were also susceptible to the disease (Spreull, 1905). He suggested that the term malarial did not

apply to the disease and proposed the name Bluetongue, after one of the symptoms, a cyanotic and swollen tongue. By 1944 Du Toit had confirmed that the disease - as well as the related orbiviral disease, African horse sickness - could be transmitted by insects when he demonstrated that a species of biting midge of the genus *Culicoides* could transfer the disease from infected to uninfected animals (Du Toit, 1944).

Until 1943, when an epidemic occurred in Cyprus, Bluetongue was thought to be confined to Africa. Subsequent outbreaks were reported in Israel in 1951, Pakistan in 1962 and India in 1963. An epidemic in Spain and Portugal in 1956-1957 killed 17,900 sheep - 75% of affected animals - within the first four months. In North America in 1952, a disease of sheep known as "soremuzzle" was described (Hardy & Price, 1952). It was later identified as Bluetongue and the virus was subsequently isolated. With the advent of serological testing it was found that the disease was more widely distributed than initially thought. Bluetongue virus (BTV) is now believed to be present in livestock in most tropical and sub-tropical countries between latitudes 40°N and 35°S. In 1988 the sheep population in these regions was about 830 million or 71% of the world sheep population.

1.2 BLUETONGUE DISEASE

The wide distribution of BTV led to Bluetongue being described as an emerging disease (Howell, 1960). It is believed that outbreaks of the disease occur when susceptible animals are moved into regions where BTV is endemic or when infected arthropod vectors are carried by the wind to regions where endemic vectors and susceptible animals are found (Sellers, 1975, Shimshony *et al.*, 1988).

The symptom for which the disease is named, a dark blue and swollen tongue, is actually very rare and transitory, and is often missed. The first symptoms include a high fever lasting up to 14 days, although 5-7 is typical (Erasmus, 1975). An increased respiratory rate, hyperaemia and swelling of the buccal and nasal mucosa accompany the fever. Frothy salivation, a swollen tongue and licking of the lips and nostrils also occur early on in infection. Cracking of the epidermis at the folds of the lips follow along with encrustation of these areas and oedema of the face, ears and eyelids. Haemorrhages develop in the mucous membrane of the gingiva and oral cavity and it is at this point that the tongue may become blue and swollen and protrude from the mouth.

The epithelial lesions in the mouth may become chronic leading to excoriation which in turn causes bleeding lesions that can become infected and necrotic. Haemorrhages develop at the coronet of the hoof and the periople (skin-horn junction), parts of the body likely to be cooler. Infected sheep develop stiffness, lethargy and anorexia related to the appearance of these haemorrhages. There can be severe skeletal muscle damage causing extreme weakness and muscular degeneration. Lesions on the smooth muscle of the oesophagus and pharyngeal area often cause vomiting which is usually followed by pneumonia and torticollis, frequently ending in death.

1.3 CLASSIFICATION AND SEROLOGY

In early work BTV was grown in embryonated eggs (Mason & Neitz, 1940). Growth in cell culture led to easier virus propagation giving rise to better serological assays and allowing the virus to be characterised (Haig *et al.*, 1956).

BTV was first observed by electron microscopy in 1966 (Owen & Munz, 1966) and was purified in 1969 (Verwoerd, 1969). Verwoerd showed that the genome was segmented and consisted of double-stranded RNA (dsRNA). He proposed a new taxonomic group including other dsRNA viruses and arthropod-borne viruses similar to BTV. The International Committee on Taxonomy of Viruses decided that this group of viruses would be defined by the genus *Orbivirus* (Latin "*orbis*" meaning ring or circle) within the family Reoviridae (Fenner, 1976). The other genera are *Rotavirus, Orthoreovirus, Aquareovirus, Phytoreovirus, Fijivirus, Oryzavirus, Cypovirus* and *Coltivirus*. BTV is now the prototype virus of the *Orbivirus* genus. It shares many similar characteristics with both reovirus and rotavirus such as a double-stranded segmented genome, bi-shelled capsid and the virion associated transcriptase (Verwoerd *et al.*, 1972, Verwoerd & Huismans, 1972). Other arthropod-borne orbiviruses include African horse-sickness virus (AHSV) and epizootic haemorrhagic disease virus (EHDV).

Early attempts at vaccination met with limited success. Theiler used a mild strain of BTV that had been serially passaged in sheep. This strain was used until 1948 when Neitz showed that antigenically distinct types of BTV existed, explaining the poor protection provided by Theilier's strain (Parsonson, 1991).

There are 14 orbivirus serogroups (Mertens & Roy, 1994) and 25 BTV serotypes (Knudson & Shope, 1985, Davies *et al.*, 1992), shown in Table 1.1. The serogroups are based on cross-reactions in fluorescent antibody assays, complement fixation tests and agar gel immunodiffusion tests. BTV serotypes were initially defined by serum neutralisation tests but are now usually defined by a plaque reduction test (Della Porta, 1985).

1.4 GENOME

The dsRNA segments are grouped according to size and numbered according to decreasing size as determined by migration on agarose gels (Van Dijk & Huismans, 1988, Pedley *et al.*, 1988). The coding assignments of the individual segments (Table 1.2) has been determined by isolating individual segments and their subsequent translation *in vitro* (Mertens *et al.*, 1984, Van Dijk & Huismans, 1988).

Each of the ten genome segments contains conserved 5' and 3' terminal hexanucleotides (Rao *et al.*, 1983, Mertens & Sangar, 1985). Similarly conserved sequences have also been found in EHDV and AHSV (Mertens & Sangar, 1985, Iwata *et al.*, 1992a, Iwata *et al.*, 1992b), although the AHSV sequences appear to be more variable. In addition, each segment has an inverted repeat sequence of five to 14 nucleotides which has been predicted to allow the formation of a panhandle-type structure when the genome is at a single-stranded stage (Cowley *et al.*, 1991). The extent of base pairing within this region varies from segment to segment, although at least five of the 5' and 3' hexanucleotides always remain unpaired (Fig 1.1). Similar structures have also been found in influenza virus (Hsu *et al.*, 1987), a negative-stranded, segmented RNA virus and wound tumour virus (Anzola *et al.*, 1987, Stoeckle *et al.*, 1987), a member of the Reoviridae family. The panhandle structure in influenza virus is important for transcription (Fodor *et al.*, 1994, Pritlove *et al.*, 1995) and the recently proposed RNA-fork model involved in the initiation of transcription (Fodor *et al.*, 1995, Kim *et al.*, 1997) is generally similar to the predicted BTV structure.

All segments have a 5' and 3' non-coding region. The 5' non-coding regions vary in size from 8-34 nucleotides while the 3' regions are between 31 and 116

nucleotides in length (Roy, 1991). Type 1 cap structures ($m^7GpppG^{(m)}G$) similar to those found in reovirus (Furuichi *et al.*, 1975a, Furuichi *et al.*, 1975b, Shatkin *et al.*, 1976) and rotavirus (Imai *et al.*, 1983) are found at the 5' termini of both mRNA transcripts and genomic RNA (Mertens *et al.*, 1991). It is not known whether the minus-strand is capped and no polyadenylation signals or 3' poly-A tails have been described for either the messenger or genomic RNA.

Table 1.1: Orbivirus serogroups (Mertens & Roy, 1994).

Serogroup	Number of serotypes
African horse sickness	9
Bluetongue	25
Changuinola	12
Corriparta	3
Epizootic haemorrhagic disease	8
Equine encephalosis	7
Eubenadgee	4
Kemerovo (includes Broadhaven virus)	40
Lebombo	1
Orungo	4
Palyam	11
Umatilla	3
Wallal	2
Warrego	2

Table 1.2: Coding arrangement of BTV serotype 10. Updated from Roy *et al.*, (1990b).

Genome segment	Length (bp)	Gene product	Protein function	No. of amino acids	Protein size (kDa)
L1	3944	VP1	Minor core protein, RNA polymerase	1302	149.6
L2	2926	VP2	Outer capsid protein	956	111.1
L3	2772	VP3	Inner shell of core	901	103.3
M4	1981	VP4	Minor core protein, guanylyltransferase, methyltransferase, NTPase	644	75.3
M5	1639	VP5	Outer capsid protein	526	59.2
M6	1770	NS1	Forms tubules	552	64.4
S7	1156	VP7	Outer shell of core, forms trimers	349	38.5
S8	1123	NS2	Forms viral inclusion bodies, binds ssRNA	357	41.0
S9	1049	VP6	Minor core protein, RNA helicase, NTPase activity, binds ss and ds RNA and DNA	325	35.8
S10	822	NS3/NS3A	Integral membrane protein, aids virus release	229	25.6

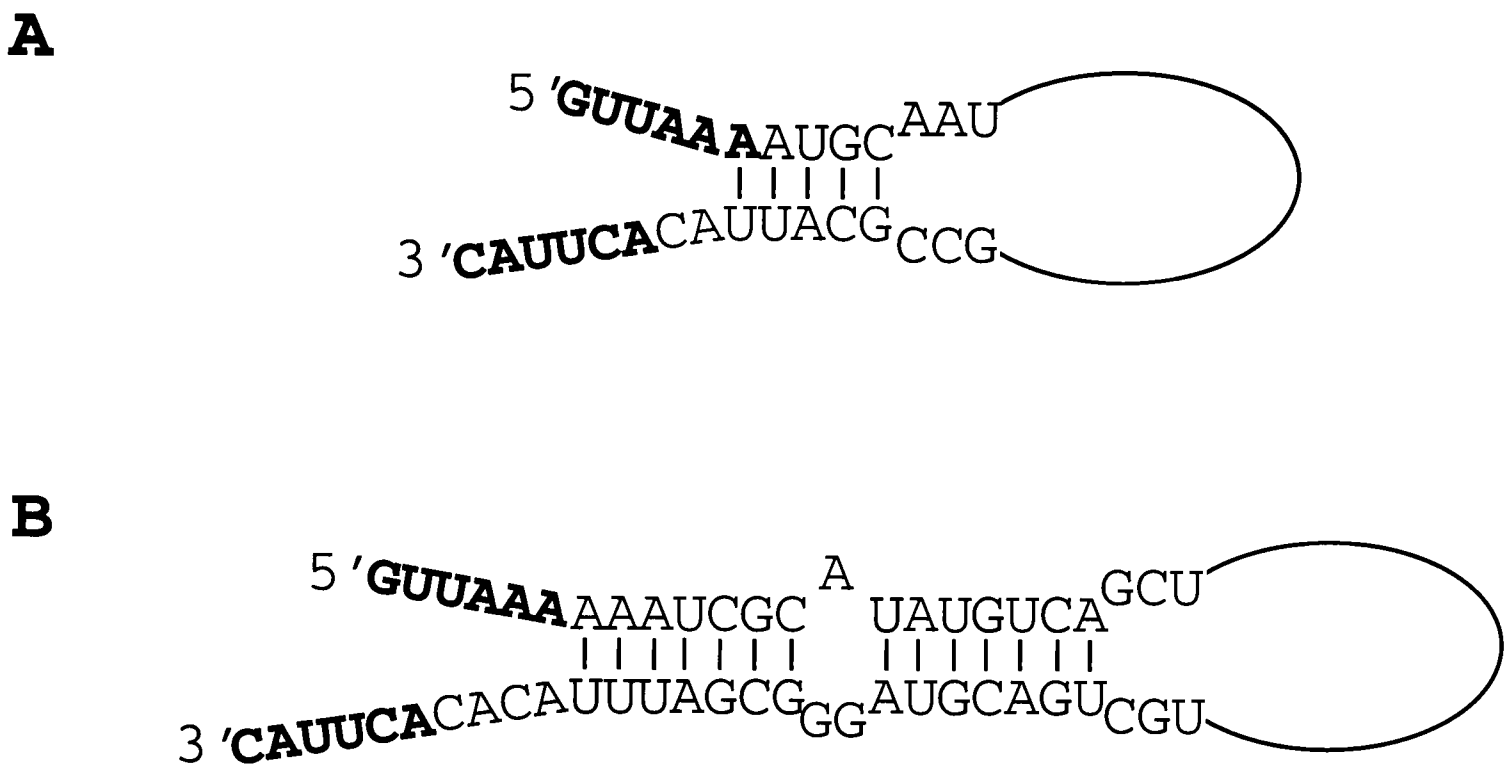

Fig 1.1: Predicted terminal structures for BTV-10. **A:** Segment L1. One of the simpler terminal structures. **B:** Segment S9. A more complex terminal structure. Conserved hexanucleotides are shown in bold. Based on data from Cowley *et al.*, 1992.

1.5 STRUCTURAL PROTEINS

Electron microscopy revealed BTV particles to be icosahedral, non-enveloped double capsids (Studdert *et al.*, 1966) with a diameter of 81 nm (Hewat *et al.*, 1992b). These particles are complex in structure and contain seven structural proteins, four major and three minor (Fig 1.2). The structure of BTV is very similar to that of Broadhaven virus, an orbivirus in the Kemerovo complex (Schoehn *et al.*, 1997) and is similar in organisation to rotavirus (Prasad *et al.*, 1988, Yeager *et al.*, 1990, Prasad *et al.*, 1996) and reovirus (Metcalf *et al.*, 1991, Dryden *et al.*, 1993, Shaw *et al.*, 1996).

1.5.1 Outer Capsid Proteins VP2 and VP5

The outer capsid is composed of VP2 and VP5 (Fig 1.2 & 1.3A) which together make up 40% of the total viral protein (Huismans & Van Dijk, 1990). VP2 is the serotype specific antigen and haemagglutinin (Huismans & Erasmus, 1981, Grubman *et al.*, 1983, Kahlon *et al.*, 1983, Cowley & Gorman, 1987) while VP5 is the group specific antigen (Mertens *et al.*, 1989, Marshall & Roy, 1990). In keeping with their roles as serotype and group specific antigens, there is a high degree of variability of VP2 and VP5. Both proteins can be removed from virus particles by protease treatment. VP2 is cleaved first followed by VP5, leaving an exposed core with an active RNA polymerase (Martin & Zweerink, 1972, Van Dijk & Huismans, 1980). VP5 is glycosylated with a short N-linked sugar chain (Yang & Li, 1993).

1.5.2 Core Proteins VP3 and VP7

BTV cores contain the three minor core proteins (VP1, VP4 and VP6) enveloped by the major structural proteins VP3 and VP7. The structure of native cores

has been determined by cryo-electron microscopy (Hewat *et al.*, 1992b, Prasad *et al.*, 1992). These cores have a diameter of 69 nm and icosahedral symmetry with a triangulation number of 13. VP7 in the outer core layer is composed of five- and six-membered rings or clusters of VP7 trimers (Fig 1.3B). The clusters are arranged so that there are 132 channels. The VP7 trimers form 260 prominent protrusions per core (a total of 780 VP7 molecules per particle). The inner layer of VP3, with a radius of 21.5 to 28 nm, forms a surface upon which the VP7 trimers sit. They are arranged as 24 pentamers with a total of 120 molecules per core (Hewat *et al.*, 1992a). The crystal structure of VP7 has been determined (Basak *et al.*, 1992, Grimes *et al.*, 1995) and support the cryo-EM data in terms of orientation and trimeric nature. It also reveals that VP7 monomers consist of two domains. The lower domain sits on the VP3 layer and is formed from the amino and carboxy portions of the protein. The upper domain interacts with VP5 and is formed from the middle of the protein.

Recombinant VP3 and VP7 and VP2, VP3, VP5 and VP7 co-expressed in insect cells using the baculovirus expression system can spontaneously assemble into core-like particles (CLP's) and virus-like particles (VLP's) respectively (French *et al.*, 1990, French & Roy, 1990, Belyaev & Roy, 1993). The particles appear identical to authentic cores and virions by electron microscopy. Neither the minor core proteins, non-structural proteins or viral RNA appear to be required to form these structures (French *et al.*, 1990, French & Roy, 1990). Further manipulation of the baculovirus expression system has led to the incorporation of the minor core proteins VP1, VP4 and VP6 into CLP's (Loudon & Roy, 1991, Le Blois *et al.*, 1992).

1.5.3 Minor Core proteins VP1, VP4 and VP6

The minor core proteins VP1, VP4 and VP6, along with the ten dsRNA segments fill the VP3 core. These proteins are responsible for many of the enzymatic activities required for replication and (+)-strand synthesis (Huismans & Verwoerd, 1973) but the characterisation of these proteins is far from complete.

The largest viral protein, VP1, is 150 kDa and is produced in small amounts in infected cells. It has sequence homology with known RNA polymerases and with the *E.coli* RNA polymerase β-subunit (Roy *et al.*, 1988). The protein has two GDD motifs found in RNA polymerases (Roy *et al.*, 1988, Huang *et al.*, 1995). Further evidence pointing to VP1 as the RNA-dependent RNA polymerase comes from experiments showing that insect cell lysates containing baculovirus virus expressed VP1 has an RNA-dependent RNA polymerase activity (Urakawa *et al.*, 1989). The protein also has three leucine-zipper motifs, the significance of which is unknown (Huang *et al.*, 1995).

Like VP1, VP4 is produced in small amounts. It is a 75.3 kDa protein that binds GTP and is the guanylyltransferase involved in mRNA capping (Mertens *et al.*, 1991, Le Blois *et al.*, 1992). It also has a transmethylase and NTPase activity also involved in the capping reaction (Martinez-Costas *et al.*, 1997). VP4 forms dimers and a leucine-zipper motif found near the carboxy terminus of the protein is involved in dimer formation (Ramadevi *et al.*, 1997).

The third minor core protein, VP6 (35.8 kDa), binds both single-stranded and double-stranded DNA and RNA non-specifically (Roy *et al.*, 1990a). It is the RNA helicase responsible for the unwinding of the dsRNA genome before the synthesis of mRNA (Staeuber *et al.*, 1997).

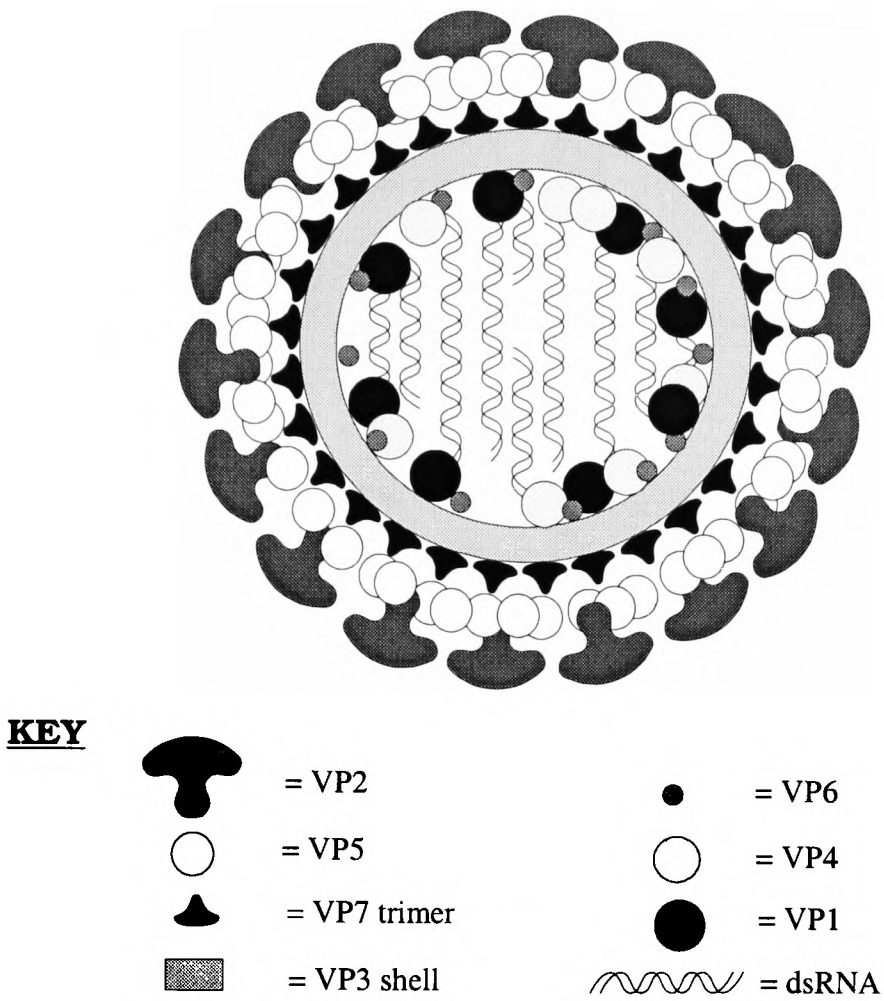

Fig 1.2: Structural arrangement of BTV virions (Roy, 1993).

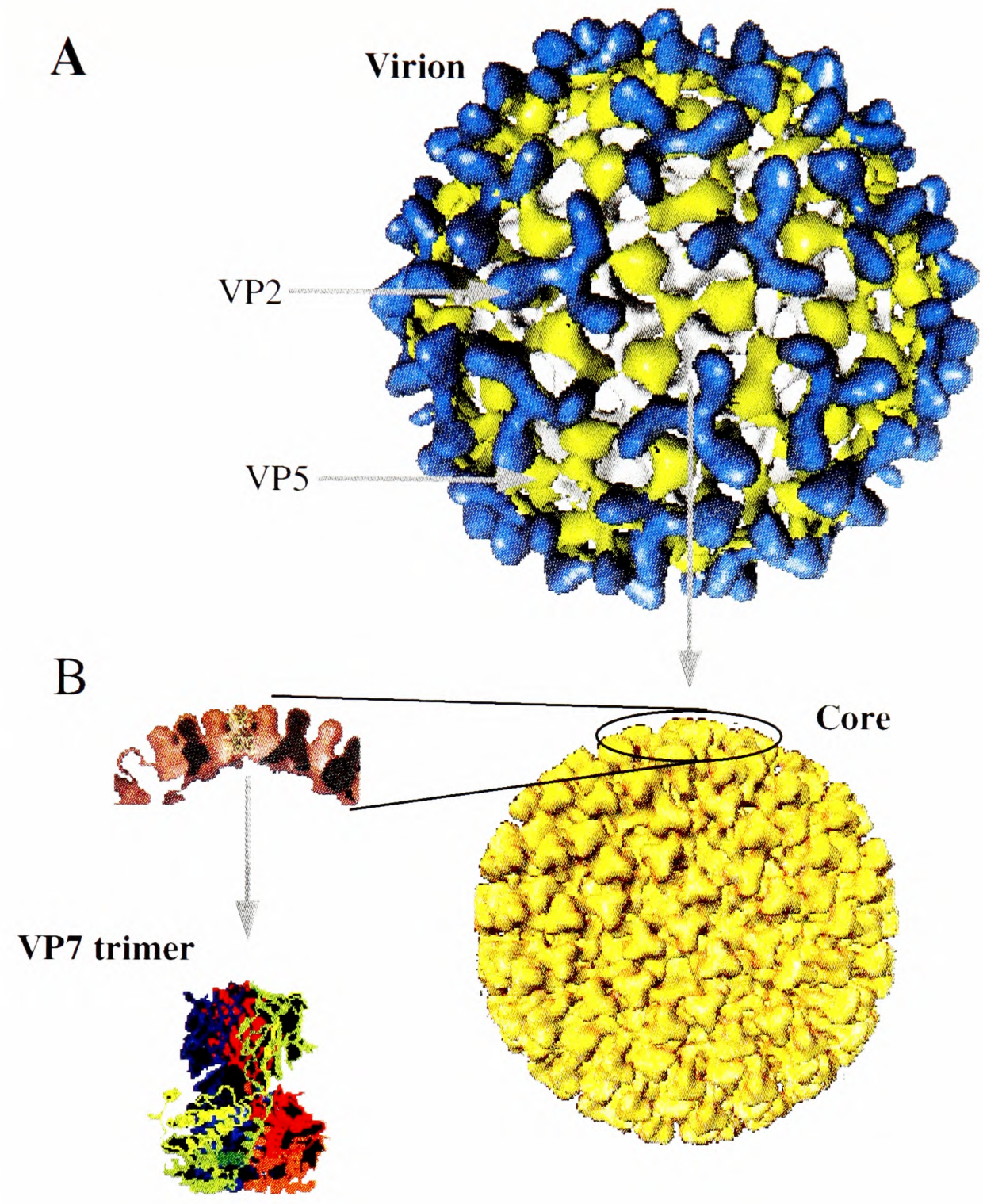

Fig 1.3: Structural arrangement of BTV virions and cores. **A**: VP2 (blue) and VP5 (yellow) forming a layer of the inner capsid as determined by cryo-EM (Hewat *et al.*. 1992a). Note the holes through which the cores are visible. **B**: Core particle showing the location of the VP7 trimers and the crystal structure of VP7 (Prasad *et al.*. 1992, Grimes *et al.*. 1995).

1.6 NON-STRUCTURAL PROTEINS

Four non-structural proteins are synthesised in BTV infected cells. NS1 and NS2 are the major non-structural proteins, while NS3 and NS3A, synthesised from the same segment, are found at much lower levels (Huismans, 1979, Mertens *et al.*, 1984).

1.6.1 NS1

The virus specific tubules seen in BTV - and other orbivirus - infected cells are formed from the 64kDa protein NS1 (Huismans & Els, 1979, Urakawa & Roy, 1988). The tubules consist of helically coiled ribbons of NS1 dimers with a diameter of 52 nm and can be up to 1000 nm long (Hewat *et al.*, 1992c). NS1 is the most abundant virus-specific protein.

Several conserved hydrophobic regions exist in the carboxy half of the protein (Roy *et al.*, 1990b). A number of conserved cysteine residues are located within these regions, many clustered in pairs separated by two to five amino acids. Cysteine residues at position 337 and 340 are required, along with amino- and carboxy-terminal amino acids, for tubule formation (Monastyrskaya *et al.*, 1994). These cysteine residues may be involved in the formation of a zinc finger-like structure as they are also required for the binding of zinc by NS1 (unpublished data). This structure possibly plays a role in the dimerisation of NS1 or the polymerisation of the dimers into tubules. No other BTV proteins are required for tubule formation as baculovirus expressed NS1 assembles into tubules in insect cells (Urakawa & Roy, 1988).

NS1 tubules are found attached to intermediate filaments of the cell cytoskeleton (Eaton *et al.*, 1987) and NS1 has also been identified associated with cytoskeleton attached virus-like particles and viruses released from infected cells (Eaton *et al.*, 1988). As antibodies against VP3 and VP7 also react with material associated with tubules (Hyatt & Eaton, 1988), it has been suggested that NS1 may be involved in the transport of virus particles in infected cells and that the observed tubules are a repository for NS1 used earlier in morphogenesis.

1.6.2 NS2

NS2, the 41 kDa product of the S8 gene, binds ssRNA but does not bind dsRNA (Thomas *et al.*, 1990). The protein is generally hydrophilic and is rich in charged residues. It is the only phosphorylated BTV protein. The effect of phoshorylation on its RNA-binding capability has been investigated (Thomas *et al.*, 1990, Theron *et al.*, 1994). Thomas *et al.* reported that there was no reduction in RNA-binding when baculovirus-expressed NS2 was dephoshorylated, while Theron *et al.* used *E.coli*-expressed NS2 and observed a reduction, but not complete abrogation, of RNA-binding. NS2 forms viral inclusion bodies (VIBs) in BTV-infected cells (Brookes *et al.*, 1993) and when expressed in insect cells using recombinant baculoviruses (Thomas *et al.*, 1990) suggesting that no other viral proteins nor a full complement of viral RNAs are necessary. The effect of the presence of a full complement of BTV RNA on the assembly efficiency or stability of VIBs is not known. Neither the amino nor carboxy termini of the protein is required for VIB formation (Zhao *et al.*, 1994). VIBs are believed to be the location at which viral assembly occurs.

No RNA-binding motifs have been identified in NS2 although a group of conserved amino acids has been identified in the NS2 proteins of BTV and the related orbiviruses EHDV and AHSV, as well as in rotavirus NSP3 and reovirus σNS (van Staden *et al.*, 1991, Rao *et al.*, 1995). It has been shown that mutation of this region in EHDV diminishes RNA binding (Theron *et al.*, 1996). However mutation or deletion of the first eight amino acids in BTV NS2 and reovirus σNS - outside of this region - abolish RNA binding (Zhao *et al.*, 1994, Gillian & Nibert, 1997), suggesting that the overall structure of the protein is important.

The significance of NS2 phoshorylation is not known. Phoshorylation has been shown to play a role in the multimerization and protein-protein interactions of a number of other viral proteins (Montenarh & Muller, 1987, Gao & Lenard, 1995b, Gao & Lenard, 1995a, Spadafora *et al.*, 1996) and the phoshorylation of NS2 may be important for VIB formation or interaction with other viral or cellular proteins.

1.6.3 NS3/NS3A

The smallest BTV protein is synthesised in two forms, NS3 and NS3A, as a result of transcription initiation at a second in-frame initiation codon (Lee & Roy, 1986, French *et al.*, 1989, Wade Evans, 1990, Hwang *et al.*, 1992). NS3 is 229 aa long and has a molecular weight of 25 kDa while NS3A is 13 aa shorter and is 24 kDa. They are produced in small amounts in infected cells (Huismans, 1979) and are both glycosylated with N-linked carbohydrates (Wu *et al.*, 1992). They are integral membrane proteins that localise to the plasma membrane after transportation through the golgi apparatus (Hyatt *et al.*, 1991, Wu *et al.*, 1992) and contain two conserved hydrophobic regions that may serve as transmembrane domains (Lee & Roy, 1986,

Gould, 1988, Hwang *et al.*, 1992). The NS3 proteins have also been found associated smooth-surfaced, intracellular vesicles and it is believed that they aid the release of virus particles from infected cells (Hyatt *et al.*, 1993).

Recent data obtained by two-hybrid protein-protein interaction assays suggests that NS3, but not NS3A, can interact with two cellular proteins, the calpactin light chain (p11) and bithoraxoid (Andrew Beaton, personal communication). While little is known about bithoraxoid, the calpactin family of proteins, of which p11 is a member, are known to be calcium binding proteins that interact with phospholipids and cytoskeletal proteins (Gerke & Weber, 1985, Geisow *et al.*, 1986, Glenney, 1986). By undergoing a conformational change, calpactin is thought to allow the fusion of two membranes leading to exocytosis (Nakata *et al.*, 1990). NS3 is predicted to form an N-terminal amphipathic alpha helix that may interact with p11, aiding exocytosis. Although NS3A is only 13 aa shorter than NS3, it is not predicted to form the necessary alpha helix.

1.7 REPLICATION

Although little is known about the replication of BTV and other orbiviruses it is believed that their replication cycles are generally similar to that of the extensively studied reoviruses (Roy, 1996b). It is thought that all members of the *Reoviridae* use a similar replication strategy (Joklik, 1981).

BTV enters susceptible cells by endocytosis and replicates in the cytoplasm, shutting down host cell protein synthesis (Huismans, 1970). Following entry the virus penetrates the lysosomal or endosomal compartment where the low pH uncoats the virus, activating the transcriptase (Van Dijk & Huismans, 1980, Huismans *et al.*,

1987b). The addition of compounds that raise the lysosomal or endosomal pH prevents endocytosed virus particles from entering the cytoplasm (Hyatt *et al.*, 1989). At 1-2 hpi the viral core particle enters the cytoplasm (Huismans *et al.*, 1987b).

The activation of the BTV transcriptase complex by the removal of the outer capsid proteins allows access of nucleotide triphosphates to the genome and the extrusion of nascent mRNA into the cytoplasm (Van Dijk & Huismans, 1980, Mertens *et al.*, 1987). Although the transcriptase has a low optimum temperature (28°C), transcription is efficient at 37°C (Verwoerd & Huismans, 1972, Van Dijk & Huismans, 1980, Van Dijk & Huismans, 1982). This low temperature optimum may explain, in part, the development of haemorrhages observed in parts of infected sheep thought to be at a lower temperature (see Bluetongue disease). The loss of VP7 from intercellular cores is believed to stop transcription as cores depleted of VP7 *in vitro* cannot transcribe (Huismans *et al.*, 1987b).

The mRNA molecules are capped and methylated by VP4 (Mertens *et al.*, 1991) and are extruded into the cytoplasm. The molar ratios of the different mRNA species remains the same throughout the infection cycle and the first virus-specific proteins are detected 2-4 hpi (Huismans & Van Dijk, 1990, Whetter *et al.*, 1990). The rate of protein synthesis increases rapidly until 11-13 hpi and then slows and continues until cell death.

As stated earlier, viral inclusion bodies composed of NS2 are considered to be the site of viral assembly. The possible roles of NS2 in various stages of replication and assembly will be discussed in the introduction to the following Chapters. One each of the ten ssRNA segments are packaged within a core of VP3 pentamers along with the minor core proteins VP1, VP4 and VP6. Neither the mechanism nor the

proteins involved in packaging the RNA species is known for BTV or any other members of the *Reoviridae*. The VP3 core is stabilised by a layer of VP7 trimers. The outer capsid proteins VP2 and VP5 are thought to assemble onto the virion either within the VIBs or as it emerges from the VIB as particles with both proteins have been found associated with the periphery of the VIBs (Eaton *et al.*, 1990).

Virus particles leave the infected cell by passage, either individually or in groups, through a locally disrupted plasma membrane (Hyatt *et al.*, 1989). This egress involves NS3/3A and does not appear to have a deleterious effect on host cell viability (Hyatt *et al.*, 1991).

1.8 ROTAVIRUSES

Rotavirus and reovirus are both members of the *Reoviridae* family and have a number of similarities with BTV at the molecular and structural level. While structural protein homologues can be identified between the three virus groups, non-structural protein homologues are not easily classified. In order to provide an overall view of replication within the *Reoviridae* family, the rotavirus proteins will be discussed below.

Rotaviruses cause gastro-enteritis in humans and animals. They pose a serious health risk, particularly in developing countries, where the chronic diarrhoea they cause can be fatal in young children (Estes & Cohen, 1989). Of the six serogroups, A - F, groups A, B and C can infect both humans and animals and are the most extensively characterised.

The 11 segments of dsRNA that make up the rotavirus genome are enclosed within the viral core. The segments vary in length from 3302 to 667 bp and with the exception of segment 11, which contains two open reading frames (Mattion *et al.*, 1991), the gene segments are monocistronic (Table 1.3).

The plus sense RNA strands are capped at the 5' end with sequence $m^7GpppG^{(m)}GPy$ and lack a poly(A) tail at the 3' end (Imai *et al.*, 1983, McCrae & McCorquodale, 1983, Spencer & Garcia, 1984). The viral RNA-dependent RNA polymerase is required to transcribe functional mRNAs as the genomic dsRNA is not infective (Cohen, 1977).

Consensus sequences are found at the termini of each segment. The 5' consensus sequence is 5'-GGC(A/U)(A/U)U(A/U)A(A/U)(A/U)-3' while the 3' consensus sequence is 5'-U(G/U)(U/G)(G/U)(A/G)CC-3'. These consensus sequences

are located immediately adjacent to a non-coding regions of variable length, unique to each segment (Imai *et al.*, 1983, McCrae & McCorquodale, 1983).

The structural proteins VP4 and VP7 form the outer layer of the rotavirus virion (Fig 1.4). VP4 is cleaved to form VP5* and VP8* which, as dimers, form 20 nm long spikes on the surface, visualised by image reconstruction of cryo-electron micrographs (Prasad *et al.*, 1988, Prasad *et al.*, 1990, Yeager *et al.*, 1990, Anthony *et al.*, 1991, Shaw *et al.*, 1993, Yeager *et al.*, 1994).

VP4 is the cell attachment protein (Ludert *et al.*, 1996) and trypsin cleavage of VP4 is required for virion entry (Fukuhara *et al.*, 1988, Nandi *et al.*, 1992). Following cleavage both fragments remain associated with the virion and viral infectivity is enhanced (Estes *et al.*, 1981, Kalica *et al.*, 1983, Prasad *et al.*, 1990). Antibodies to VP4 as well as VP5* and VP8* neutralise rotavirus *in vitro* (Greenberg *et al.*, 1983, Burns *et al.*, 1988). Direct membrane penetration is thought to be the mode of entry (Kaljot *et al.*, 1988, Falconer *et al.*, 1995).

The VP4 spikes protrude through holes in the surface formed by trimers of the other outer shell protein VP7. VP7 is a highly immunogenic glycoprotein that can induce neutralising antibodies (Ericson *et al.*, 1983) and permeablise cell membrane vesicles (Charpilienne *et al.*, 1997). It localises to the endoplasmic reticulum where it is an integral membrane protein (Petrie *et al.*, 1982, Kabcenell & Atkinson, 1985). There is a signal sequence (aa 1-50) for translocation to the ER located in the N-terminal that is removed on entry of the protein to the ER and ER retention signals are located between aa 51 -111 (Ericson *et al.*, 1983, Poruchynsky & Atkinson, 1988).

Table 1.3: Rotavirus proteins

Protein	Genome segment	Protein size (Kd)	Location and Function
VP1	1	125	Inner core, RNA polymerase, binds 3' end of viral mRNA, localises to viroplasms.
VP2	2	94	Inner core, binds RNA non-specifically.
VP3	3	88	Inner core, guanylyltransferase.
VP4	4	86.8	Outer-shell, haemagglutinin, cleaved into VP5* and VP8*
VP5*	-		Outer-shell
VP8*	-		Outer-shell
NSP1	5	58.6	Cytoskeleton, zinc finger motif involved in binding 5'end of viral mRNA
VP6	6	44.8	Inner core
NSP2	8	35	Viroplasms, multimeric, binds ssRNA non-specifically.
NSP3	7	34	Cytoskeleton, binds 3' end of viral mRNA.
VP7	9	37.2	Outer-shell.
NSP4	10	28	ER
NSP5/5A	11	26	Viroplasms, glycosylated, phosphorylated, has kinase activity.

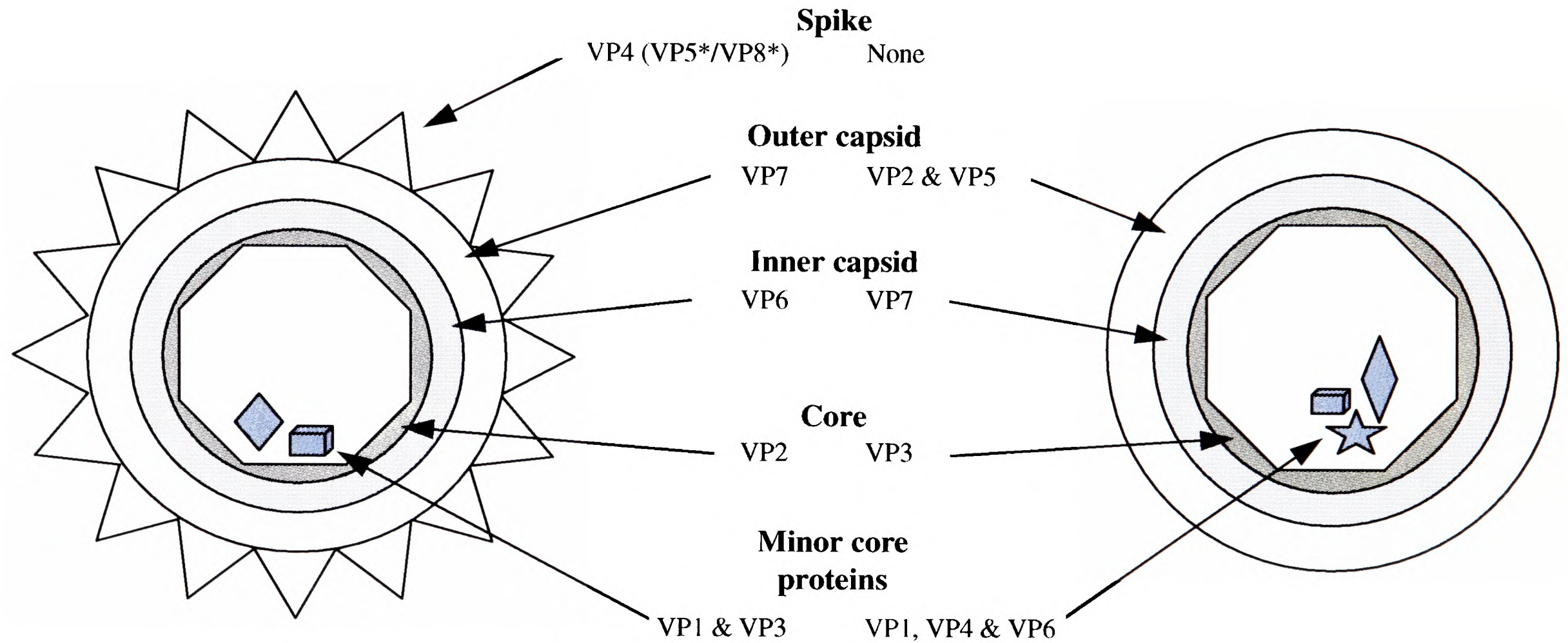

Fig 1.4: Comparison of the layered arrangement of rotavirus and BTV structural proteins.

VP6 is the most abundant structural protein and coats the surface of the single-shelled particle (Prasad *et al.*, 1988, Yeager *et al.*, 1990). The protein forms trimers and is crucial for the transcriptase activity of single-shelled particles. Removal of VP6 from single-shelled particles results in core particles and the loss of mRNA synthesis that can be restored by the addition of excess VP6 (Bican *et al.*, 1982, Sandino *et al.*, 1986). However VP6 is not required for rotavirus replication (Patton & Gallegos, 1988, Gallegos & Patton, 1989, Mansell & Patton, 1990). Mapping studies have localised the trimerisation domain to the middle of the protein (aa 105 - 328) (Clapp & Patton, 1991) with a single amino acid change at proline 306 affecting the stability of trimers (Shen *et al.*, 1994). The domain required for interaction with cores is located in the carboxy terminus (aa 251 - 397) and although these domains overlap, trimerisation and assembly are independent (Clapp & Patton, 1991).

Rotavirus cores are made up of dimeric VP2 (Labbe *et al.*, 1991, Zeng *et al.*, 1994). VP2 is a 103 kDa protein with hydrophilic N-terminus and two leucine-zipper motifs that may be involved in either dimerisation or the formation of cores (Kumar *et al.*, 1989, Mitchell & Both, 1990a). The N-terminus of the protein (aa 1-132) is responsible for binding ssRNA and dsRNA in a non-specific manner (Boyle & Holmes, 1986, Labbe *et al.*, 1994). VP2 is myristoylated and it has been proposed that this myristoylation may play a role in core assembly (Clark & Desselberger, 1988). A temperature sensitive mutant with a substitution at aa 387 of VP2 does not assemble into cores (Mansell *et al.*, 1994). VP2 is essential for rotavirus replication (Mansell & Patton, 1990) and it has been proposed that it interacts with a VP1-RNA replication complex (Patton, 1996).

The minor core protein, VP1, has sequence homology to known RNA-dependent RNA polymerases (Cohen *et al.*, 1989, Fukuhara *et al.*, 1989) and labelling experiments have confirmed its role as the RNA-dependent RNA polymerase (Valenzuela *et al.*, 1991). Both VP1 and VP2 are required for replicase activity (Zeng *et al.*, 1996). Purified VP1 has no polymerase activity on its own but it binds specifically to the 3' ends of rotavirus mRNA (Patton, 1996).

The other minor core protein, VP3, is a 98 kDa protein that bears homology to other RNA polymerases (Mitchell & Both, 1990a). Experimental evidence suggests that it is the guanylyltransferase as it specifically binds GTP covalently and reversibly in the presence of magnesium to form a VP3-GMP complex (Pizarro *et al.*, 1991, Liu *et al.*, 1992). Particles containing temperature sensitive VP3 mutants assembled at the non-permissive temperature do not contain RNA, indicating a possible packaging role for VP3 (Vasquez *et al.*, 1993).

Rotaviruses encode five non-structural proteins. The largest, NSP1 is a 53 kDa protein detected early in infection and expressed in low levels (Ericson *et al.*, 1982). The protein contains at least one conserved zinc finger motif (Mitchell & Both, 1990b, Hua *et al.*, 1993) and can bind zinc (Brottier *et al.*, 1992). NSP1 is an RNA-binding protein that binds to all 11 viral RNAs and this activity has been localised to the zinc finger region of the protein (Brottier *et al.*, 1992, Hua *et al.*, 1994). Rotaviruses with rearrangements in the gene encoding NSP1 suggest large parts of the protein are not required for replication (Tian *et al.*, 1993, Hua & Patton, 1994). One study reported that a variant encoding a protein corresponding to the first 40 aa of NSP1 was viable in cell culture (Taniguchi *et al.*, 1996). This variant lacked the zinc finger region of the protein suggesting that it is not required for replication.

In contrast to NSP1, NSP2 is the most abundant non-structural protein in infected cells. The 35 kDA protein appears to be the main constituent of viroplasms, the proposed site of viral assembly (Petrie *et al.*, 1984). It is a basic protein that binds RNA in a non-specific manner and forms multimers (Kattoura *et al.*, 1992, Kattoura *et al.*, 1994). Analysis of different NSP2 gene sequences has identified a conserved putative RNA binding domain between aa 205 and 241 (Patton *et al.*, 1993). A temperature sensitive mutant with a lesion mapping to the gene encoding NSP2 produced less RNA, failed to produce viroplasms in infected cells and produced a large proportion of empty viral particles at the non-permissive temperature (Ramig, 1982, Ramig & Petrie, 1984, Gombold *et al.*, 1985, Chen *et al.*, 1990). NSP2 is known to interact with the polymerase VP1 (Kattoura *et al.*, 1994) and replicase complexes composed of VP1, VP2 and VP6 have been recovered by immunoprecipitation with a monoclonal antibody to NSP2 (Aponte *et al.*, 1996). It also interacts with NSP5 and may be important for the localisation of NSP5 to viroplasms (Poncet *et al.*, 1997a). Based on viroplasm formation and the apparent non-specific RNA binding activity, NSP2 is very similar to BTV NS2 and reovirus σNS.

NSP3 (36 kDa) specifically binds the 3' ends of rotavirus mRNA with four 3' terminal nucleotides being the minimal recognised sequence (Poncet *et al.*, 1993, Poncet *et al.*, 1994). The protein can discriminate between the RNAs of different rotavirus groups. It also binds dsRNA specifically and this is thought to interfere with the activation of a dsRNA-dependant interferon induced protein kinase that regulates phosphorylation of a translation initiation factor (Langland *et al.*, 1994). A conserved basic region identified in NSP3 is thought to be involved in RNA binding in rotavirus

as well as other members of the Reoviridae (van Staden *et al.*, 1991, Mattion *et al.*, 1992, Rao *et al.*, 1995). NSP3 has been detected in association with the cytoskeleton, forms homomultimers and can interact with NSP1 and NSP5 (Estes & Cohen, 1989, Mattion *et al.*, 1992, Poncet *et al.*, 1997a).

NSP4 is a 20.3 kDa protein glycosylated by the addition of N-linked sugar chains (Kabcenell & Atkinson, 1985). It is found in cells associated with the ER membrane and membrane vesicles within the ER in a homotetrameric form (Petrie *et al.*, 1984, Maass & Atkinson, 1990, Taylor *et al.*, 1996). These vesicles are unique intermediates in rotavirus morphogenesis not observed in other members of the *Reoviridae* family. These vesicles are the structure from which single shelled particles bud to the ER for the assembly of VP7 (Petrie *et al.*, 1982, Poruchynsky & Atkinson, 1991, Poruchynsky *et al.*, 1991). Two glycosylation signals and an ER translocation signal are located in the N-terminal portion of the protein (Both *et al.*, 1983). Hydrophobic domains in this region are thought to anchor the protein into the ER membrane and about 131 aa of the C-terminal portion of NSP4 are believed to be located in the cytoplasm (Chan *et al.*, 1988, Bergmann *et al.*, 1989). This cytoplasmic part of the protein contains a virus binding domain and can interact with VP4 and VP6 (Maass & Atkinson, 1990, Taylor *et al.*, 1996). This suggests that NSP4 is a receptor that can recognise both VP4 and single shelled particles during the budding of single shelled particles into the ER (Au *et al.*, 1993).

An intracellular increase in free calcium brought about by the release of calcium from the ER has been linked with the expression of NSP4 (Tian *et al.*, 1994, Tian *et al.*, 1995) This increase is a result of the membrane destabilising property of NSP4, localised to aa 114-135 (Tian *et al.*, 1996). Diarrhoea caused by rotavirus

infection is probably the result of an NSP4 induced ion imbalance in cells of the gastrointestinal tract (Ball *et al.*, 1996, Dong *et al.*, 1997). A peptide corresponding to aa 114-135 also increases intracellular calcium and causes diarrhoea in suckling mice.

NSP5 undergoes phosphorylation and O-linked glycosylation and as a result has predicted and apparent molecular weights of 21 and 26 kDa respectively (Welch *et al.*, 1989, Gonzalez & Burrone, 1991). A second out-of-phase reading frame produces an 11 kDa protein, NSP5A or NSP6 (Gallegos & Patton, 1989, Welch *et al.*, 1989). NSP5 has kinase activity and is phosphorylated on serine residues at multiple sites (Blackhall *et al.*, 1997). It localises to viroplasms, a feature related to its kinase activity (Gallegos & Patton, 1989, Poncet *et al.*, 1997a).

The intermediates involved in the replication of rotavirus - replicase intermediates (RI) - have been well characterised and provide an overview of the early events occurring during morphogenesis (Patton, 1986, Stacy Phipps & Patton, 1987, Patton & Gallegos, 1988, Gallegos & Patton, 1989, Patton, 1990, Patton & Gallegos, 1990). It is believed that there are three RIs involved in the assembly of core single-shelled particles (Table 1.4). The first intermediate formed, the precore RI, contains VP1, VP3, the non-structural proteins NSP1, NSP2, NSP3 and NSP5 and viral RNA. These intermediates do not have replicase activity which is probably due to the absence of VP2 in the precore RI (Mansell & Patton, 1990, Patton, 1996). Replicase activity is first observed in core RIs which differ in protein content from precore RIs only by the addition of VP2. As VP6 is added to form single-shelled particles, NSP1, NSP3 and NSP5 are lost from the intermediates and this may correspond with the egress of these particles from the viroplasms.

The single-shelled particles enter the ER, assisted by NSP4, where they are transiently enveloped before emerging as double-shelled particles containing VP4 and VP7. Mature virions are released by cell lysis although many particles remain associated with cell debris (Altenburg *et al.*, 1980, Musalem & Espejo, 1985).

Table 1.4: Rotavirus replication intermediates and their replicase activity

	Precore RI	Core RI	Single-shelled RI
VP1	+	+	+
VP2		+	+
VP3	+	+	+
VP6	-	-	+
NSP2	+	+	+
NSP1, NSP3, NSP5	+	+	-
RNA	+	+	+
Replicase activity	-	+	+

1.9 OBJECTIVES

While the major structural components of BTV have been well studied, little is known about the role played by the minor core proteins in replication and even less about the non-structural proteins. The lack of a reverse genetics system for BTV and other members of the *Reoviridae* has hampered the characterisation of the role of individual proteins in replication and assembly. In order to provide further information on the role of the non-structural proteins in BTV replication and assembly, this research was designed to investigate the role of NS2 in the replication cycle.

As NS2 is synthesised to high levels in infected cells, binds ssRNA and forms viroplasms it is likely that it plays a key role in the assembly of nascent virions. As such it would be critical to the understanding of the BTV infection cycle and the development of any reverse genetics system. The identification of specific NS2 binding sequences in the RNA segments would then allow a different strategy for the incorporation of altered genes into assembling virions.

With this in mind the primary objectives were:

1. To purify NS2 to a high degree of homogeneity.
2. To initiate structural studies on NS2.
3. To characterise the RNA sequence involved in NS2 binding.
4. To investigate the function of NS2 in replication.

Chapter 2

MATERIALS AND METHODS

This Chapter describes the materials and methods used in the research, and includes both standard procedures and those methods which were adapted and modified during the research.

2.1 General Reagents and Buffers

2.1.1 Chemicals

All chemicals were of analytical reagent grade unless stated otherwise. Most reagents were obtained from British Drug House (BDH), Poole, England, UK; Sigma Chemical Company Ltd., Poole, UK; Pharmacia Fine Chemicals, Sweden and Gibco BRL, UK. Some reagents were obtained from other companies as stated in the text.

2.1.2 Enzymes

Restriction enzymes and enzymes for DNA or RNA modification were purchased mainly from New England Biolabs Ltd., UK, Amersham International Plc, UK, Promega UK and Boehringer Mannheim, Germany.

2.1.3 Water

Water used in enzyme reactions and "sterile water" specified in the text were purified through a Millipore Corporation Milli-Q reagent system and sterilised by autoclaving. Deionised water was used for all other purposes.

2.1.4 Liquid Media

All media was prepared by the Media Preparation section of NERC Institute of Virology and Environmental Microbiology or purchased from Gibco-BRL. TC100 (pH 6.2) was supplemented with 5-10% foetal calf serum (FCS), 50 mg/l of streptomycin and 50,000 International units/l of penicillin. L15 was supplemented with 1-10% FCS. FCS was purchased frozen from Gibco BRL. The serum was thawed and incubated at 56°C for 30 min. The heat-inactivated serum was divided into aliquots and stored at -20°C.

2.1.5 Radiochemicals

Radioactive chemicals were purchased from DuPont-NEN.

[γ^{32}P]ATP (5000Ci/mmol; 10 μCi/μl)

[α^{32}P]ATP (3000Ci/mmol; 10 μCi/μl)

[α^{32}P]GTP (3000Ci/mmol; 10 μCi/μl)

[α^{32}P]UTP (3000Ci/mmol; 20 μCi/μl)

[^{32}P]-orthophosphate (5μCi/μl)

[^{35}S]-methionine (1200-1300Ci/mmol; 10-15 μCi/μl)

2.1.6 Antibodies

Rabbit anti-NS2 polyclonal antibodies were raised against baculovirus-expressed purified BTV-10 NS2 in rabbits. Anti-rabbit alkaline phosphatase conjugated antibodies were purchased from Sigma Chemical Company Ltd.

2.1.7 Buffers

6x DNA loading buffer

0.25% bromophenol blue

30% glycerol

10x TBE

108 g Tris base

55 g boric acid

40 ml 500 mM EDTA pH8.0

water to 1 L

10x TAE

48.4g Tris base

5.7ml glacial acetic acid

20ml 500mM EDTA pH 8.0

water to 1L

Plasmid preparation soln. I

50 mM glucose

10 mM EDTA

25 mM Tris-HCl pH8.0

Plasmid preparation soln II

0.2 M NaOH

1% SDS

Plasmid preparation soln. III

5 M potassium acetate

pH4.8 w/glacial acetic acid

RNA sample buffer (premix)

15 ml deionised formamide

0.54 ml formalin (40% formaldehyde)

3 ml 10x MOPS buffer

15 mM EDTA

10x RNA loading buffer

50% glycerol (Rnase free)

1 mM EDTA

0.4% bromophenol blue

Tris-EDTA (TE) buffer

10 mM Tris-HCl pH7.4

1 mM EDTA

Phosphate buffered saline- (PBS)

7.54 mM Na_2HPO_4

2.5 mM NaH_2PO_4

145.45 mM NaCl

pH7.2

SDS-PAGE buffer

0.192 M glycine

0.025 M Tris base

0.1% SDS

2x SDS-PAGE sample buffer

20% glycerol

2% SDS

0.01% bromophenol blue

5 mM Tris-HCl (pH6.8)

5% β-mercaptoethanol

Protein stain

40% methanol

10% glacial acetic acid

0.2% w/v Coomassie brilliant-blue

Destain solution

40% methanol

10% acetic acid

Western blot transfer buffer

0.2 M glycine

0.025 M Tris base

methanaol 20%

pH8.3

RIPA buffer

0.15 M NaCl

1% Na deoxycholate

1% Triton-X 100

0.1% SDS

0.1 M Tris-HCl (pH7.4)

10x RNA binding buffer

100mM HEPES pH 7.8

400mM KCl

10mM EDTA

50% glycerol

10mM DTT

10x MOPS running buffer

400mM MOPS

50mM sodium acetate

5mM EDTA

Add 800ml water

pH 7.0 with 10M NaOH

Make to 1L.

2.2 Standard Methods

2.2.1 Sterilisation

Glassware, plasticware (reaction tubes and pipette tips), liquid reagents and buffers were sterilised by autoclaving at 121°C for 20 min. Utensils were then dried at 37°C for several hours. During all nucleic acid manipulations, disposable gloves were worn and sterile reagents and utensils were used.

2.2.2 Centrifugation

Small volumes (up to 1.5 ml) were centrifuged in an Eppendorf microcentrifuge at 14,000 rpm unless stated otherwise. Low speed centrifugation was carried out in a Beckman GPKR centrifuge or in a Sorvall RC-5B centrifuge. Ultracentrifugation was carried out in a Beckman L8-55 Ultracentrifuge using various rotors: Ti50, Ti70, SW28, SW41, TH641, etc.

2.2.3 Autoradiography

Kodak XAR film was used for autoradiography and was processed in an X-Omat automatic developer.

2.3 Nucleic Acid Methods

2.3.1 Phenol/chloroform extraction of nucleic acids

The combination of phenol and chloroform denatures and removes proteins from DNA and RNA solutions. Chloroform preparations were mixed with isoamyl alcohol (24:1). Phenol/chloroform extraction was performed by adding an equal volume of buffered phenol to a sample, vortexing and centrifugation in a microcentrifuge to make sure that the two phases were completely separated. Traces of phenol were then removed by subsequent extraction of the aqueous layer with a half-volume of chloroform. The upper aqueous layer containing nucleic acids was retained.

2.3.2 Precipitation of nucleic acids with ethanol or isopropanol.

Nucleic acids were precipitated from solutions by the addition of one-tenth volume of 3 M sodium acetate (pH 5.2) and then either 2 to 2.5 volumes of cold ethanol or 1 volume of cold isopropanol (-20^{o}C). The mixture was vortexed and incubated either at -20^{o}C for at least 12 h, or at -70^{o}C for 1 h, or frozen using liquid nitrogen and centrifuged straight away. Precipitated nucleic acids were recovered from the suspension by centrifugation in a microcentrifuge at 14,000 rpm for 10 min. The pellet was washed with cold 70% (v/v) ethanol and dried under vacuum in a Savant Speed-Vac concentrator. DNA was normally resuspended in an appropriate volume of TE buffer (pH 8.0) and stored at -20^{o}C. RNA was either left in ethanol or isopropanol for long-term storage at -20^{o}C, or was resuspended in sterile water and kept at -20^{o}C.

2.3.3 Spectrophotometry

The concentrations of DNA and RNA in solutions were estimated using the absorbance of the solution at 260 nm (A_{260}). This was measured using a CE 6600 Multimode computing UV spectrophotometer. Concentrations were calculated using the following assumptions (Maniatis *et al.*, 1982):

1 A_{260} unit of dsDNA = 50 μg/ml.

1 A_{260} unit of ssRNA = 40 μg/ml.

1 A_{260} unit of ssDNA oligonucleotide = 30 μg/ml.

2.3.4 Oligonucleotide sequence design

Oligonucleotide designs were analysed using software program, Oligo 4.1 (Rychlik, 1992). PCR primers were designed to keep intra- and intermolecular base-pairing to a minimum. Where internal base-pairing was unavoidable, the initial annealing temperatures for PCR primers were designed to be more than 10°C above calculated melting temperature of the internal base-pairing. Oligonucleotides used for sequencing and primer extensions were designed to have annealing temperatures of 45 to 50°C and a minimum of secondary structure.

2.3.5 Purification of oligonucleotides

Oligonucleotides were synthesised by Mrs V. Cooper on an Applied Biosystems oligonucleotide synthesiser (Dept. of Organic Chemistry, University of

Oxford), and deprotected by incubation at 56°C for at least 4 h. They were purified by extraction with butan-1-ol.

For butanol extraction 100 µl of deprotected oligonucleotide were mixed with 1 ml of butan-1-ol, vortexed for 15 sec and precipitated by centrifugation in a microcentrifuge for 10 min. The pellet was then dried in the Speed-Vac and resuspended in a small volume of water. Oligonucleotides were diluted to the working concentration of 100 ng/µl and stored at -20°C.

2.3.6 Restriction enzyme reactions

Most enzymes were used according to the manufacturer's instructions and employing the buffers provided. A typical reaction mixture for enzymatic digestion included the following: 1 µl of 10 X restriction buffer, DNA (1-5 µg), and water to give a final volume of 10 µl, and an enzyme dilution providing the units required to digest the DNA under the reaction conditions. A reaction mixture was incubated for 1 - 3 h at the specified temperature.

2.3.7 Dephosphorylation of DNA

In order to minimise recircularisation, vectors were dephosphorylated using Calf intestinal alkaline phosphatase (CIAP) to remove 5' terminal phosphates. In a typical reaction (50 µl) some 1-5 µg DNA were added to 5 µl of 10 X CIP buffer (500 mM Tris-HCl, pH 9.0, 10 mM $MgCl_2$, 1 mM $ZnCl_2$, 10 mM spermidine) with 1 µl of 1 unit/ml CIAP and water added to the required volume. For overhang fragments, a reaction was incubated at 37°C for 30 min, then a further 1 µl CIAP was added and

reaction was continued for another 30 min. For blunt-ended fragments, the reaction was incubated at 37°C for 15 min, then at 56°C for 15 min. The incubation was then repeated with a further 1 µl of CIP.

Reactions were stopped by addition of 5 µl of 10% (w/v) SDS and heating at 65°C for 10 min. The fragment was then separated by agarose gel electrophoresis and purified using a GeneClean kit as described below.

2.3.8 Ligation of restricted DNA fragments

DNA ligations were normally performed in an ice bucket full of iced water which was allowed to gradually warm up to room temperature overnight. Generally, for DNA fragment/vector ligation a molar ratio of 5:1 was used. For both overhang and blunt-end ligations the following buffer was used: a five-fold dilution in sterile water of 5 X ligase buffer (250 mM Tris-HCl, pH 7.6, 50 mM $MgCl_2$, 25% (w/v) polyethylene glycol 8000, 5 mM ATP, 5 mM DTT) with 1-2 units of T4 DNA ligase.

2.3.9 Agarose gel electrophoresis

DNA and RNA molecules were separated according to size when subjected to gel electrophoresis. Horizontal gels of 0.6 - 2% (w/v) agarose were used in the presence of ethidium bromide (final concentration of 1 µg/ml). Gels were run in 1 X TBE or TAE buffer, and DNA was loaded in agarose gel loading buffer. Molecular weight markers were derived from lambda DNA (Gibco BRL) digested with *Hind*III and *Eco*RI. DNA was visualised using a Photodyne UV transilluminator. Photographs

were taken using a Polaroid MP4 land camera with Polaroid High speed 5X4 land film and a Mitsubishi video CCD camera and copy processor.

2.3.10 Denaturing electrophoresis of RNA in formaldehyde-agarose gels

Formaldehyde at 0.25 M final concentration was added to agarose gels and included in the 10 x MOPS running buffer at the same concentration to reduce skewing of RNA bands during electrophoresis. Agarose concentrations varied from 1% to 2%. Proteins and low molecular weight products (e.g., unincorporated nucleotides) were removed from RNA by phenol/chloroform extractions followed by chromatography through G25 spin columns equilibrated with RNase-free TE buffer. RNA samples were mixed with 2 to 3 volumes of RNA sample buffer then denatured by heating at 80°C for 2 mins followed by snap-cooling on ice. A 1/10th volume of loading buffer was added to the samples immediately prior to electrophoresis. Gels used directly for autoradiography were fixed for 60 mins then partly dried between paper towels before wrapping in plastic film and exposing to film at either room temperature (with no intensifying screen) or at -70°C with one screen.

2.3.11 Polyacrylamide gel electrophoresis

Vertical polyacrylamide gel electrophoresis was used to separate and purify small labelled RNA fragments. Typically 8-20% gels were used. An appropriate amount of 40% (w/v) 38:2 acrylamide: bisacrylamide solution was added to 25 g of urea, 5 ml of 10 X TBE and water to provide the final volume of 50 ml. After the urea

was completely dissolved 300 µl of 10% (w/v) APS and 60 µl TEMED were added. The gel was poured immediately. Urea was omitted for non-denaturing gels.

2.3.12 Purification of DNA fragments from agarose gels

DNA fragments resolved in an agarose gel were visualised as described above and cut out from the gel using a sterile razor blade. Then they were purified using either the GeneClean kits supplied by BIO 101, USA, or the Qiaex kits supplied by Qiagen, USA, following the manufacturer's instructions.

2.3.13 Preparation of competent cells

The *Escherichia coli* used routinely for cloning procedures was strain XL1 (blue phenotype): end A1, hsd R17 (rk-, mk+), sup E44, thi-1, λ-rec A1, gyr A96, rel A1, (lac-), [F', pro AB, lac1qZΔ M15, Tn 10 (tet^r)]. LB were used to grow liquid cultures. For LB plates, 15 g bactoagar was added to 1 litre of LB

A single colony was picked from an agar plate and inoculated in 10 ml of LB medium and grown overnight at 37°C in a shaker. Next morning 1 ml of the overnight culture was transferred into 100 ml of pre-warmed LB and incubated at 37°C until the optical density of the culture at 600 nm (OD_{600}) reached 0.3. The cells were then chilled on ice for 10 min, and centrifuged in a cold centrifuge for 10 min at 2500 rpm. The supernatant was discarded and the cells resuspended in 40 ml of ice-cold TFb1 (30 mM potassium acetate, 100 mM RbCl, 10 mM $CaCl_2$-$2H_2O$, 50 mM $MnCl_2$-$4H_2O$, pH 5.8, 15% (v/v) glycerol, previously sterilised by filtration). After incubating on ice for 5 min, cells were re-centrifuged under the same conditions. They were then

resuspended in 4 ml of sterile cold TFb2 (10 mM MOPS, 75 mM $CaCl_2$-$2H_2O$, 10 mM RbCl, pH 6.5, 15% (v/v) glycerol), incubated on ice for another 15 min, and dispensed in sterile Eppendorf tubes. Cells were frozen in a bath of ethanol and dry ice, and transferred to a -70°C freezer, where they were stored for several months.

2.3.14 Transformation of *E. coli* with plasmid DNA

An aliquot of competent cells was thawed on ice. Volumes of 2-10 µl of DNA solution, or ligation mixture, were added to the competent cells (100 µl) and mixed gently on ice. The cells were kept on ice for 30 - 60 min and then heat shocked at 42°C for 1 min. After the heat shock, 1 ml of LB (at room temperature) was added and the suspension was incubated in a 37°C shaker for 45 - 60 min. The cells were then plated on LB agar plates containing an appropriate antibiotic (usually 100 µg/ml of ampicillin) and incubated at 37°C overnight.

2.3.15 Mini-preparation of plasmid DNA

A single bacterial colony was used to inoculate 5 ml of L-broth containing an appropriate antibiotic. After an overnight incubation in the 37°C shaker, cells were harvested by spinning them down at 3000 rpm for 10 min. The cell pellet was resuspended in 100 µl of plasmid preparation solution 1, transferred into an Eppendorf tube and 200 µl of the freshly prepared plasmid preparation solution 2 was added. Cells were gently mixed with soln 2, and left on ice for 5 min, after which 150 µl of

plasmid preparation solution 3 was added. Cells were left on ice for another 15 min and then centrifuged in the microcentrifuge for 5 min at 14,000 rpm. Cell DNA, and the other debris was left in the pellet and the supernatant containing the plasmid DNA was transferred into a fresh Eppendorf tube and mixed with 300 µl of cold isopropanol. After incubation on ice for 30 min, the plasmid DNA was pelleted by centrifugation for 10 min at 14,000 rpm.

DNA was then washed with 70% (v/v) ethanol to remove the salts, and dried in a Speed-Vac. When dry, the DNA was resuspended in 150 µl of TE, treated with ribonuclease A (10 µl of 1 mg/ml solution prepared as described in Maniatis *et al.*, (1989) for 30 min at 37°C. Plasmid DNA preparation was extracted with phenol/chloroform, precipitated with ethanol and dissolved in a small volume of TE.

2.3.16 Maxi-preparation of plasmid DNA using caesium chloride

400 ml of LB supplemented with an appropriate antibiotic were inoculated with a single bacterial colony and shaken overnight at 37°C. The cells were pelleted and resuspended in 4 ml of Solution 1 in a Corex centrifuge tube. The bacteria were lysed on ice by the addition of 8 ml of freshly made Solution 2 (5 min incubation). Then 6 ml of Solution 3 were added, followed by incubation on ice for 15 min. The chromosomal DNA and cell debris were pelleted by centrifugation in a Sorvall RC-5B centrifuge for 10 min at 10,000 rpm. The supernatant was transferred to a fresh tube, and the plasmid DNA precipitated on ice during 30 min with 11 ml of cold isopropanol. Plasmid DNA was then pelleted, thoroughly washed with 70% (v/v) ethanol and dried. DNA was dissolved in 2 ml of TE, 200 µl of ethidium bromide

solution (10 mg/ml) was added and the resulting mixture pipetted through a syringe. The plasmid solution was then mixed with 8 ml of CsCl (8 g/ml solution in TE) in a quickseal Beckman centrifuge tube. The tube was filled with TE, balanced and sealed. DNA was centrifuged at 45,000 rpm for 36 h in a Ti70 rotor. The plasmid band was usually visible without UV light. The DNA was harvested, ethidium bromide was extracted with water-saturated isoamyl alcohol, and CsCl removed by dialysis against TE (4^{o}C, 3 changes of 1 l volumes of TE).

2.3.17 Polymerase chain reaction (PCR)

Plasmid DNA for PCR was added to 100 µl of a solution containing 10 mM Tris-HCl, pH 8.8, 1.5 mM $MgCl_2$, 50 mM KCl, 200 µM dNTPs, 5 pmol of the forward and reverse primers (approximately 5 ng each) and 2 units of VENT polymerase (NEB). Approximately 200 µl of liquid paraffin was added to each tube. PCR involved various cycles outlined in the text. Five µl samples were analysed on an agarose gel. Prior to restriction enzyme digest, the PCR products were treated with proteinase K. To accomplish this, Tris-HCl, pH 8.0 (final concentration 10 mM), EDTA, pH 8.0 (final concentration 5 mM) and SDS solution (final concentration 0.1% (w/v) were added to 92 µl of PCR mixture together with 2 µg of proteinase K. The mixture was incubated at 37^{o}C for 30 min, then the proteinase K was heat-inactivated by incubation at 70^{o}C for 10 min Following phenol extraction the PCR products were precipitated with cold ethanol, dissolved in water and digested, as required, with an appropriate restriction enzyme.

2.3.18 5' end labelling of synthetic RNA probes

Synthetic RNA probes were labelled at the 5' end with [γ-^{32}P]ATP using T4 polynucleotide kinase (PNK). Probes corresponding to the rotavirus 5' and 3', the BTV 3' and reovirus 3' consensus sequence were a gift from Dr. Jean Cohen, (INRA, France) as were the rotavirus proteins used as controls. BTV 5', M4NTS and S10NTS probes were purchased from Cruachem, (Glasgow, Scotland). Each 10µl reaction contained 0.5µM synthetic RNA, 1x kinase buffer (supplied), 10µCi [γ-^{32}P]ATP and 10 units PNK (New England Biolabs). Reactions were incubated at 37°C for 30 min and were stopped by the addition of 10µl 25mM EDTA. Probes were gel-purified and diluted before use.

2.3.19 *In vitro* transcription and labelling.

Twenty µL reactions were generally used for producing *in vitro* RNA transcripts for analytical purposes. RNA transcripts were produced and labelled using a T7 RiboMAX large scale RNA production system (Promega) with modifications to the manufacturers instructions. Each transcription reaction was set up to include supplied buffer, 4mM each of ATP, GTP and CTP, 0.5mM UTP, 1-2µg template DNA, 10 µCi [α^{32}P]UTP and 2µl supplied enzyme mix in a 20µl volume.

The reactions were incubated at 37°C for 2-3.5 hrs. Two units of RQ1 RNAse-free DNAse was then added and incubated for a further 15 min. Following extraction with phenol/chloroform and purification on a G25 spin column (Pharmacia), the probes were precipitated with isopropanol in the presence of 0.3M sodium acetate pH5.2. The probes were resuspended in water, typically 200µl, and 10µl was spotted

onto filter paper, precipitated with TCA and counted in a scintillation counter. Capped transcripts were produced by reducing the GTP concentration 10-fold and adding 1 μL of 5 mM $m^7G(5')ppp(5')G$ to the reaction. Luciferase template DNA was used to make non-BTV RNA.

2.3.20 Ultraviolet crosslinking assays

The RNA binding buffer (10x stock) used in all experiments contained 100mM HEPES pH 7.8, 400mM KCl, 10mM EDTA, 50% glycerol and 10mM dithiothreitol and was diluted accordingly for each reaction. Cold RNA (10-15μg) was also added to reduce non-specific binding in some experiments. Crosslinking experiments were performed in an Amersham RPN 2500 UV crosslinker fitted with 254nm tubes. RNA binding buffer, NS2 and labelled probe were combined in 96-well, U-bottomed microtitre plates to give a 20μl reaction volume. After 30 min at room temperature, the reactions were exposed to UV light for 10 min on ice. Reactions were transferred to separate microfuge tubes and 50 units T1 RNAse was added. Following incubation at 37°C for 30 min, 10 μl 3x SDS-PAGE sample buffer was added. Samples were denatured by heating to 100°C for 3 min or microwaving for 1 min (Horscroft & Roy, 1997) and electrophoresed on a 10% SDS-PAGE gel at 200V until the dye front reached the bottom of the gel. Gels were fixed in acetic acid/methanol and dried at 80°C for 2 hrs prior to exposure to x-ray film at -70°C.

2.3.21 Gel retardation assays

Binding reactions prior to gel retardation analysis were similar to UV crosslinking reactions. Cold RNA was omitted from reactions with the short synthetic RNA probes. Various amounts of probe and protein were incubated with binding buffer for 30 min at either 30°C or room temperature. Samples were loaded directly onto gels without RNAse digestion or heating. A small amount of bromophenol blue was added as a dye.

Two types of gels were used. Non-denaturing 8% acrylamide gels were used for gel retardation assays with short synthetic RNA probes. Agarose gels (1%) were used in gel retardation assays involving longer, *in vitro* transcribed RNA probes. Acrylamide gels were dried at 80°C for 2 hrs, while agarose gels were dried onto paper under vacuum, without heat, for 1 hr. They were exposed to x-ray film at -70°C.

2.4 Protein Methods

2.4.1 Preparation of whole cell lysates

The small-scale preparation of cell lysates was performed in a 24 well plate or a 35 mm dish. The cells were harvested in culture medium, pelleted by centrifugation, washed with PBS, centrifuged again and lysed using an appropriate volume of RIPA buffer. For larger number of cells (e.g., from 10-500 ml) cultures of the cells were similarly harvested and washed with PBS, then resuspended at a ratio of 1:10 or 1:20 by volume in lysis buffer (TNN: 50 mM Tris-HCl, pH 8.0, 150 mM NaCl, 0.5% v/v Nonidet P 40), or STE (10 mM Tris-HCl, pH 8.0, 150 mM NaCl, 1 mM EDTA) supplemented with 0.5% (v/v) Triton X100. The cells were incubated on ice for 5 - 10 min, and homogenised.

For further purification, cell lysates were spun at 3,000 rpm for 5 min to remove nuclei and cell debris. Material present in supernatant fluids were further purified as required.

2.4.2 Protein SDS-PAGE

Proteins were resolved by SDS-PAGE using appropriate polyacrylamide gels and buffers (Laemmli, 1970). The procedure employed a stacking gel consisting of a 5% (w/v) polyacrylamide that overlaid a 10% or 12% polyacrylamide gel, depending on the experiment. The running buffer was 1 X SDS-PAGE buffer (200 mM glycine, 25 mM Tris-HCl, pH 8.8, 0.1% (w/v) SDS). Gels were prepared with 30% (w/v) acrylamide- 0.8% bisacrylamide. The lower resolving gel contained 375 mM Tris-HCl,

pH 8.3 and 0.1% (w/v) SDS, and was polymerised in the presence of TEMED and 10% (w/v) APS. The gel was poured between the plates of an ATTO gel apparatus (from Genetic Research Instrumental Ltd, UK) so that 4 cm were left for the stacking gel. Water was layered on top. Once the gel had polymerised, the water was removed, and a stacking gel, containing 135 mM Tris-HCl, pH 6.8, with 0.1% (w/v) SDS and similar volumes of TEMED and APS, were added and a comb was inserted to provide sample wells.

Protein solutions were mixed with an equal volume of 2 X SDS-PAGE sample buffer (10 mM Tris-HCl, pH 6.8, 10% (w/v) SDS, 10% (v/v) β-mercaptoethanol, 25% (v/v) glycerol, 0.02% (w/v) bromphenol blue) and boiled at 100^{o}C for 10-20 min. Proteins in the sample buffer were applied to the wells of the gel. Pre-stained protein molecular weight markers (Sigma (SDS-7B)) included species ranging in size from 26.5 kDa to 180 kDa.

Gels were electrophoresed at 100V until the dye front reached the resolving gel and then at 160V until the dye front migrated out of the base of the gel. To visualise proteins, the gel was soaked in Coomassie Brilliant Blue stain for 30 min (0.25% (w/v) Coomassie Brilliant blue stain, 45% (v/v) methanol, 10% (v/v) acetic acid), then destained in 45% (v/v) methanol and 10% (v/v) acetic acid. Gels were dried in a vacuum drier for 2 h at 85^{o}C.

2.4.3 Western blot (immunoblot) analysis

After resolution by SDS-PAGE, a gel was soaked for 5 min in blotting buffer (3.03 g Tris, 14.41 g glycine, methanol (to 20% v/v) and water to 1 litre, pH 8.3). A

PVDF-Immobilon membrane (Millipore Corp., Bedford, Mass.), previously soaked in methanol and then in blotting buffer was prepared. The gel and membrane were sandwiched between 3MM Watman filter paper soaked in blotting buffer using a Sartorius semi-dry electroblotter. A current of 100 mA (30V limiting) was applied for 1 h.

Western blot analysis was performed as described by (Burnette, 1981). The PVDF membrane on which the proteins were transferred, was soaked in blocking buffer (PBS with 5% (w/v) skimmed milk, 0.05% (v/v) Tween 20) for 1 h to overnight. The membrane was then drained and agitated gently at room temperature for 1 h with 10 ml of blocking buffer and a 1:1000 dilution of the primary antibody. The membrane was then washed in PBS with 0.05% (v/v) Tween 20 for 30 min (three changes of washing buffer), incubated with a 1:1000 dilution (in blocking buffer) of the secondary antibody (goat anti-mouse, or goat anti-rabbit) conjugated with alkaline phosphatase. After 1 h incubation, the membrane was washed as before and treated with the alkaline phosphatase substrate mixture, containing 44 µl of nitroblue tetrazolium chloride (NBT) and 33 µl of 5-bromo-4-chloro-3-indolylphosphate p-toluidine (BCIP) (both from Gibco BRL) in 10 ml of reaction buffer (100 mM Tris-HCl, pH 9.5, 100 mM NaCl, 50 mM $MgCl_2$). After the reaction was complete, the membrane was washed with water and dried at room temperature.

2.4.4 Purification of recombinant baculovirus expressed NS2

Sf cells were infected with AcBTV10-NS2 at a moi of 5 and harvested 3 days after infection by centrifugation at 2400 x g for 10 min. The pellet was washed once

with PBS and resuspended in NS2 lysis buffer (0.1 M NaH_2PO_4-Na_2HPO_4 buffer (NaPi) pH 8.0, 0.1 M NaCl, 1mM EDTA, 1mM DTT, 0.5% Triton X-100, 1mM Pefabloc SC (Pentapharm AG, Switzerland), 1mM APMSF, 10μM E-64) using 5ml per 100ml culture fluid. Cells were lysed by ten strokes of a Dounce homogeniser and cell debris pelleted at 60K rpm for 45 min in a Ti70 rotor at 10°C. The supernatant was passed through a Q-sepharose column (Pharmacia) equilibrated with 0.1M NaCl, 1mM EDTA and the protein was eluted by a 0.1 to 0.5 M NaCl, 1mM EDTA gradient. Fractions above 0.25M NaCl were analysed by SDS-PAGE. The peaks were pooled, diluted 1:4 with 0.1M NaPi pH 8.0, 1mM EDTA and passed through a Heparin column (Pharmacia) equilibrated with 25mM NaPi pH 8.0, 0.1M NaCl, 1mM EDTA. The column was washed with 25mM NaPi pH 8.0, 0.1M NaCl, 1mM EDTA. Step gradients of 0.4M NaCl, 0.5M NaCl, and 1.0M NaCl in 25mM NaPi pH 8.0, 1mM EDTA were applied and fractions collected. Fractions were analysed by SDS-PAGE. Peaks were pooled, diluted 1:8 with 25mM NaPi pH 8.0, 1mM EDTA and passed through a poly-uridine column (Sigma) equilibrated with 25mM NaPi pH 8.0, 0.1M NaCl, 1mM EDTA. The column was washed with 25mM NaPi pH 8.0, 0.1M NaCl, 1mM EDTA. Step gradients of 0.4M NaCl, 0.5M NaCl, and 1.0M NaCl in 25mM NaPi pH 8.0, 1mM EDTA were applied and fractions collected. Fractions were analysed by SDS-PAGE and concentrated using Centricon-10 (Ambion) centrifuge concentrators with a molecular weight cut-off of 10kDa. Aliquots of NS2 were stored at -70°C.

2.4.5 Metabolic radioisotope labelling of proteins

Sf cells in a 35 mm dish were infected with a recombinant baculovirus as described above. At 24 or 48 h p.i. the culture medium was removed, the cells washed twice with methionine-free TC100 medium and incubated with 1 ml of methionine-free TC100 for 1 h at 28°C to starve the cells of methionine. This medium was then removed and substituted with 1 ml of methionine-free TC100 supplemented with 2 µl of [^{35}S] methionine (total activity 20 µCi). Cells were incubated in this medium for 2 h at 28°C after which time the medium was removed, the cells washed in PBS and harvested as described above. The cell lysates were used for immunoprecipitation.

To label BTV-infected BHK cells, the same procedures were employed, except that L-15 was used with or without methionine. To label with ^{32}Pi, 100µCi [^{32}P]-orthophosphate and phosphate-free L-15 was used.

2.4.6 Immunoprecipitation

The cells from one 35 mm Petri dish were lysed on ice with 100-400 ml of RIPA buffer for 10 min and clarified by centrifugation at 12,000g for 3 mins in a microfuge. Proteins were immunoprecipitated by adding polyclonal rabbit antiserum to give a dilution of 1:100-1:500 to the lysates. Samples were incubated at 4°C with agitation for 2 hr - overnight then Sepharose protein A (SIGMA) was added for a minimum of 2 hrs under the same conditions. The antigen/antibody/Sepharose complexes were pelleted by centrifugation for 30 secs in a microfuge and washed with RIPA buffer. The complexes were pelleted and washed a further 2 times, then analysed by SDS-PAGE and autoradiography, or autofluorography.

2.4.7 *In vitro* translation

Transcription-translation reactions were performed as recommended by the manufacturers (Single Tube Protein System 2, Novagen) with either BTV M6 cDNA or the supplied control. NS2 was added to various concentrations and the products labelled with [^{35}S]-methionine followed by SDS-PAGE. For translation from exogenous RNA rabbit reticulocyte lysate (Promega) reactions were programmed with BTV M6 RNA or the supplied luciferase control RNA. The products were labelled with [^{35}S]-methionine in the presence of various concentrations of NS2. All translation products were resolved on 10% SDS-PAGE gels, dried and exposed to x-ray film at room temperature.

2.4.8 Circular dichroism

CD spectra were obtained with a Jasco J720 spectropolarimeter using a 1mm quartz cell, with samples held at 30°C. Thirty-two scans were performed over a wavelength ranges from 190-300nm at 1nm intervals. NS2 samples were measured in 25mM sodium phosphate pH 7.8. Baseline measurements were recorded under the same conditions on 25mM sodium phosphate pH7.8. Other conditions are reported in the text. The data was corrected for baseline measurements and smoothed before plotting with Microsoft Excel (Microsoft Corp., USA). For

2.4.9 TLC phosphohydrolase assay

Reactions were set up as described in the text. Briefly, 1-1.5mg purified NS2, 50mM Tris buffer pH8.0, divalent cation and [α^{32}P]-nucleotide triphosphate were combined to give a final volume of 10µl. The mixtures were incubated at 37°C for 30 mins and the reaction was stopped by adding an equal volume of 10%TCA. An aliquot (1.0-2.5µl) of the stopped reaction was spotted onto polyethylene amine (PEI) cellulose thin layer chromatography plates (Merck) and developed by ascending chromatography in 0.75M KH_2PO_4 buffer (pH3.5). After drying the plates were exposed to x-ray film.

2.4.10 *In vitro* kinase assay

10µl of cell lysate or immunoprecipitated protein was incubated with 5µCi of [γ-^{32}P]ATP in 10mM Tris-HCl, pH 8.0, 10mM $MgCl_2$, in a total volume of 20µl, at R.T. for 30 mins. The reaction was stopped by adding an equal volume of 25mM EDTA and the protein samples were resolved by SDS-PAGE. Radiolabeled proteins were detected by autoradiography.

2.4.11 Chemical crosslinking

Infected and uninfected cells were lysed and supernatants prepared as indicated in the text. Buffers containing primary amines e.g. Tris were avoided and were generally replaced with HEPES buffer. DSP and EGS were purchased from Pierce and dissolved in DMSO to 100mM. The crosslinkers were used at final concentrations ranging from 40µM to 5mM.

Crosslinking reactions were set-up by mixing 100µl supernatant with 1µl of crosslinking reagent (or DMSO for control reactions) and incubating either on ice or at room temperature for 30 mins. The reactions were quenched by adding glycine to a final concentration of 50mM and incubating for a further 10 mins. Proteins were immunoprecipitated as outlined in the text and analysed by SDS-PAGE under reducing conditions for DSP crosslinking. For EGS crosslinking the crosslinks were cleaved by incubation with 1M hydroxlyamine at 37°C for 4 hrs before resolution by SDS-PAGE.

2.5 Cell Culture

2.5.1 Materials

Protocols for work with insect cells and baculoviruses followed the methods and recommendations described by King and Possee (1992). Cell lines derived from *Spodoptera frugiperda (Sf)*, the fall army worm, were used for the expression of foreign genes using baculovirus AcNPV. The original cell line, *Sf*21 (IPLB-21; Vaughn *et al.*, 1977), was derived form ovarian tissue. This cell line was normally used for expressing foreign proteins in infected *Sf*21 monolayer cultures, and for plaque assays (see below). An alternative cell line, *Sf*9, used for the expression of recombinant proteins in spinner flask cultures was a clonal derivative of *Sf* 21.

The medium used to grow *Sf* cells was TC100. Foetal calf serum and antibiotics (penicillin and streptomycin) were obtained from Gibco BRL, UK.

2.5.2 Culture of insect cells

Media were incubated at 28^{o}C prior to use. Cultures were maintained at 28^{o}C. Since *Sf* cells have a doubling time of 18 - 24 h, they were sub-cultured every 3 days. Cells were stored frozen and recovered as required. To freeze *Sf* cells, low passage cultures were grown to a density of 1.5 X 10^{6} cells/ml, gently pelleted by centrifugation and resuspended in medium to a density of 5 X 10^{7} cells/ml. Dimethyl sulphoxide (DMSO) was added (to 20% (v/v)), and the cells frozen in 1 ml aliquots at -70^{o}C. For recovery from liquid nitrogen, frozen *Sf* cells were gently thawed at room

temperature, then transferred to a 25 cm^2 plastic flask with fresh TC100 medium containing 10% (v/v) FCS, and incubated at 28°C for 24 h. The medium was changed, and cells were passaged as normal. In routine work, cells were not allowed to grow beyond a density of 1.5 X 10^6 cells/ml, and were usually seeded at a density of 1-2 X 10^5 cells/ml.

2.5.2.1 Monolayer cultures

Cells were maintained in log-phase in sub-confluent monolayers in plastic tissue culture flasks, or in 35 mm plastic Petri dishes. Monolayers were generally incubated at 28°C, but could be grown more slowly at room temperature (20 - 22°C). Monolayers were used for growing the cells which had been frozen, for determining virus titres by plaque assay (see below), and for expressing proteins using recombinant baculoviruses.

2.5.2.2 Suspension cultures

Cells were maintained in log-phase in glass round bottomed flasks. Volumes of 20 - 500 ml were grown in flasks that were at least twice the size of the culture to allow adequate aeration. Cultures were stirred at 40-100 rpm on magnetic stirrers and grown at 28°C. Cells were counted using a haemocytometer. Trypan Blue stain (1:10 diluted in PBS) was added to the cells at a 1:1 (v/v) ratio to stain dead cells and to count the viable cells.

2.5.2.3 Infection of *Sf* cells in monolayers

Sub-confluent cell monolayers in 35 mm Petri dishes were used for virus infections. The medium was removed and the virus added directly to the monolayer in a small volume (up to 300 µl) of TC100 per 35 mm Petri dish. The virus was left to absorb for 1 h at room temperature, then the inoculum removed and replaced with 1.5 ml of fresh TC100 containing 10% (v/v) FCS. The cells were incubated in a moist environment for 3-4 days which provided a high titre of extracellular virus particles in the supernatant (usually 5×10^7 - 1×10^8 pfu/ml)

2.5.2.4 Infection of *Sf* cells in suspension

Suspension cultures at the density of 5×10^5 cells/ml were used for the propagation of baculoviruses. The required volume of virus was added directly to the cells without spinning them down. The usual MOI was 0.1 pfu/cell. Infected cells were incubated at 28°C for 5-6 days and their condition monitored periodically. When the number of dead cells was over 50% of the observed population, the virus stock was harvested by centrifuging for 15 min at 3,000 rpm. The supernatant (virus stock) was saved in a sterile bottle, and the titre of the virus stock determined by plaque assay.

A different method was used for infection of *Sf* cells in order to produce baculovirus expressed foreign proteins. Cells (100-500 ml) were grown in suspension culture to the density of 1 -1.5 $\times 10^6$ cells/ml. The MOI used was usually 5 pfu/cell. The virus was allowed to absorb to the cells by incubating them at room temperature for 1 h with slow stirring. The cells were incubated at 28°C for 72 h. They were then harvested and the expressed proteins extracted.

2.5.2.5 Titration of a virus stock

Virus titration was performed as recommended by Brown and Faulkner (1977). Petri dishes (35 mm) were seeded with 1 -1.5 X 10^6 cells which were left to attach for 30 min and form sub-confluent monolayers. The culture medium was then removed, and the monolayers were inoculated with 200 µl of a virus stock at appropriate dilutions (usually 10^{-4} - 10^{-7}) in TC100. The virus was allowed to absorb to the cells for 1 h at room temperature. The inoculum was removed and the cells overlaid with 2 ml of TC100 with 5% (v/v) FCS and 1.5% (w/v) of molten LMP agarose solution pre-cooled to 40°C. The overlay was allowed to set for 5 min, then 1 ml of TC100 medium with 10% (v/v) FCS was added to the dish. Dishes were incubated in a moist environment for 4 days at 28°C. Plaques were stained with 6% (v/v) Neutral Red, freshly diluted in NPV-PBS (8.2 g NaCl, 2 g KCl, 0.2 g KH_2PO_4, 1.14 g Na_3PO_4 in 1 l of solution, pH 7.3). The medium was removed from the solid overlay, and 1 ml of diluted stain was added directly to each dish. Dishes were then left to stain for 1 h at 28°C. The stain was removed from the dishes which were then left for several hours at room temperature by which time the virus plaques were visible. Plaques were counted and the titres of the original virus stocks were calculated.

2.5.3 Mammalian cell culture

BHK-21 cells were used for the routine propagation of BTV-10. The medium used was L-15. Penicillin and streptomycin were added to 50 units/ml. FCS was added to 1-10% (v/v). Cells were trypsinised in trypsin-EDTA (Sigma) to disrupt the cell monolayer before sub-culturing. Cells were grown at 37°C.

2.5.3.1 Titration of BTV virus

Virus stocks were routinely kept at 4°C. 35mm plastic dishes were seeded with BHK cells which were grown until 90% confluence. A series of dilutions of BTV-10 virus in EMEM (no FCS) was made (typically 10^{-3}, 10^{-4}, 10^{-5}). The medium was aspirated off the dishes and 100µl of diluted virus was added to the cell monolayer. After 1 h at 37°C, 2ml of an agarose overlay consisting of 1.5% low gelling temperature agarose in 1 x EMEM was added, with the addition of EMEM (with FCS and antibiotics) after 20 mins. The dishes were incubated at 37°C for 3 days, whereon the medium was removed, and 1.5ml neutral red stain was added. After 1-2 h at 37°C, the stain was removed, and the plaques counted.

2.5.3.2 Infection of BHK cells with BTV-10

All work with plaque cloned US BTV-10 was carried out in the Institute's P3 isolation laboratory. BHK cells were grown to 80% confluence, the medium removed and the cells washed with PBS prior to infection. Titrated BTV virus stocks were pre-warmed and the cells were infected at a MOI of 5 pfu/cell. The virus was left to absorb on the monolayer for 1 h at 37^{O}C, then the inoculum was removed and L-15 supplemented with 5% (v/v) FCS and antibiotics was added.

Chapter 3

STRUCTURAL STUDIES ON NS2

3.1 INTRODUCTION

Structural studies on a protein can shed light on its form and function by identifying structural homologues and specific structural features. The structures of a number of RNA-binding proteins have been determined and co-crystallisation of RNA with protein allows the precise identification of the nucleotides and amino acids directly involved in interactions (Ni *et al.*, 1995, Nagai, 1996).

The determination of the three-dimensional (3-D) structure of a protein relies on the application of X-ray crystallography, nuclear magnetic resonance (NMR) spectroscopy or cryo-electron microscopy (cryo-EM). In addition circular dichroism has been used to determine secondary structure. However, there are certain prerequisites and limitations associated with each of these techniques and often a combination of methods are used to gain an overall view of a particular protein structure (Rossmann *et al.*, 1994, Consonni *et al.*, 1996, Massiah *et al.*, 1996, Chang *et al.*, 1997, Wikoff *et al.*, 1997).

Developments in molecular biology over the last two decades have meant that it is now possible to produce large amounts of rare proteins *in vitro*, enabling an explosion in structural studies. The use of crystals and X-ray diffraction to determine protein structure was first performed in the 1930's and the improvement of crystallisation methods in the 1960's and 70's (dialysis and vapour phase diffusion and the use of additives such as polyamines and non-ionic detergents) has made it a popular method for protein structure determination (Giege & Ducruix, 1992). However, not all proteins can be crystallised or if crystals do form they may not diffract to high resolution. There may also be problems with finding suitable heavy

atom derivatives, essential for structure determination. NMR was developed as an alternative to X-ray crystallography for the determination of protein 3-D structures although it is often used to complement X-ray data and *vice versa.* This technique provides data on the structure of a protein in solution, which may be significantly different from its crystalline structure. Since the protein is in solution crystallisation is not necessary and it is possible to vary the solution (e.g. buffers, pH, temperature and ionic strength) to compare the structure of a protein under different conditions. The limitations of NMR however, confine its applications. There is a theoretical upper molecular weight limit of 50-60 kDa with current technology allowing the structure determination of proteins up to about 30 kDa (Kay & Gardner, 1997). The protein must also be capable of remaining in solution at concentrations of up to 1 mM.

The nature of conditions required for crystal formation and the size limitations of NMR spectroscopy mean that macromolecular complexes, important in many biological processes, do not easily yield structural data. Cryo-EM of frozen-hydrated samples followed by the 3-D reconstruction of their images can provide quaternary structural information, particularly of relatively large complexes (Wade & Hewat, 1994, Bringas, 1997). Atomic level structural information obtained by crystallography or NMR can be combined with cryo-EM data to provide an overall picture of the protein or complex (Rossmann *et al.*, 1994, Grimes *et al.*, 1995, Wikoff *et al.*, 1997). As the software responsible for the reconstruction of the cryo-EM images becomes more advanced, the resolution of structures visualised by cryo-EM will improve, possibly allowing the determination of protein structures to near X-ray resolution.

Although CD spectroscopy cannot provide detailed 3-D structural data, it can provide useful secondary structure data to improve the understanding of structures

obtained by other methods, particularly the NMR spectroscopy of peptides (Cheng *et al.*, 1996, Consonni *et al.*, 1996, Chang *et al.*, 1997). CD spectroscopy is a fairly simple technique and provides information on the relative amounts of α-helices and β-sheets in a protein or peptide (Johnson Jr., 1990). Its main advantage is in comparing similar proteins or observing structural changes in a protein during folding or denaturation. For the latter application the use of a stopped-flow system allows the intermediate structures in protein folding to be identified (Hooke *et al.*, 1994, Lu *et al.*, 1997).

For any of the above mentioned structural methods, purified protein is an important prerequisite. In addition the protein will probably be required in large quantities and at a high concentration. In this Chapter the purification and concentration of BTV NS2 is presented along with experiments performed to obtain structural data on NS2. This information can contribute to the understanding of how NS2 forms VIBs and binds RNA.

3.2 RESULTS

3.2.1 Purification of NS2

Previous work on NS2 used purified protein but the yield of these preparations was not very high (Thomas *et al.*, 1990, Zhao *et al.*, 1994). In order to increase the yield of protein a new purification scheme was developed with the assistance of Hans van der Zandt of EMBL, Germany. The details of NS2 purification can be found in the Materials and Methods. An outline of the purification scheme and rationale is presented below.

A recombinant baculovirus expressing NS2 to high levels (AcBTV10.8) was used to express the protein in insect cells (Thomas *et al.*, 1990). At 72-96 hpi the cells were harvested by low speed centrifugation and washed with PBS. Lysis was achieved by dounce homogenisation of cells resuspended in lysis buffer (0.1 M NaH_2PO_4-Na_2HPO_4 buffer (NaPi) pH 8.0, 0.1 M NaCl, 1mM EDTA, 1mM DTT, 0.5% Triton X-100) containing a combination of protease inhibitors. The lysate was clarified by high speed ultracentrifugation.

Ion-exchange chromatography was selected as the first stage of purification. This method is an easy and flexible method for the separation of proteins based on their charge. It is widely used in the purification of a number of proteins including the BTV proteins VP4, VP6 and VP7 purified in our laboratory (Basak *et al.*, 1992, Martinez-Costas *et al.*, 1997, Staeuber *et al.*, 1997). Ion-exchange chromatography has two forms, anion exchange and cation exchange. Anion exchange columns

contain positively charged groups that bind negatively charged or anionic proteins (at the pH of the buffer).

A strong anion exchange column, Q-sepharose (Pharmacia), consisting of a quaternary aminoethyl group coupled to agarose was used. The column was attached to a Pharmacia low pressure chromatography system incorporating a UV-monitor, conductivity meter and a fraction collector, and equilibrated with buffer A (0.1M phosphate buffer, 0.1M NaCl and 1mM EDTA). The clarified lysate was applied to the column and a gradient formed by mixing buffer A and buffer B (0.1M phosphate buffer, 0.5M NaCl and 1mM EDTA) was applied (Fig 3.1A). Fractions above 0.3M NaCl (50% buffer B) were analysed by SDS-PAGE to identify the fractions containing NS2 (Fig 3.1B). Lanes 7 and 8 contain the most concentrated NS2 and, although not pure, they contain significantly less contaminants than the original lysate (lane 1).

Subsequent stages in the purification scheme exploited the ability of NS2 to bind RNA. Heparin is a sulphated polysaccharide that mimics nucleic acids. Columns containing immobilized heparin are used in a similar fashion to ion-exchange columns as the interactions are mainly electrostatic. Proteins that can bind nucleic acids bind to the immobilized heparin and are eluted at a higher concentration of counter ions.

The fractions containing NS2 from the Q-sepharose column were pooled and the NaCl concentration of solution was estimated by referring to the conductivity trace from the gradient. The solution was diluted with 0.1M phosphate buffer pH 8.0 containing 1mM EDTA so as to give a final NaCl concentration of 0.1M. A heparin column (Pharmacia) was equilibrated with 25mM phosphate buffer pH 8.0 containing 0.1M NaCl and 1mM EDTA (low salt buffer). The sample was applied by attaching a syringe to the end of a column and gradually depressing the plunger. The column was

washed with ten column volumes of low salt buffer and a step gradient was applied consisting of three column volumes each of 25mM phosphate buffer pH 8.0 and 1mM EDTA with 0.4M NaCl and with 0.5M NaCl. The column was then washed with four column volumes of buffer containing 1.0M NaCl. Fractions were collected in appropriate volumes, usually 1.0 ml, and analysed by SDS-PAGE (Fig 3.2). NS2 protein was typically found in the fractions eluted at 0.5M NaCl (Fig 3.2, lanes 5-7). Also visible in those lanes are the major break-down products of NS2, indicating the extent of degradation despite the use of protease inhibitors.

The final column used poly-uridylic acid (poly-U) to mimic RNA and therefore further purify NS2 from other nucleic acid binding proteins that may have co-purified on the heparin column. The column was constructed in the laboratory by pre-washing poly-U (Sigma) and packing it into a 5 ml syringe. The poly-U bed occupied a volume of about 1 ml. The fractions containing NS2 were pooled and diluted to 0.1M NaCl with 25mM phosphate buffer pH 8.0 containing 1mM EDTA. The column was equilibrated with low salt buffer and the sample applied. The column was washed with low salt buffer and a step gradient containing increasing amounts of NaCl (0.4, 0.5 and 1.0M) was applied. The fractions collected were analysed by SDS-PAGE (Fig 3.3). During later purifications, NS2 was eluted with 0.6M NaCl, omitting the 0.4 and 0.5M steps. This eluted the NS2 in fewer fractions giving a more concentrated protein solution.

The yield of NS2 using this method was approximately 5mg per 500ml culture medium. The protein appeared as a single band by SDS-PAGE, although more NS2 degradation products appeared gradually during storage. As a result NS2 was made and purified on a frequent basis during this research.

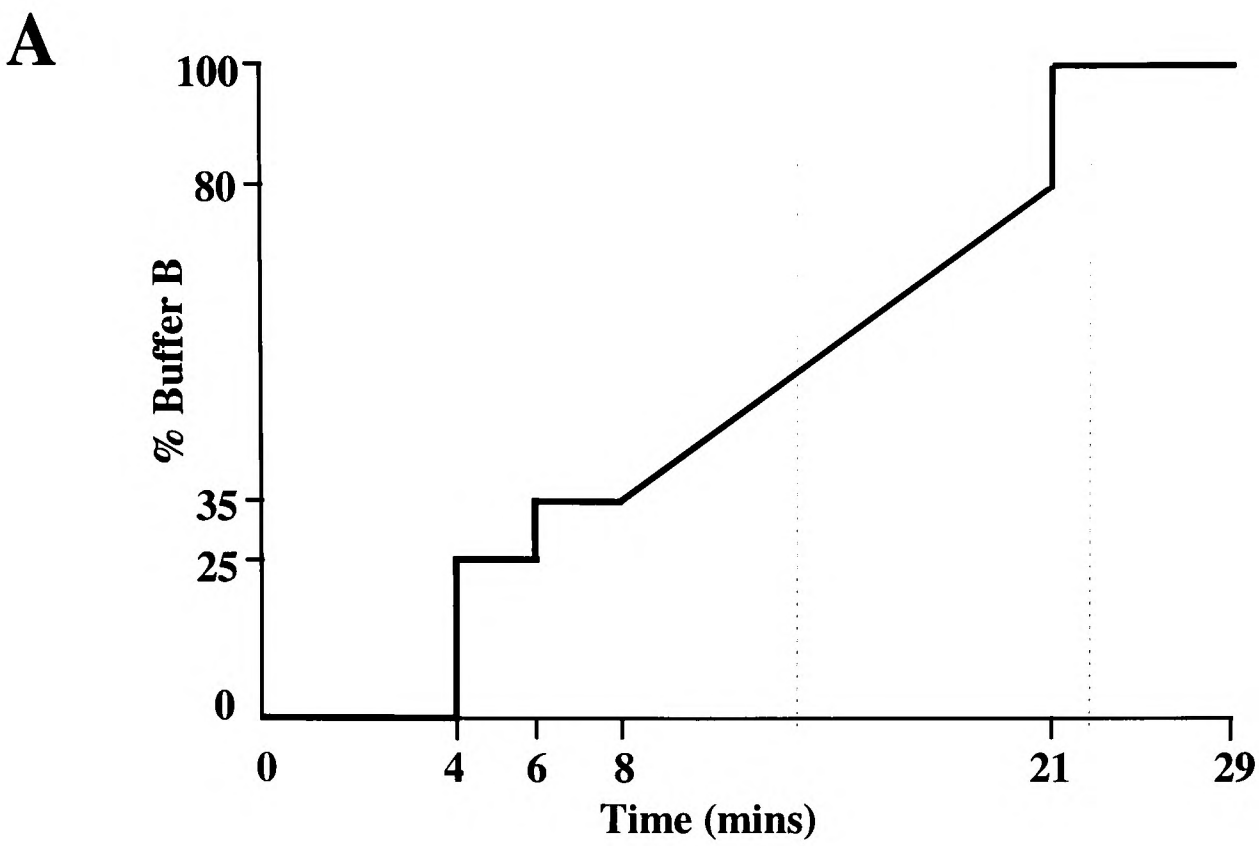

Fig 3.1: Purification of NS2 on a Q-sepharose column. A: Gradient applied to column after application of the sample. Buffer A: 0.1M phosphate buffer, 0.1M NaCl and 1mM EDTA. Buffer B: 0.1M phosphate buffer, 0.5M NaCl and 1mM EDTA. Fractions analysed by SDS-PAGE are indicated by vertical broken lines. B: SDS-PAGE analysis of fractions from Q-sepharose column. M: molecular weight markers. Lane 1: cell lysate. Lanes 2-12: fractions containing increasing salt concentrations. NS2 eluted in approx. 0.4M NaCl.

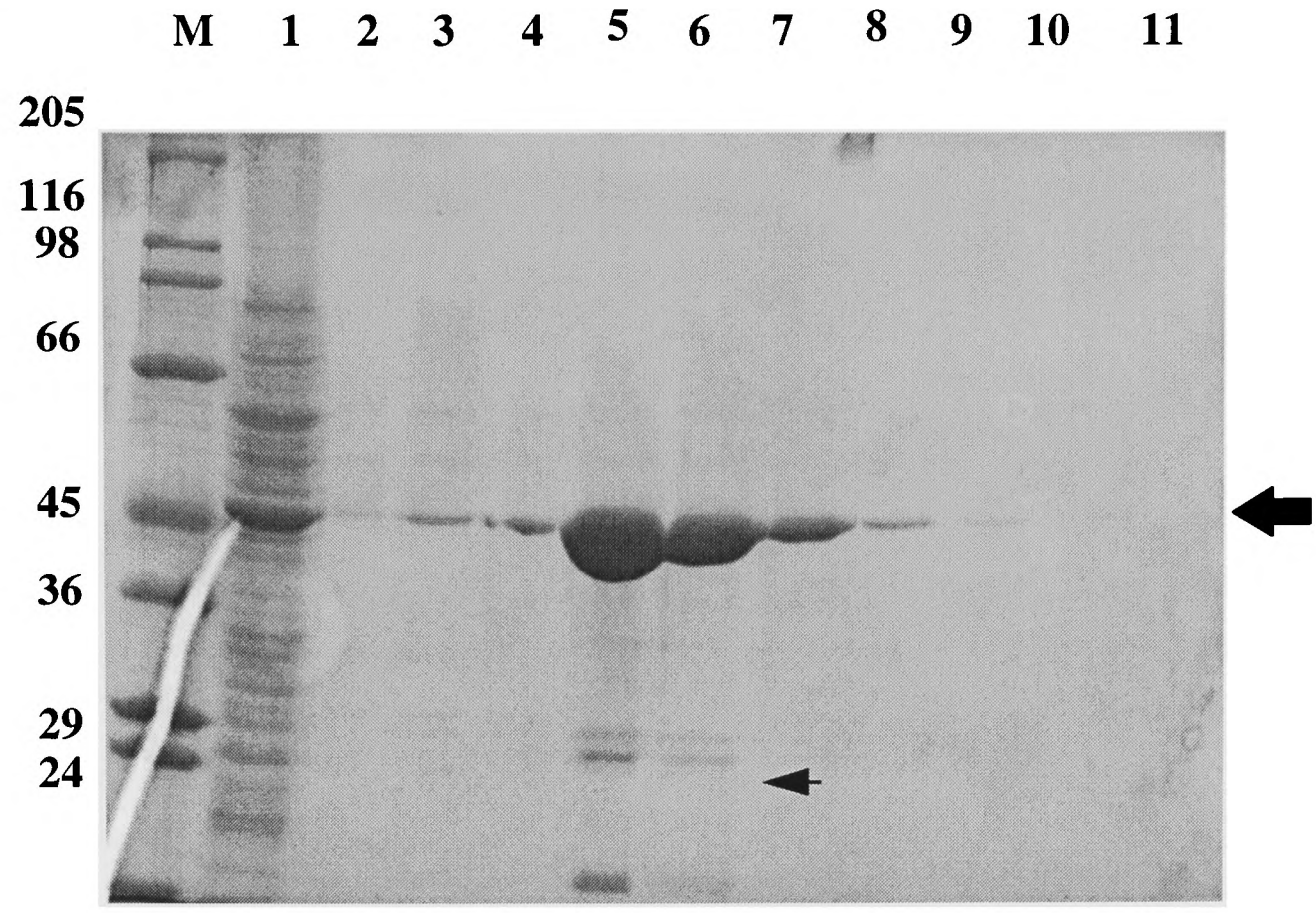

Fig 3.2: SDS-PAGE analysis of fractions eluted from heparin column. M: molecular weight markers. Lane 1: cell lysate. Lanes 2-4: 0.4M NaCl fractions. Lanes 5-7: 0.5M NaCl fractions. Lanes 8-11: 1.0M NaCl fractions. NS2 (large arrow) eluted in the 0.5M NaCl fractions. NS2 degradation products are indicated by a small arrow.

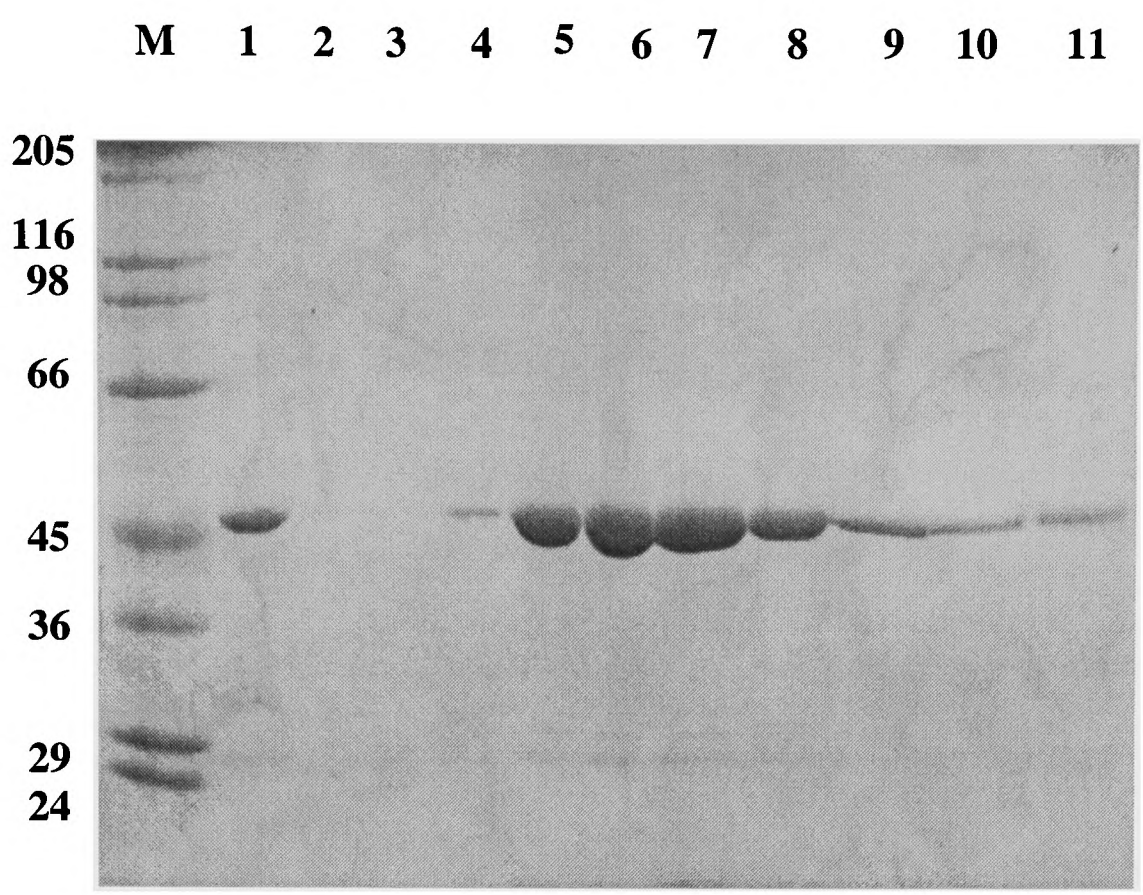

Fig 3.3: SDS-PAGE analysis of fractions from the poly-U column. M: molecular weight markers. Lane 1: NS2 purified previously. Lanes 2-4: 0.4M NaCl fractions. Lanes 5-7: 0.5M NaCl fractions. Lanes 8-11: 1.0M NaCl fractions.

3.2.2 Crystallography

The conditions under which a protein forms crystals varies greatly and cannot be predicted. A popular approach used in the determination of optimal crystallisation conditions is the use of a screening kit to rapidly and efficiently determine the conditions that produce crystallised protein. The Crystal Screen™ macromolecular crystallisation reagent kits from Hampton Research (Riverside, CA, USA) provide a total of 98 reagents to test for crystal formation at a wide range of conditions. Variables tested include precipitant, buffer, salt and pH (a range from 4 to 9).

Purified NS2 was used to set up crystallisation within 24 hours of purification, avoiding the freezing of the protein. NS2 was concentrated to approximately 10mg/ml with a Centricon-10 centrifuge concentrator with a molecular weight cut-off of 10 kDa. During concentration the protein was diluted with phosphate buffer pH 8.0 containing 400mM NaCl and 1mM EDTA thus achieving a buffer exchange into a slightly lower salt buffer. From experience and observation it was noticed that NS2 easily precipitated from solutions containing less than about 300mM NaCl on storage at 4°C. The concentration of NS2 was determined by colourimetric methods or by spectroscopy using a calculated molar extinction coefficient of 1.0.

All screening experiments were set up and incubated in a room set aside for crystallography in the Laboratory of Molecular Biophysics, Department of Biochemistry, Oxford University. The sitting drop vapour diffusion equilibration method was used. The bridges and Linbro plates used were freed of dust by spraying with compressed air and 700µl of each reagent in the Crystal Screen™ I and II kits (Table 3.1 and 3.2) were added to separate wells. NS2 was centrifuged to remove

particulate matter. One µl of concentrated NS2 was pipetted onto each bridge and mixed with 1µl of the respective reagent. Each well was sealed with a cover slide and vacuum grease and allowed to equilibrate.

The drops were examined for crystal formation at frequent intervals (up to several months after set up). From the initial screening experiment no crystals have so far been observed. Precipitates have been found in a few wells and some remain clear, giving hope that crystals may eventually form.

In the meantime further screening experiments were set up in order to assess whether a change in the preparation of the protein sample could have an effect on crystal formation. Using the concentration step in Centricon-10 filters as a method for buffer exchange, the effect of different salt concentrations or additives on crystal formation was investigated. Both higher (600mM) and lower (100mM) NaCl concentrations were tried as salt concentration has an effect on the solubility of NS2. Screens were tried with and without the divalent cation chelator EDTA, the reducing agent dithiothreitol (DTT) and the RNA mimic poly-uridine. These tests are ongoing but have not yielded crystals at the time of writing.

Table 3.1: Crystal Screen™ I reagent conditions.

Tube	Salt	Buffer	pH	Precipitant
1	0.02M Calcium chloride dihydrate	0.1M Na Acetate	4.6	30% v/v 2-methyl-2,4-pentanediol
2	None	None		0.4M K, Na Tartrate tetrahydrate
3	None	None		0.4M Ammonium dihydrogen phosphate
4	None	0.1M Tris	8.5	2.0M Ammonium sulphate
5	0.2M tri-sodium citrate dihydrate	0.1M Na HEPES	7.5	30% v/v 2-methyl-2,4-pentanediol
6	0.2M Mg chloride hexahydrate	0.1M Tris	8.5	30% w/v PEG 4000
7	None	0.1M Na Cacodylate	6.5	1.4M Sodium acetate trihydrate
8	0.2M tri-sodium citrate dihydrate	0.1M Na Cacodylate	6.5	30% v/v propan-2-ol
9	0.2M Ammonium acetate	0.1M Na Citrate	5.6	30% w/v PEG 4000
10	0.2M Ammonium acetate	0.1M Na Acetate	4.6	30% w/v PEG 4000
11	None	0.1M Na Citrate	5.6	1.0M Ammonium dihydrogen phosphate
12	0.2M Mg chloride hexahydrate	0.1M Na HEPES	7.5	30% v/v propan-2-ol
13	0.2M tri-sodium citrate dihydrate	0.1M Tris	8.5	30% v/v PEG 400
14	0.2M Calcium chloride dihydrate	0.1M Na HEPES	7.5	28% v/v PEG 400
15	0.2M Ammonium sulphate	0.1M Na Cacodylate	6.5	30% w/w PEG 8000
16	None	0.1M Na HEPES	7.5	1.5M Lithium sulphate monohydrate
17	0.2M Lithium sulphate monohydrate	0.1M Tris	8.5	30% PEG 4000

Tube	Salt	Buffer	pH	Precipitant
18	0.2M Magnesium acetate tetrahydrate	0.1M Na Cacodylate	6.5	20% PEG 8000
19	0.2M Ammonium acetate	0.1M Tris	8.5	30% v/v propan-2-ol
20	0.2M Ammonium sulphate	0.1M Na Acetate	4.6	25% w/v PEG 4000
21	0.2M Magnesium acetate tetrahydrate	0.1M Na Cacodylate	6.5	30% v/v 2-methyl-2,4-pentanediol
22	0.2M Sodium acetate trihydrate	0.1M Tris	8.5	30% w/v PEG 4000
23	0.2M Mg chloride hexahydrate	0.1M Na HEPES	7.5	30% v/v PEG 400
24	0.2M Calcium chloride dihydrate	0.1M Na Acetate	4.6	20% v/v propan-2-ol
25	None	0.1M Imidazole	6.5	1.0M Sodium acetate trihydrate
26	0.2M Ammonium acetate	0.1M Na Citrate	5.6	30% v/v 2-methyl-2,4-pentanediol
27	0.2M tri-sodium citrate dihydrate	0.1M Na HEPES	7.5	20% v/v propan-2-ol
28	0.2M Sodium acetate trihydrate	0.1M Na Cacodylate	6.5	30% w/v PEG 8000
29	None	0.1M Na HEPES	7.5	0.8M K, Na Tartrate tetrahydrate
30	0.2M Ammonium sulphate	None		30% w/v PEG 8000
31	0.2M Ammonium sulphate	None		30% w/v PEG 4000
32	None	None		2.0M Ammonium sulphate
33	None	None		4.0M Sodium formate
34	None	0.1M Na Acetate	4.6	2.0M Sodium formate
35	None	0.1M Na HEPES	7.5	0.8M K & 0.8M Na phosphate monobasic

Tube	Salt	Buffer	pH	Precipitant
36	None	0.1M Tris	8.5	8% w/v PEG 8000
37	None	0.1M Na Acetate	4.6	8% w/v PEG 4000
38	None	0.1M Na HEPES	7.5	1.4M Sodium citrate dihydrate
39	None	0.1M Na HEPES	7.5	2% v/v PEG 400 & 2.0M Ammonium sulphate
40	None	0.1M Na Citrate	5.6	20% v/v propan-2-ol & 20% w/v PEG 4000
41	None	0.1M Na HEPES	7.5	10% v/v propan-2-ol & 20% w/v PEG 4000
42	0.05M Potassium phosphate monobasic	None		20% w/v PEG 8000
43	None	None		30% w/v PEG 1500
44	None	None		0.2M Magnesium formate
45	0.2M Zinc acetate dihydrate	0.1M Na Cacodylate	6.5	18% w/v PEG 8000
46	0.2M Calcium acetate	0.1M Na Cacodylate	6.5	18% w/v PEG 8000
47	None	0.1M Na Acetate	4.6	2.0M Ammonium sulphate
48	None	0.1M Tris	8.5	2.0M Ammonium dihydrogen phosphate
49	1.0M Lithium sulphate monohydrate	None		2% w/v PEG 8000
50	0.5M Lithium sulphate monohydrate	None		15% w/v PEG 8000

Table 3.2: Crystal Screen™ II reagent conditions.

Tube	Salt	Buffer	pH	Precipitant
1	2.0M NaCl	None		10% w/v PEG 6000
2	0.01M Cetyl trimethyl-ammonium bromide	None		0.5M NaCl & 0.01M MgCl hexahydrate
3	None	None		25% v/v Ethylene glycol
4	None	None		35% v/v Dioxane
5	2.0M Ammonium sulphate	None		5% v/v isopropanol
6	None	None		1.0M Imidazole pH6.5
7	None	None		10% w/v PEG 1000, 10% w/v PEG 8000
8	1.5M NaCl	None		10% v/v Ethanol
9	None	0.1M Na Acetate	4.6	2.0M NaCl
10	0.2M NaCl	0.1M Na Acetate	4.6	30% v/v MPD
11	0.01M Cobalt chloride hexahydrate	0.1M Na Acetate	4.6	1.0M 1,6 Hexanediol
12	0.1M Cadmium chloride	0.1M Na Acetate	4.6	30% v/v PEG 400
13	0.2M Ammonium sulphate	0.1M Na Acetate	4.6	30% w/v PEG mono-methylether 2000
14	0.2M K/Na Tartrate	0.1M Na Citrate	5.6	2.0M Ammonium Sulphate
15	0.5M Ammonium sulphate	0.1M Na Citrate	5.6	1.0M Lithium sulphate
16	0.5M NaCl	0.1M Na Citrate	5.6	4% w/v polyethylene-imine
17	None	0.1M Na Citrate	5.6	35% v/v tert-butanol

Tube	Salt	Buffer	pH	Precipitant
18	0.01M Ferric chloride hexahydrate	0.1M Na Citrate	5.6	10% v/v Jaffamine M-600
19	None	0.1M Na Citrate	5.6	2.5M 1,6 Hexanediol
20	None	0.1M MES	6.5	1.6M Magnesium sulphate heptahydrate
21	0.1M Na & 0.1M K phosphate monobasic	0.1M MES	6.5	2.0M NaCl
22	None	0.1M MES	6.5	12% w/v PEG 20000
23	1.6M Ammonium sulphate	0.1M MES	6.5	10% v/v Dioxane
24	0.05M Caesium chloride	0.1M MES	6.5	30% v/v Jaffamine M-600
25	0.01M Cobalt chloride hexahydrate	0.1M MES	6.5	1.8M Ammonium Sulphate
26	0.2M Ammonium sulphate	0.1M MES	6.5	30% w/v PEG mono-methylether 5000
27	0.01M Zinc sulphate heptahydrate	0.1M MES	6.5	25% w/v PEG mono-methylether 550
28	None	None		1.6M Sodium citrate pH 6.5
29	0.5M Ammonium sulphate	0.1M HEPES	7.5	30% v/v MPD
30	None	0.1M HEPES	7.5	10% w/v PEG 6000, 5% v/v MPD
31	None	0.1M HEPES	7.5	20% v/v Jaffamine M-600
32	0.1M NaCl	0.1M HEPES	7.5	1.6M Ammonium Sulphate
33	None	0.1M HEPES	7.5	2.0M Ammonium formate
34	0.05M Cadmium sulphate octahydrate	0.1M HEPES	7.5	1.0M Sodium acetate
35	None	0.1M HEPES	7.5	70% v/v MPD

Tube	Salt	Buffer	pH	Precipitant
36	None	0.1M HEPES	7.5	4.3M NaCl
37	None	0.1M HEPES	7.5	10% w/v PEG 8000, 8% v/v ethylene glycol
38	None	0.1M HEPES	7.5	20% w/v PEG 10000
39	0.2M Magnesium chloride hexahydrate	0.1M Tris	8.5	3.4M 1,6 Hexanediol
40	0.1M Calcium chloride hexahydrate	0.1M Tris	8.5	25% v/v tert-butanol
41	0.01M Nickel chloride hexahydrate	0.1M Tris	8.5	1.0M Lithium sulphate
42	1.5M Ammonium sulphate	0.1M Tris	8.5	12% v/v gylcerol
43	0.2M Ammonium phosphate monobasic	0.1M Tris	8.5	50% v/v MPD
44	None	0.1M Tris	8.5	20% v/v ethanol
45	0.01M Nickel chloride hexahydrate	0.1M Tris	8.5	20% w/v PEG mono-methylether 2000
46	0.1M NaCl	0.1M Bicine	9.0	30% w/v PEG mono-methylether 550
47	None	0.1M Bicine	9.0	2.0M Mg chloride hexahydrate
48	2% v/v Dioxane	0.1M Bicine	9.0	10% w/v PEG 20000

Numerous factors are known to affect crystal formation, two of which are particularly likely to affect NS2 crystallisation. Sequence heterogeneities caused by the degradation of the protein being crystallised is possible as NS2 degrades relatively easily if not frozen. Overcoming this degradation is not a simple problem as a wide range of protease inhibitors has slowed down, but not completely stopped the degradation. Sequence heterogeneity can also be caused by heterogeneous post-translational modification and as NS2 is phosphorylated at multiple serine residues it can possibly be found in a number of phosphorylation states.

Conformational heterogeneity, caused by oligomerisation of a protein is another possibility. NS2 oligomerises into VIBs in infected cells. VIBs are not of a regular shape or size and would therefore be very difficult to crystallise. VIBs can be formed by the expression of NS2 by a recombinant baculovirus in insect cells but it is not known whether purified NS2 is oligomeric. In order to determine if purified NS2 was monomeric or oligomeric, size exclusion or gel permeation chromatography was used.

In size exclusion chromatography the porous gel matrix separates molecules that differ in size and weight. Large molecules applied to the column cannot enter the pores of the matrix and are therefore eluted from the column before smaller molecules. A Sephacryl S-300 column (Pharmacia) attached to the low pressure chromatography system described earlier was calibrated with proteins of known size (Fig 3.4A).

A 100µl aliquot of purified NS2 in 25mM phosphate buffer, 400mM NaCl and 1mM EDTA at a concentration of 1mg/ml was applied to the column. The column was washed with the same buffer at 0.5 ml/min and fractions collected. The fractions

were monitored for protein content by A_{280} measurements with the UV detector. Since purified protein was applied to the column the only proteins to be eluted should be NS2. The first NS2 appeared at approximately 41 mins after application to the column (Fig 3.4B, broken vertical line). This is only three minutes after the void volume (Fig 3.4B, arrow head) and indicates that purified NS2 is in a large multimeric form. On the UV trace, NS2 continued to be eluted in the following fractions in decreasing amounts. Aliquots of these fractions were analysed by SDS-PAGE to confirm that NS2 was present (Fig 3.5).

From these results it is clear that purified NS2 exists in multiple oligomeric forms and would therefore be very difficult to crystallise. NS2 first elutes from the column in a fraction greater than the largest standard indicating that the largest form of oligomer is greater than 669 kDa. By extrapolation of the curve, NS2 appears to be able to oligomerise into structures as large as 900 kDa.

A

Protein Standard	Size (kDa)	Elution Volume (ml)
Thyroglobin	669	43.5
Apoferritin	443	48.0
β-amylase	200	54.0
Alcohol dehydrogenase	150	59.0
Bovine serum albumin	66	65.0
Ovalbumin	43	66.5

B

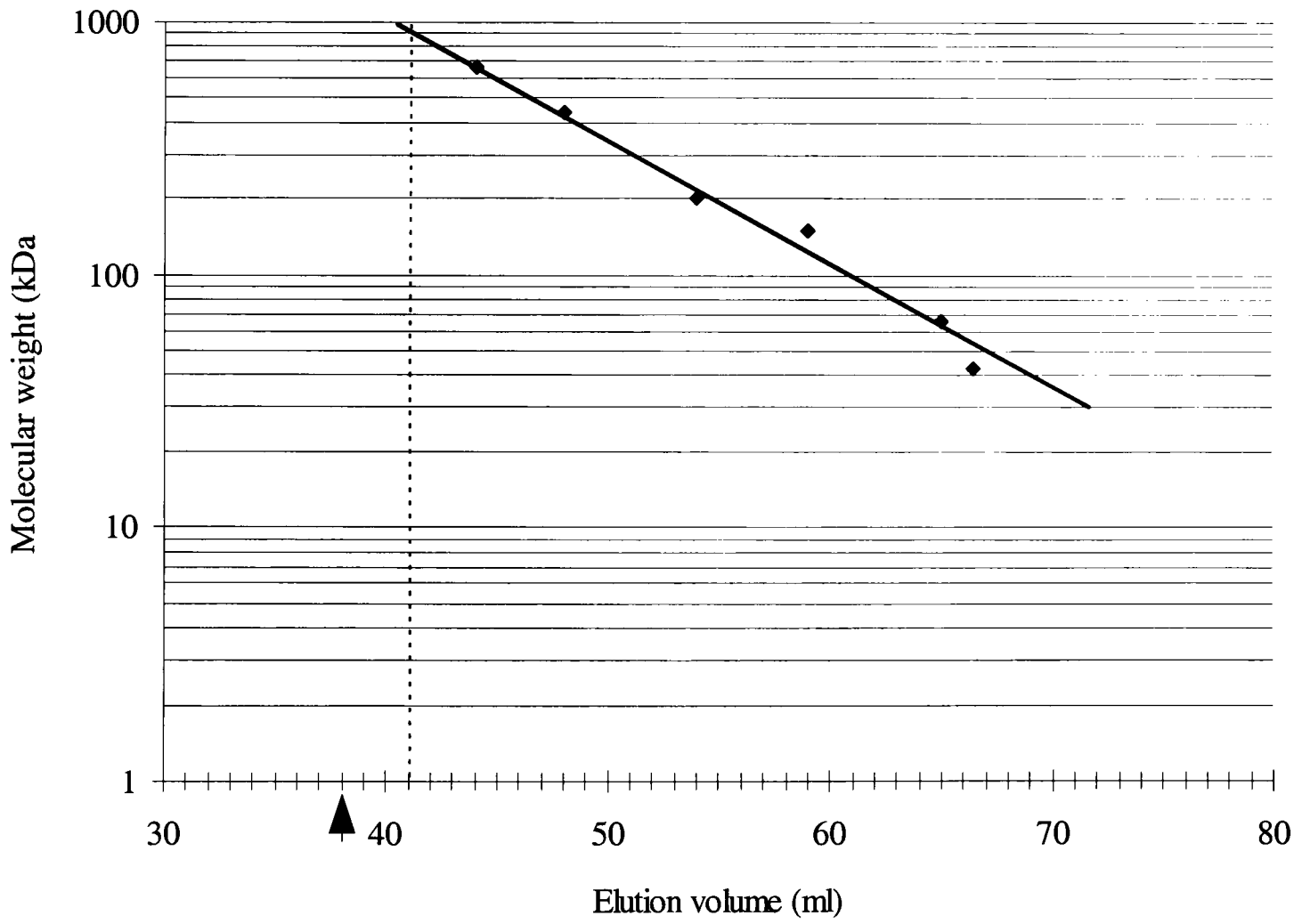

Fig 3.4: Size exclusion chromatography of purified NS2. **A**: Protein standards used to calibrate the S-300 Sephacryl 16/60 column. **B**: Standard curve plotted as a semi-log graph. The end of the void volume is indicated by an arrow head (38 mins). NS2 first eluted at 41 mins (broken vertical line).

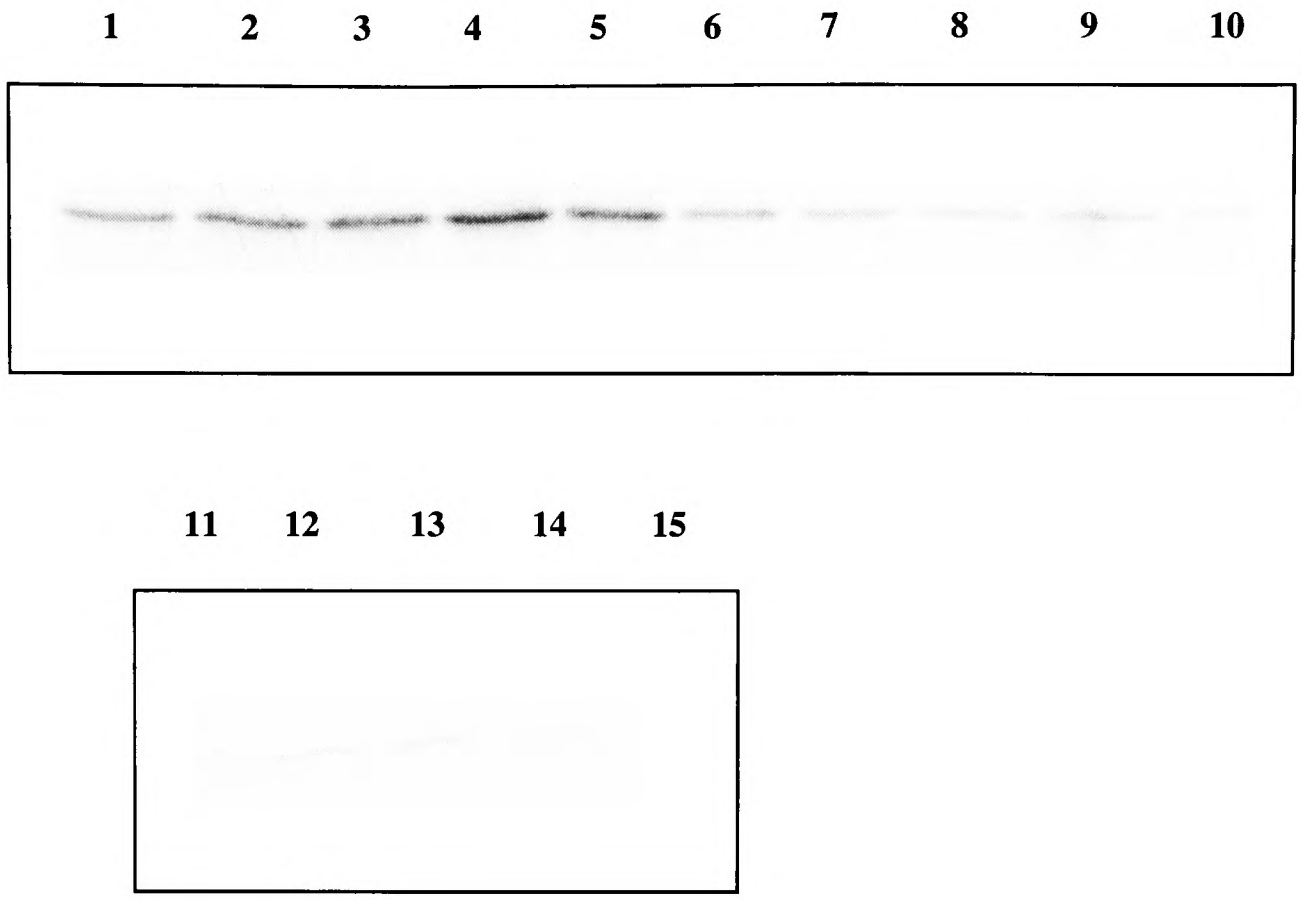

Fig 3.5: SDS-PAGE analysis of fractions eluted from the size-exclusion column to confirm the presence of NS2. Each lane represents the proteins of two fractions i.e. lane 1 represents fractions eluted at 41 and 42 mins.

3.2.3 Circular Dichroism

As NS2 is larger than the upper limit for NMR spectroscopy, it was decided to attempt circular dichroism as a means of obtaining some secondary structure data on the protein. Circular dichroism can use small amounts of relatively dilute proteins (0.1 mg/ml). However CD is very sensitive to compounds that absorb in the far UV region of the spectrum. The first step was to determine which buffer to use in obtaining CD spectra. Phosphate buffers work well in CD spectroscopy but chloride ions absorb highly (Schmid, 1997). As high concentrations of protein are not required and the time taken to obtain the spectra is short, NS2 was exchanged into 25mM phosphate buffer pH 7.8 containing 300mM sodium perchlorate ($NaClO_4$), a common replacement for NaCl in CD experiments. The NS2 sample was diluted with 25mM phosphate buffer pH 7.8 just before CD determination so as to give a solution with a $NaClO_4$ concentration of 100mM. A buffer of the same composition and concentration was used to determine the absorbance at these levels of perchlorate. For CD data to be useful the response across the photomultiplier should be less than 500mV. As can be seen in Fig 3.6, this buffer did not produce a photomultiplier voltage in excess of 500mV over the wavelengths to be used (190-260nm).

NS2, either purified and held at 4°C until the experiment or frozen and thawed before use was used. CD spectra of NS2 was obtained with a Jasco J720 spectropolarimeter using a 1mm quartz cell, with samples held at 30°C. Thirty-two scans were performed over a wavelength range from 190-260nm at 1nm intervals, on NS2 samples in 25mM sodium phosphate pH 7.8, 100mM $NaClO_4$. Baseline measurements were recorded under the same conditions. The data was corrected for baseline measurements and smoothed before plotting with Microsoft Excel (Microsoft

Corp., USA. Fig 3.7). In the structural interpretation of CD spectra, negative peaks at 210 ± 3nm and 225 ± 5nm indicate the presence of α-helices, while a positive peak at 195 ± 5nm and a broad negative peak at about 210-220nm indicate β-sheets (Woody, 1985). The data in Fig. 3.7 indicate a reduction in the amount of α-helix in NS2 when it is frozen.

In order to quantify the various amounts of the different secondary structure in NS2 the Dichroprot program (V2.2) for the interpretation of CD spectra was used (Deleage & Geourjon, 1993). The program is designed to predict the secondary structure of proteins from their experimental circular dichroism data. The data obtained by two different methods (Table 3.1) confirms the visual interpretation of the CD spectra for fresh and frozen NS2. This algorithm does not constrain the results to 100% so the figures in Table 3.1 do not add up to exactly 100%, although they are not far off. It is clear that NS2 undergoes structural changes on freeze-thawing, with both the Fasman (Perczel *et al.*, 1992) and the Yang (Yang *et al.*, 1986) methods showing a decrease in α-helical content and an increase in β-sheets. However, they differ considerably in their determination of the amounts of the various structures in each sample. The Fasman method is the newer method and is considered an improvement on many previous methods of CD spectra deconvolution. NS2 has been predicted by others to have a high α-helical content (van Staden *et al.*, 1991, Uitenweerde *et al.*, 1995) which is in agreement with the Fasman method. The reovirus σ-NS protein is also predicted to have a high α-helical content, possibly as high as 50% (Wiener & Joklik, 1987).

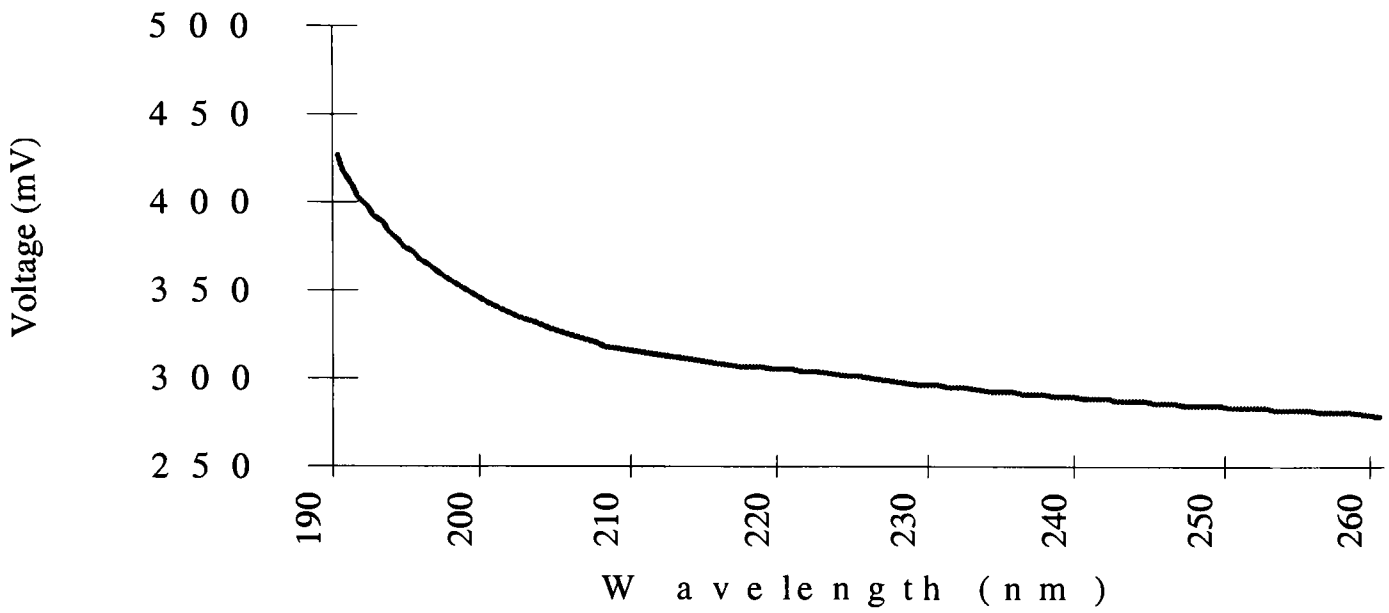

Fig 3.6: Absorbance of 25mM sodium phosphate pH 7.8, 100mM $NaClO_4$. The voltage across the photomultiplier was monitored as the wavelength decreased to determine whether the absorbance of the buffer was excessive.

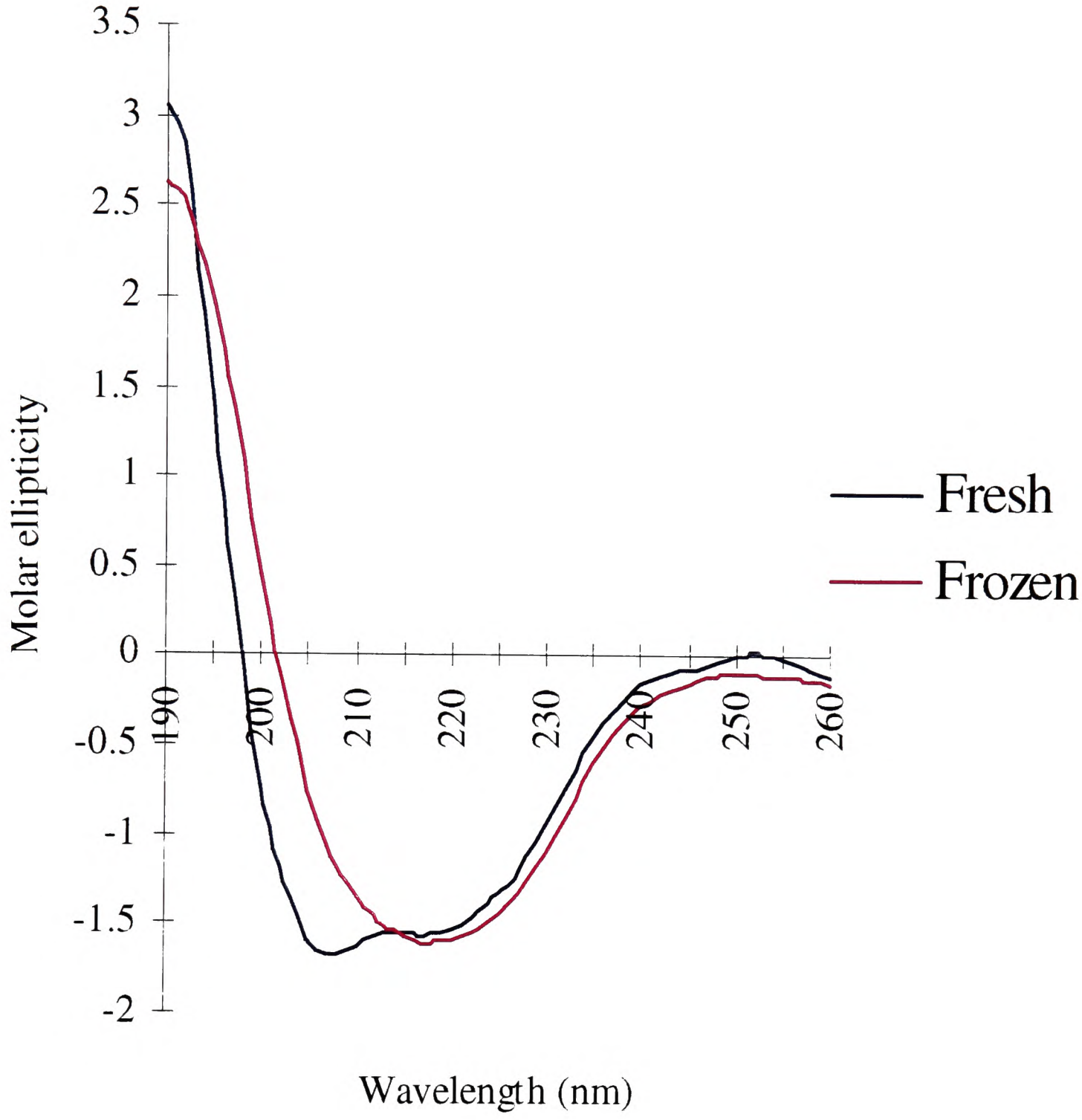

Fig 3.7: CD spectrum of NS2 in 25mM sodium phosphate pH 7.8, 100mM $NaClO_4$. The spectra was obtained with a Jasco J720 spectropolarimeter using a 1mm quartz cell, with samples held at 30°C. Thirty-two scans were performed over a wavelength range from 190-260nm at 1nm intervals. Molar ellipticity (deg cm^2 $dmol^{-1}$ $x10^4$) vs wavelength (nm) was plotted.

Table 3.3: Interpretation of the CD spectra using Dicroprot V2.2 (Deleage & Geourjon, 1993). The methods of Fasman (Perczel *et al.*, 1992) and Yang (Yang *et al.*, 1986) were used.

Structure	Fresh		Frozen	
	Fasman	**Yang**	**Fasman**	**Yang**
α-helix	53%	36%	32%	20%
β-sheet	9%	15%	37%	55%
Other	35%	54%	27%	32%

3.3 DISCUSSION

The ability to purify a protein to a high level of homogeneity and in large quantities is an important step in the study of a protein's structure and function. With the methods outlined in this chapter it has been possible to initiate structural studies on NS2. Protein purified using this method will also be used in the study of RNA-binding and the characterisation of enzymatic activity associated with NS2 described later in this thesis. In addition, this purification procedure has been used to purify NS2 for the generation of both polyclonal and monoclonal antibodies.

The procedure was designed to achieve both purification and concentration of NS2 at the same time. Chromatography on the Q-Sepharose column separated NS2 from a large amount of contaminating protein and proved to be a valuable first step. In experiments where partially purified protein was required, cell lysates were run on a Q-Sepharose column, allowing the purification of NS2 from major contaminants and also achieving a good degree of concentration.

By exploiting the ability of NS2 to bind RNA, both the heparin and poly-U columns were used to further purify the protein from other proteins. The heparin column was employed first as it has a broader range of activity in that it mimics nucleic acids and can bind proteins that bind both DNA and RNA. The poly-U column, on the other hand, binds RNA binding-proteins. The use of a high-salt elution buffer made it possible to collect NS2 in a concentrated form, a requirement for setting up crystallisation experiments.

Although a number of methods exist for the determination of a proteins secondary structure, crystallography was selected as the first method to attempt. At 41 kDa, NS2 is too large a protein for the current NMR technology. Although cryo-EM is

rapidly becoming a very powerful technique for the determination of 3-D structure, it is not yet possible to resolve structures to near atomic level. Also, it would not be suitable to obtain the structure of NS2 as a monomer. It may, however, prove useful in examining the structure of VIBs, as the main strength of cryo-EM lies in its ability to resolve macromolecular complexes.

Crystallography has been used successfully in our laboratory with the study of orbiviral VP7 (Basak *et al.*, 1992, Grimes *et al.*, 1995, Basak *et al.*, 1996) and retroviral matrix protein (Belyaev *et al.*, 1994). A wealth of experience in crystallography is available within the laboratory, where a number of other crystallisation experiments are underway, and in the Laboratory of Molecular Biophysics, with whom we have close ties.

Experience in protein crystallography, however, is no guarantee of success. Despite trying a wide range of conditions it has not been possible to crystallise NS2 to date. Two possible reasons for the inability to obtain crystals are sequence heterogeneity and conformational heterogeneity. In order to reduce sequence heterogeneity, crystallisation trials were set up as soon as possible after purification of NS2 so as to avoid excessive degradation. The possibility that conformational heterogeneity may also contribute to the difficulty in crystallising NS2 was investigated by size-exclusion chromatography. NS2 was found to be in a multimeric form of variable size even after purification. This is likely to be a major problem in current and future attempts at the crystallisation of NS2. Interestingly, it was reported at a recent conference that difficulty in crystallising reovirus σ-NS may be due to its multimeric nature (Gillian & Nibert, 1997).

Although it is not possible to obtain 3-D structural data using CD spectroscopy, useful secondary structure information can be provided. Here CD

spectroscopy has confirmed that NS2 has a high α-helical content. More importantly it has illustrated the extent of structural change that the protein undergoes on freezing, a fact that must be considered in future work. The enzymatic activity of BTV VP6 is abrogated by freeze-thawing, a feature that delayed the identification of the protein as a ds-RNA helicase. The sensitivity of CD spectroscopy makes it a useful technique for the rapid determination of changes in a proteins secondary structure.

Chapter 4

SEQUENCE SPECIFICITY OF NS2 RNA-BINDING

4.1 INTRODUCTION

The specific interactions between proteins and nucleic acids are precise processes and are central to numerous cellular processes. These interactions can be with either RNA or DNA. Much of the research on post-transcriptional regulation, RNA splicing and viral assembly focus on RNA-protein interactions. In general, research on RNA-protein complexes focuses on three main areas - the RNA target sites, the protein structures recognising RNA and studies on the mechanisms by which proteins and RNA targets interact (Draper, 1995).

The mechanisms of RNA-protein interaction have been extensively studied in other systems, particularly in HIV tat-TAR and rev-RRE complexes (Heaphy *et al.*, 1990, Delling *et al.*, 1992, Frankel, 1992, Williamson *et al.*, 1995, Jain & Belasco, 1996, Wemmer, 1996), and the assembly of bacteriophages and viruses (Rossmann *et al.*, 1983, Timmins *et al.*, 1994, Rumenapf *et al.*, 1995). A prerequisite for the determination of the interaction mechanism is a knowledge of both the protein structures involved and the RNA target. RNA secondary structures have been shown to play a crucial role in most specific RNA-protein interactions studied (Clever *et al.*, 1995, Kurg *et al.*, 1995, Tabernero *et al.*, 1996) including rotavirus (Patton, 1995). Four rotavirus proteins specifically bind the ends of rotavirus RNA segments and secondary structures at the termini are believed to play a role in some of these interactions. In the rotavirus non-structural protein NSP3 however, the protein binds the short 3' consensus sequence (Poncet *et al.*, 1993), the rotavirus equivalent of the BTV 3' hexanucleotide. A minimal sequence of four nucleotides is required for this specific binding and secondary structure involvement is thought to be unlikely (Poncet *et al.*, 1994).

Previous studies on NS2 showed that the amino terminal of the protein was essential for RNA binding (Zhao *et al.*, 1994). By using deletion and site-directed mutants, charged amino acids within the first eight residues of the protein were shown to be required for high affinity binding. A group of conserved amino acids has been identified in the NS2 proteins of BTV, EHDV and AHSV, as well as in rotavirus NSP3 and reovirus σNS (van Staden *et al.*, 1991, Rao *et al.*, 1995). This nine residue long region, located between amino acids 75 and 83 in BTV and EHDV, 77 and 85 in AHSV, 104 and 112 in rotavirus and 176 and 184 in reovirus, is believed to constitute an RNA-binding motif. Mutation of this region in EHDV reduces RNA-binding (Theron *et al.*, 1996). However mutations outside of this region in BTV NS2 (Zhao *et al.*, 1994) and reovirus σNS (Gillian & Nibert, 1997) abolish RNA binding, suggesting that the overall structure of the protein is important.

The characterisation of RNA-protein interactions is reliant on two types of analyses - cross-linking and gel-shift analysis. Cross-linking assays are an important tool in the analysis of RNA-RNA, RNA-protein and protein-protein interactions *in vivo* and *in vitro*. The use of ultraviolet (UV) light at 254nm is a popular method for the study of RNA-protein interactions (Brimacombe *et al.*, 1988, Pashev *et al.*, 1991). This method allows the identification of close interactions as cross-linking only occurs between molecules one covalent bond length or less away and it is known as a zero length cross-linker (Pashev *et al.*, 1991, Will *et al.*, 1994). Gel-shift analysis on the other hand does not rely on the induction of cross-linkage and can only be performed by assembling the RNA-protein complex components *in vitro*. It is less sensitive than UV cross-linking as the RNA and protein can dissociate during the running of the gel (Budowsky & Abdurashidova, 1989). However, since it does not

require the involvement of any external cross-linking agent it is more representative of the stability of interactions that occur *in vivo*.

Given the importance of RNA binding proteins and their specific interactions with their target RNA sequences in the assembly and replication of many viruses, it was decided to study the role of BTV non-structural proteins in packaging and assembly. Since packaging occurs at the level of ssRNA and NS2 binds ss- but not dsRNA, the identification of the RNA sequences recognised by NS2 was undertaken. Sequence specific binding by NS2, or any other BTV RNA-binding protein, has not been previously demonstrated.

4.2 RESULTS

4.2.1 BTV NS2 binds the 5' consensus sequence of rotavirus.

As other RNA-binding proteins of the Reoviridae bind the ends of their RNA molecules (Poncet *et al.*, 1993, Patton, 1995, Patton, 1996), short synthetic RNA probes were used corresponding to the 5' and 3' consensus sequences of rotavirus and the 3' consensus sequence of BTV in binding assays. Rotavirus NSP3 binds the rotavirus 3'consensus sequence while NSP1 does not bind either consensus sequence (Poncet *et al.*, 1994). These were included as positive and negative controls for specific binding respectively. By gel-shift analysis NS2 was shown to bind only the 5'consensus sequence of rotavirus (Fig 4.1). NS2 did not bind a reovirus or BTV 3' consensus sequence probe (data not shown).

In a similar experiment, increasing amounts of NS2 was incubated with a constant amount of rotavirus 5' probe. That gel shift showed that NS2 binds this rotavirus probe in a dose-dependant manner (Fig 4.2).

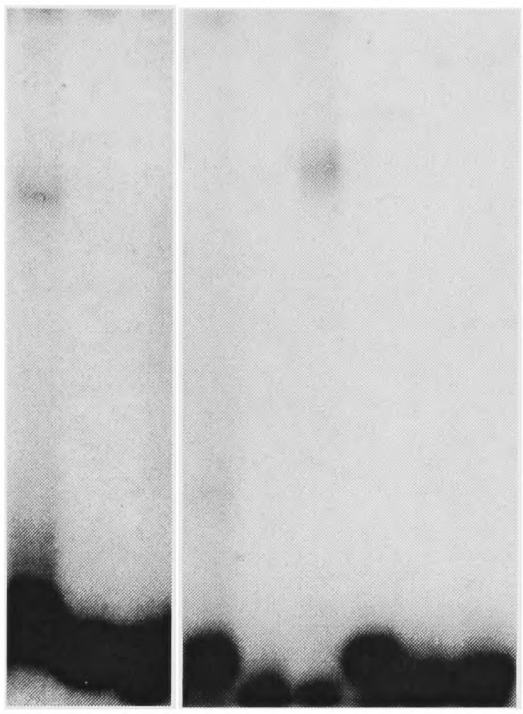

Probe	A	B	C	A	B	C	A	B	C
Protein	NS2			NSP3			NSP1		

Probes Used:
A: Rotavirus 5' GGCUUUAAAAG
B: Bluetongue 3' UCACACUUAC
C: Rotavirus 3' AUGUGACC

Fig 4.1: Gel shift of BTV NS2 and rotavirus NSP3 and NSP1 with synthetic RNA probes. Approx. 2μg protein and 2.5nM 5' end labelled probe were used in each reaction. Reactions were incubated at 30°C for 30 min before electrophoresis on an 8% low ionic strength acrylamide gel. Lane 1-3 NS2, lane 4-6 NSP3 lane 7-9 NSP1. NS2 specifically binds the rotavirus 5' synthetic RNA probe.

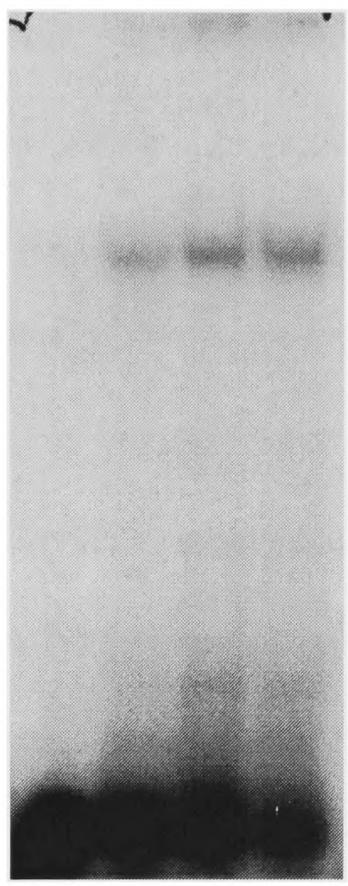

Protein (μg)	0	1	2	4

Fig 4.2: NS2 binding to rotavirus 5' synthetic RNA probe. Various amounts of NS2 (0, 1, 2 and 4 μg) were incubated at 30°C with 2.5nM rotavirus 5' consensus probe for 30 min and then electrophoresed on an 8% low ionic strength acrylamide gel. Increasing the amount of NS2 increased the amount of probe retarded.

4.2.2 Sequence identification in all ten BTV segments

Since NS2 specifically bound a sequence from rotavirus, all ten BTV segments were searched for occurrences of that sequence. Using the findpattern command in GCG7 (Wisconsin Package Version 7.0, Genetics Computer Group, Madison, Wisc.), one region in each BTV segment, with a high degree of homology to the rotavirus 5' consensus sequence, was identified (Table 4.1). For each segment, at least 7 out of 11 bases exactly matched the rotavirus 5' consensus sequence, with most of the observed variation occurring at the first and last nucleotide. There appears to be no definite motif as each sequence varies slightly from the rotavirus 5' consensus sequence. The location of this sequence - the NS2 target sequence or NTS - varied within the genome, e.g. it could be found near the 5' end, near the 3' end or in the middle.

Segment (size: bp)	Start (bp)	Sequence	Matches
L1 (3954)	3161	G G C U U U g A A c G	9/11
L2 (2926)	196	G G C U c U A A A u u	8/11
L3 (2772)	2297	G G C U U U A A g g c	8/11
M4 (2011)	121	G G C U U g A A A A u	9/11
M5 (1639)	674	G G C U a U A c A A G	9/11
M6 (1770)	128	c a C U U a A A A A G	8/11
S7 (1156)	782	a a C U U U A A A c c	7/11
S8 (1123)	148	a G C U U U u A A A c	9/11
S9 (1046)	69	G G a g U U A A A A c	8/11
S10 (822)	494	u G g U U U A A A A G	9/11
Rota 5'		G G C U U U A A A A G	

Table 4.1: Alignment of rotavirus 5' consensus sequence with all 10 BTV segments (mRNA strand). The table shows the size of each segment, the location and sequence of the homologous region in each segment and the number of exact matches. Mismatches are indicated in lower case.

4.2.3 The NS2 target sequence is essential for NS2 binding

To determine whether the NTS played a role in NS2 binding to Bluetongue viral RNA, deletions were created in segment M4 and these truncated segments were used as labelled probes in UV crosslinking experiments. Segment M4 was amplified by PCR using a forward primer to incorporate a T7 promoter site. The cDNA was digested with *Dra*I and *Hind*III to produce 110 bp (5'-) and 308 bp (5'+) cDNA fragments respectively (Fig 4.3). Labelled probes were generated by *in vitro* transcription, incorporating [α^{32}P]UTP into the RNA and used in UV crosslinking assays with NS2. Following crosslinking the complexes were electrophoresed on a 10% SDS-PAGE gel. Both the full-length (FL) and (5'+) probes were bound by NS2 while the (5'-) probe, without a NTS, was not bound (Fig 4.4).

To obtain further evidence of the role of the NTS in NS2 binding, another BTV segment, S10, was mutated and used in binding assays. Full-length S10 cDNA in pUC19 (pBTV-S10) was digested with *Sty*I to remove an internal 604 bp fragment, leaving 128 bp at the 5' end and 90 bp at the 3' end (Fig 4.5). Following purification, the plasmid was religated with 2 units of T4 DNA ligase (NEB) in a 20µl reaction. Two and ten µl portions of the ligation reaction were used to transform XL-1 Blue *E.coli*. To identify colonies containing the correct clone, white colonies were selected and were screened by PCR after the preparation of plasmid DNA by mini preps. This internally deleted S10 cDNA (5'3') and full-length S10 (FL) were amplified by PCR using existing primers.

In order to remove the 5' and 3' non-coding regions of S10, a pair of primers was designed to PCR amplify only the coding region. The forward primer, 3'S10T7F, also added a T7 promoter site. The sequence of the primers was:

3'S10T7F: 5'GCGTAATACGACTCACTATAGGTTTTGAAATGCCATTAAC3'

5'S10R: 5'GCATACCTTGGCGGTTGAGAAATGG3'

The T7 promoter sequence is underlined. The resultant cDNA, lacking 19 bp at the 5' end and 116 bp at the 3' end, was called Δ5'3'.

Amplification of FL, 5'3' and Δ5'3' was achieved by 1 cycle of denaturation at 95°C for 2 minutes, annealing at 54°C for 1 minute and extension at 72°C for 1 minute, followed by 30 cycles of 95°C for 1 minute, 54°C for 1 minute and 72°C for 1 minute. The reactions were then held at 72°C for 10 minutes to ensure that all products were fully extended. The products were purified using Wizard PCR prep columns.

Labelled probes were synthesised and used in a gel-shift assay with NS2. The NTS containing probes were bound by NS2, while the probe lacking an NTS, 5'3', did not (Fig 4.6), indicating that the NTS, and not the viral RNA ends, were essential for NS2 binding.

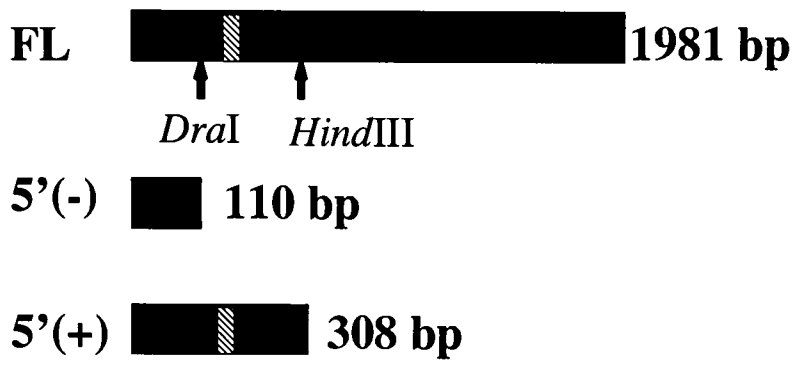

Fig 4.3: M4 ssRNA probes. cDNA constructs used in transcription reactions to produce ssRNA with or without a NS2 target sequence, indicated by shaded region.

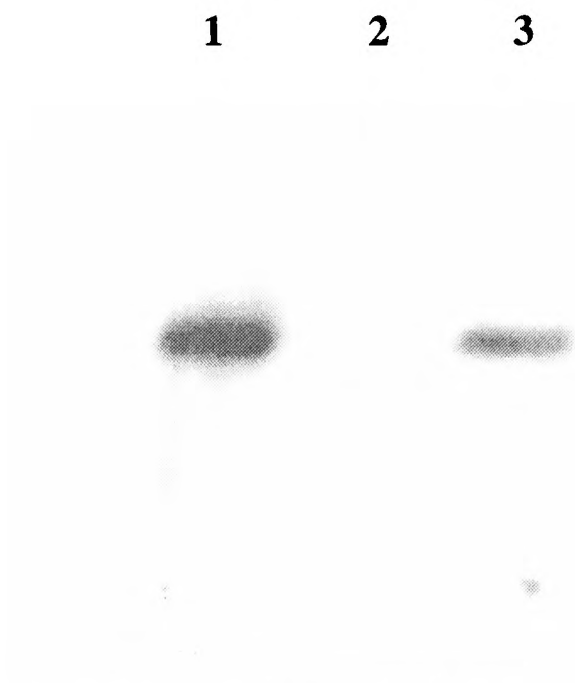

FL	5'(-)	5'(+)

Fig 4.4: UV crosslinked NS2 and M4 ssRNA probes resolved by SDS-PAGE. Approx. 10μg NS2 and 10,000 cpm probe were used in each reaction. Lane 1 FL probe, lane 2 5'(-) probe, lane 3 5'(+) probe. NS2 bound only the probes containing an NTS (lanes 1 and 3).

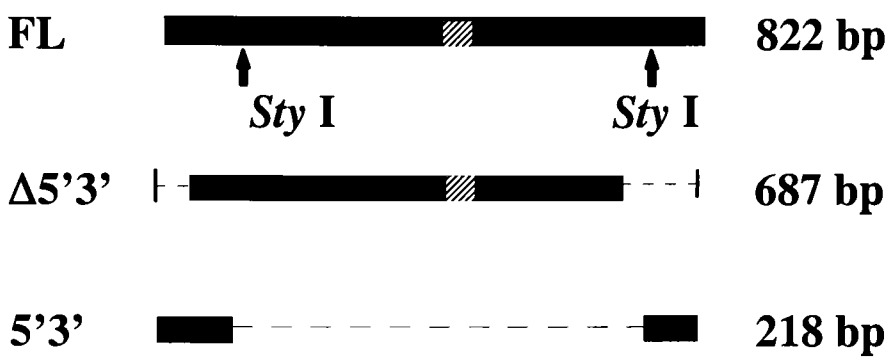

Fig 4.5: S10 ssRNA probes. cDNA constructs used in transcription reactions to produce ssRNA with or without an NS2 target sequence, indicated by shaded region.

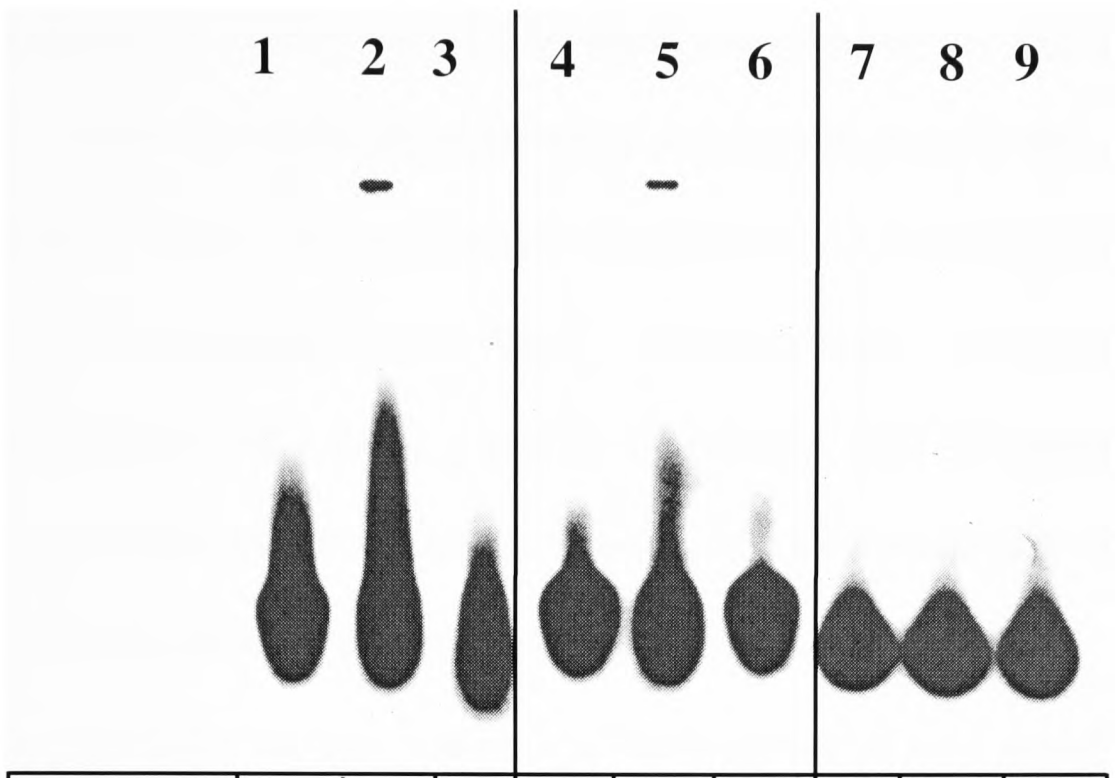

Protein	-	+	+	-	+	+	-	+	+
Buffer	+	+	-	+	+	-	+	+	-
Probe	FL	FL	FL	Δ5'3'	Δ5'3'	Δ5'3'	5'3'	5'3'	5'3'

Fig 4.6: Gel retardation of probe by NS2. Approx. 6μg NS2 and 25,000 cpm of probe were used as indicated. NS2 bound only the probes with an NTS (lanes 2 and 5).

4.2.4 The NS2 target sequence is sufficient for NS2 binding

Since NS2 was capable of binding the short rotavirus 5' consensus sequence, I wanted to determine whether the NTS, by itself, was sufficient for NS2 binding. Two synthetic 11 nucleotide RNA oligonucleotides corresponding to the M4 and S10 NTS were purchased. These were end labelled and used in uv-crosslinking experiments in the absence of cold non-BTV RNA (Fig 4.7). Both of the BTV probes bound to NS2 but not to rotavirus NSP3 (lanes 2 and 3). Conversely, only the rotavirus 3' probe bound to NSP3 (lane 4). RNA bound to larger (> 195 kDa) multimeric forms of NS2 was observed with the BTV probes (lanes 2 and 3).

The specificity of this binding was demonstrated in a uv-crosslinking assay with competition by either specific or non-specific RNA. The S10 synthetic RNA probe was end-labelled and UV-crosslinked to NS2. During the incubation of protein and RNA various amounts of either cold full length S10 RNA or cold luciferase RNA was added as indicated in Fig 4.8. Cold S10 RNA competed with the labelled S10 probe for binding to NS2 (lanes 3-6) while cold luciferase RNA, at the same concentrations, had no effect (lanes 7-10).

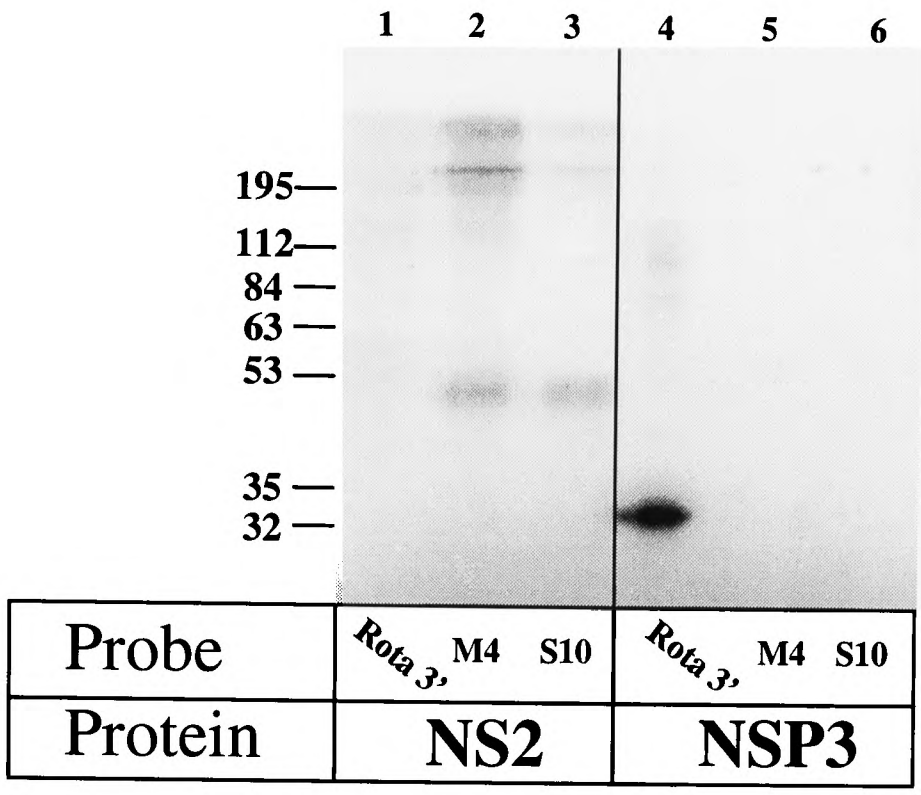

Fig 4.7: UV crosslinking of NS2 and short synthetic RNA probes. Approx. 6μg NS2 and 10,000 cpm of probe were incubated at room temperature in RNA-binding buffer for 30 min. Following exposure to UV light for 10 min, complexes were resolved on a 10% SDS-PAGE gel. The M4NTS and S10NTS probes were bound by NS2 (lanes 2 and 3) The reactions were also performed with rotavirus NSP3 as a control (lanes 4-6).

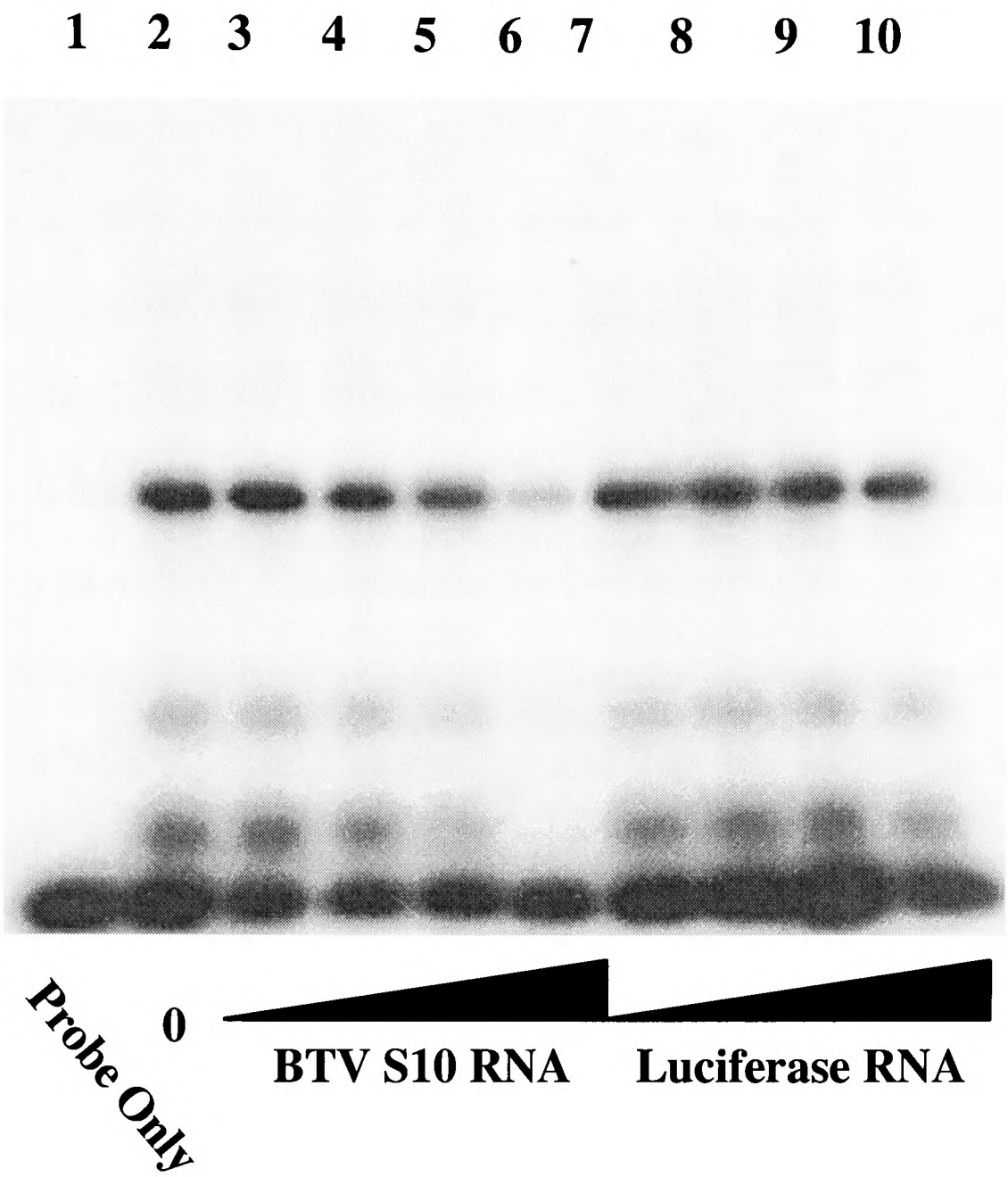

Fig 4.8: Competition assay. Approx. 6μg NS2 and 20,000 cpm S10NTS probe were incubated for 30 mins at room temperature with either full length BTV S10 (lanes 3-6) or luciferase RNA (lanes 7-10) at a concentration of 0.28-280ng/μl in 10-fold increments. The reactions were UV-crosslinked for 15 mins and autoradiographed after SDS-PAGE and drying.

4.2.5 The NS2 target sequence confers RNA binding to non-BTV RNA

To obtain further evidence to confirm the role of the NTS in NS2 specific binding I set up an experiment to test whether the aptamer could confer specific binding to non-BTV RNA. Using PCR and appropriate primers, I amplified an 85bp region of the baculovirus p10 promoter and simultaneously added a T7 promoter sequence to the 5' end and various sequences to the 3' end. On transcription, in the presence of [α^{32}P]-UTP, labelled probes were produced (Fig 4.9). These probes, along with labelled luciferase RNA were used in uv crosslinking experiments (Fig 4.10). All four probes were bound by NS2 when no cold RNA was included in the reactions (lanes 1-4), although there appeared to be a higher affinity for the probes containing the NTS (lanes 2 and 3). The addition of cold RNA reduced the amount of probe bound (lanes 5-12), particularly when BTV S10 RNA was used as competitor (lanes 9-12). Cold S10 RNA appeared to compete off the p10S10 probe more efficiently than the p10M4 probe (Fig 4.10, lanes 10 and 11, cf. lanes 6 and 7), suggesting that there may be some form of recognition of the different segments by NS2. The faster migrating bands observed (lanes 2, 3, 6, 7, 10 and 11) correspond to an NS2 degradation product occasionally seen during purification.

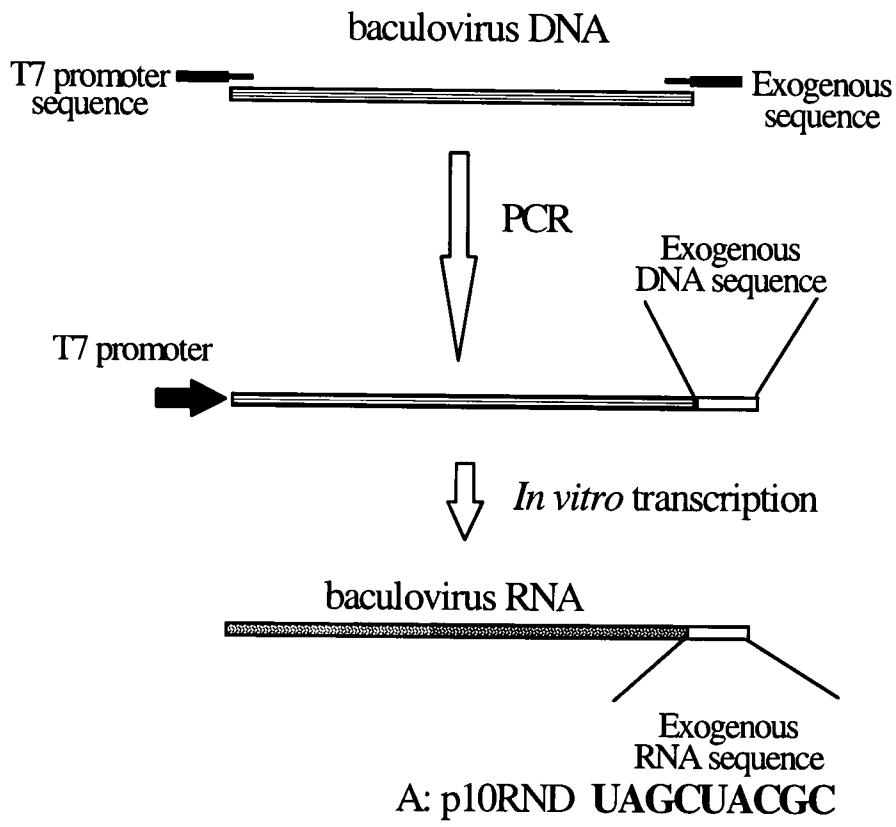

Fig 4.9: Labelled RNA used in UV crosslinking. A region of the baculovirus p10 promoter was amplified by PCR with the addition of a T7 promoter to the 5' end and the sequences A, B and C to the 3' end. Full length luciferase RNA was also used (D).

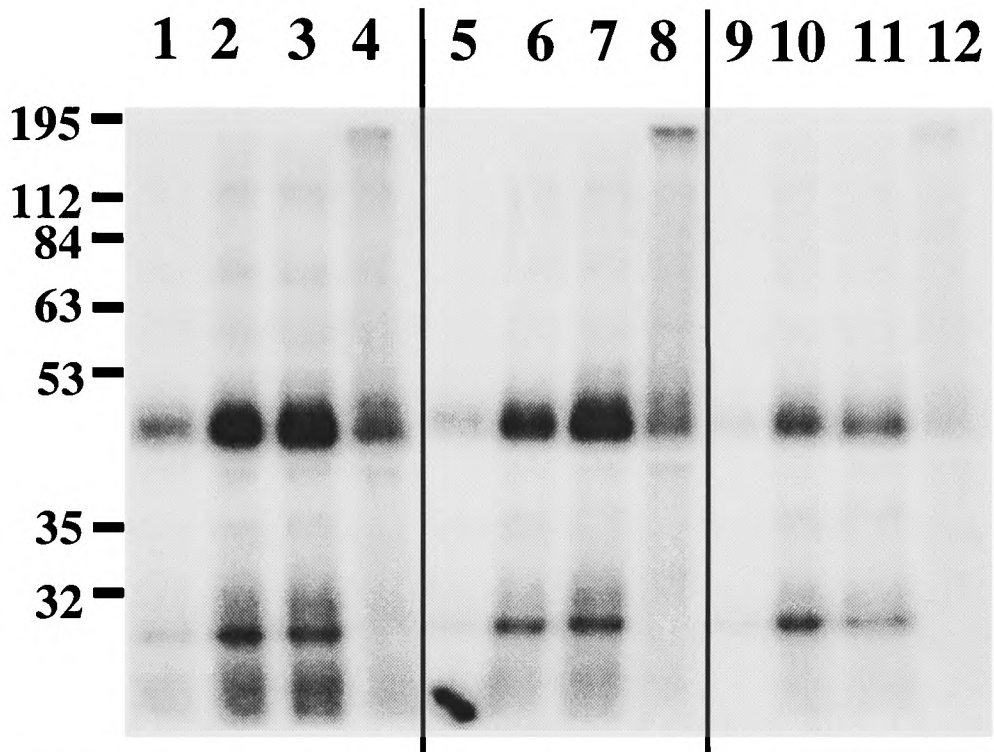

Labelled RNA	A	B	C	D	A	B	C	D	A	B	C	D
Cold RNA	None				Poly U				S10			

Fig 4.10: UV crosslinking and competition analysis of NS2 with BTV and non-BTV RNA. Approx. 8μg NS2 was pre-incubated with or without 5μg cold RNA (poly-U or BTV S10) as indicated, in RNA-binding buffer. After 10 min, 20,000 cpm of indicated probe was added and incubated for a further 25 min. Reactions were exposed to UV light for 10 min and excess RNA was digested with T1 RNAse. All probes were bound by NS2 in the absence of cold RNA (lanes 1-4) and the probes lacking an NTS were competed off by cold poly-u (lanes 5 and 8) and BTV S10 RNA (lanes 9 and 12). Competition with S10 RNA was more efficient (lanes 5-8 cf. lanes 9-12).

4.3 DISCUSSION

The results presented in this chapter demonstrate for the first time, sequence specificity in RNA binding by NS2. Previous studies on BTV RNA binding proteins have failed to identify sequence or structural specificity in any of the proteins (Huismans *et al.*, 1987a, Roy *et al.*, 1990a, Thomas *et al.*, 1990, Loudon & Roy, 1992, Theron *et al.*, 1994, Uitenweerde *et al.*, 1995) while Theron and Nels (Theron & Nel, 1997) have demonstrated that NS2 has a higher affinity for one segment of BTV RNA over non-BTV RNA.

It was initially surprising to find that NS2 bound the rotavirus 5' end rather than BTV viral ends, but this binding was reproducible in uv-crosslinking and gel shift experiments. In order to determine the significance of these results I looked for this sequence in BTV RNA. Once similar consensus sequences were identified in all 10 viral segments it was possible to investigate the role of this sequence. For two segments, M4 and S10, the deletion of the NTS abolished binding by NS2. The results indicate that this aptamer is necessary and sufficient for specific binding by NS2 to BTV ssRNA. In addition, competition experiments demonstrated the specificity of the binding.

It may be possible that NS2 has two distinct RNA binding activities. It is clear that NS2 can bind all RNA in UV-crosslinking assays (Fig 4.10, lanes 1-4). However the inclusion of cold non-BTV RNA can compete off some binding by full-length BTV RNA. It is possible that with full length BTV RNA, some binding is occurring at the non-specific binding site with the rest occurring at the specific site. The addition of non-BTV RNA could result in competition with BTV RNA for binding at the non-

specific site but not the specific site. This would mask any specific binding occurring, possibly explaining the failure of previous attempts to detect specific binding by NS2.

The NTS identified here is unusual. It appears to be linear since the formation of secondary structure seems unlikely in the short synthetic RNA aptamers used as probes. Examination of computer generated fold prediction for three BTV RNA segments does not suggest that the NTS is presented to NS2 in the context of a secondary structure common to all segments. Although rare, linear binding signals have been identified, most notably in the related rotaviruses. NSP3 binds a linear sequence found at the 3' end of all rotavirus RNA segments (Poncet *et al.*, 1994). Other linear RNA binding proteins include the T4 regA protein (Draper, 1995) and the Lupus antigen (Stefano, 1984). However all of these linear signals are found at the end of an RNA molecule. NSP3 and the Lupus antigen recognise a sequence at the 3' end while T4 regA recognises a signal at the 5'end. NS2 on the other hand, recognises an aptamer that occurs at different locations within different RNA molecules. This unique feature may provide a mechanism by which NS2 can differentiate between various segments, facilitating the correct packaging of only one copy of each segment into every virion.

Other possible roles for NS2 include the sequestration of viral RNA for assortment and packaging by some other protein, or as part of the replicase complex. The former seems more likely given that the sites of viral assembly, the viral inclusion bodies (VIBs), are composed of NS2, although the latter cannot be ruled out.

Chapter 5

FUNCTIONAL INTERACTIONS OF NS2 WITH RNA AND PROTEINS

5.1 Introduction

The interaction of proteins with RNA *in vivo* have a variety of functions. These include the control of gene expression (Marello *et al.*, 1992, Williamson *et al.*, 1995) and the packaging of viral genomes (Pickett & Peabody, 1993, Wang *et al.*, 1994). Some proteins can function in both of these roles (Pollack & Ganem, 1994) or can undergo conformational changes on binding RNA that allow them to perform additional roles (LeCuyer *et al.*, 1995). In the case of the dsRNA bacteriophage ϕ6, the packaging of ssRNA of particular sizes is dependent on the packaging of another segment causing an expansion of the procapsid (Qiao *et al.*, 1997). It appears that the packaging of the whole genome is closely linked to second strand synthesis and the signalling involved may correlate with conformational changes in other proteins of the procapsid.

Protein-protein interactions are also essential, not only in viral assembly (Gibson, 1996, Johnson, 1996, Roy, 1996b) but also in the control of transcription and replication (Lai *et al.*, 1994, Johnston *et al.*, 1996, Veschambre *et al.*, 1997). The inhibition of host-cell protein synthesis in virus-infected cells may rely on protein-protein interactions although the state of phosphorylation can also play a role (Duncan, 1990, Zhang *et al.*, 1994, Bresnahan *et al.*, 1996, Zoll *et al.*, 1996). Host-cell shutdown is also a feature of orbiviral infections although the mechanism is unknown (Huismans, 1971, Huismans, 1979). In research presented at a recent conference it has been proposed that interactions between a rotavirus non-structural protein and the translation initiation factor eIF4G may be responsible for the shut down of cellular protein synthesis (Poncet *et al.*, 1997b).

The generally accepted role of NS2-containing VIBs as the site of viral assembly and the observation of viral proteins closely associated with VIBs suggests that protein-protein interactions are likely to occur between NS2 and other viral proteins. With regard to cellular proteins, a preliminary study employing BTV NS2 in the yeast two-hybrid system detected over 1000 interactions (Andrew Beaton, personal communication). While it is highly likely that a significant number of these interactions are false positives, interaction of NS2 with cellular proteins is probable and these interactions are being investigated as part of a separate project.

While the RNA-binding capabilities of NS2 have been recognised and characterised, this does not preclude additional roles for NS2 in replication and assembly. Active replicase complexes have not yet been identified in BTV and the components of such a complex are not known. NS2 most resembles the rotavirus protein NSP2 which has been shown to interact with VP1, the viral RNA-dependant RNA polymerase (Kattoura *et al.*, 1994). In addition monoclonal antibodies against NSP2 have been used to immunoprecipitate active replicase complexes containing VP1, VP2 and VP6 from rotavirus infected cells (Aponte *et al.*, 1996).

In order to shed some light on the function of NS2 in the viral lifecycle an attempt has been made to characterise NS2 in terms of its effect on translation and interaction with other viral proteins. In this Chapter I shall present data showing that NS2 can down-regulate the translation of BTV RNA and can interact with the viral polymerase VP1.

5.2 Results

5.2.1 NS2 specifically inhibits the translation of BTV RNA

As a number of RNA binding proteins have an effect on translation (Ranjan *et al.*, 1993, Standart & Jackson, 1994, Wolffe, 1994, Sommerville & Ladomery, 1996b) the effect of NS2 on *in vitro* translation reactions was investigated. The approach used initially was to set up *in vitro* transcription-translation reactions containing either BTV M6 cDNA or β-galactosidase cDNA. Segment M6 was selected as it encodes for NS1 which forms tubules in infected cells. NS1 does not interact with RNA and therefore could not interact with RNA in the reaction. Transcription-translation reactions were performed as recommended by the manufacturers (Single Tube Protein System 2, Novagen) except that NS2, in various amounts, was added at the start of the reactions. The transcription part of the reaction was carried out at 30°C for 30 mins. The translation components were then added along with ^{35}S-methionine and the reactions incubated at 30°C for 60 mins. The reaction products were analysed by SDS-PAGE and autoradiography (Fig 5.1). It can be seen that by adding increasing amounts of NS2 to the transcription-translation reaction a reduction in the amount of BTV specific product (NS1) formed was observed (Fig 5.1, lanes 6-9). This reduction did not occur when the reaction was programmed with the β-galactosidase gene (lanes 1-4) indicating that the specificity of the inhibition is for BTV. The amounts of NS2 in the tubes ranged from 1.7-167ng/μl with respect to the volume in the transcription reaction and 0.4-40ng/μl with respect to the final volume in the translation reaction.

This inhibitory effect did not appear to be a gradual effect as there was a sharp drop-off of NS1 production at the highest concentrations of NS2 used. The fact that β-

galactosidase production was unaffected suggests that NS2 was not inactivating a component of the translation reaction and that NS2 was interacting with a BTV specific component. As the RNA was the only component that was BTV specific it was reasoned that this inhibition was occurring at the RNA level.

To extend the observations on this effect, a similar experiment was performed with the addition of NS2 to rabbit reticulocyte lysate translation reactions programmed with either luciferase or BTV M6 RNA. The M6 RNA was produced by transcription using a Ribomax RNA transcription kit (Promega) as described in the materials and methods and luciferase RNA was supplied as a control with the rabbit reticulocyte lysate reagents (Promega). The same amounts of NS2 as used in the previous experiment were added to the translation reactions and incubated at 30°C for 60 mins. The results again indicated that NS2 can inhibit the translation of BTV RNA (Fig 5.2, lanes 5-8) while luciferase production was unaffected (Fig 5.2, lanes 1-4).

As both RNA and NS2 were added in this second experiment it was possible to determine the ratio of RNA-protein in the reaction. Each reaction contained 50ng of either BTV M6 or luciferase RNA and either 10, 100 or 1000ng of NS2. This gave a ratio of RNA:NS2 of either 5:1, 1:2 or 1:20. Inhibition was observed at the highest concentration of NS2 or a ratio of 1:20. However, in experiments where a 10-fold lower concentration of RNA was used, giving ratios of 1:2, 1:20 or 1:200, inhibition was still observed at the highest NS2 concentration used. This was at a ratio of 1:200 indicating that it was not the ratio of RNA-protein that was causing the inhibition.

It seems likely that it is the multimerisation of NS2 at a particular concentration, irrespective of the amount of RNA present, that is responsible for the inhibition of translation. If an RNA molecule is bound to NS2 when it multimerises to form a VIB, that RNA molecule will be unavailable for translation.

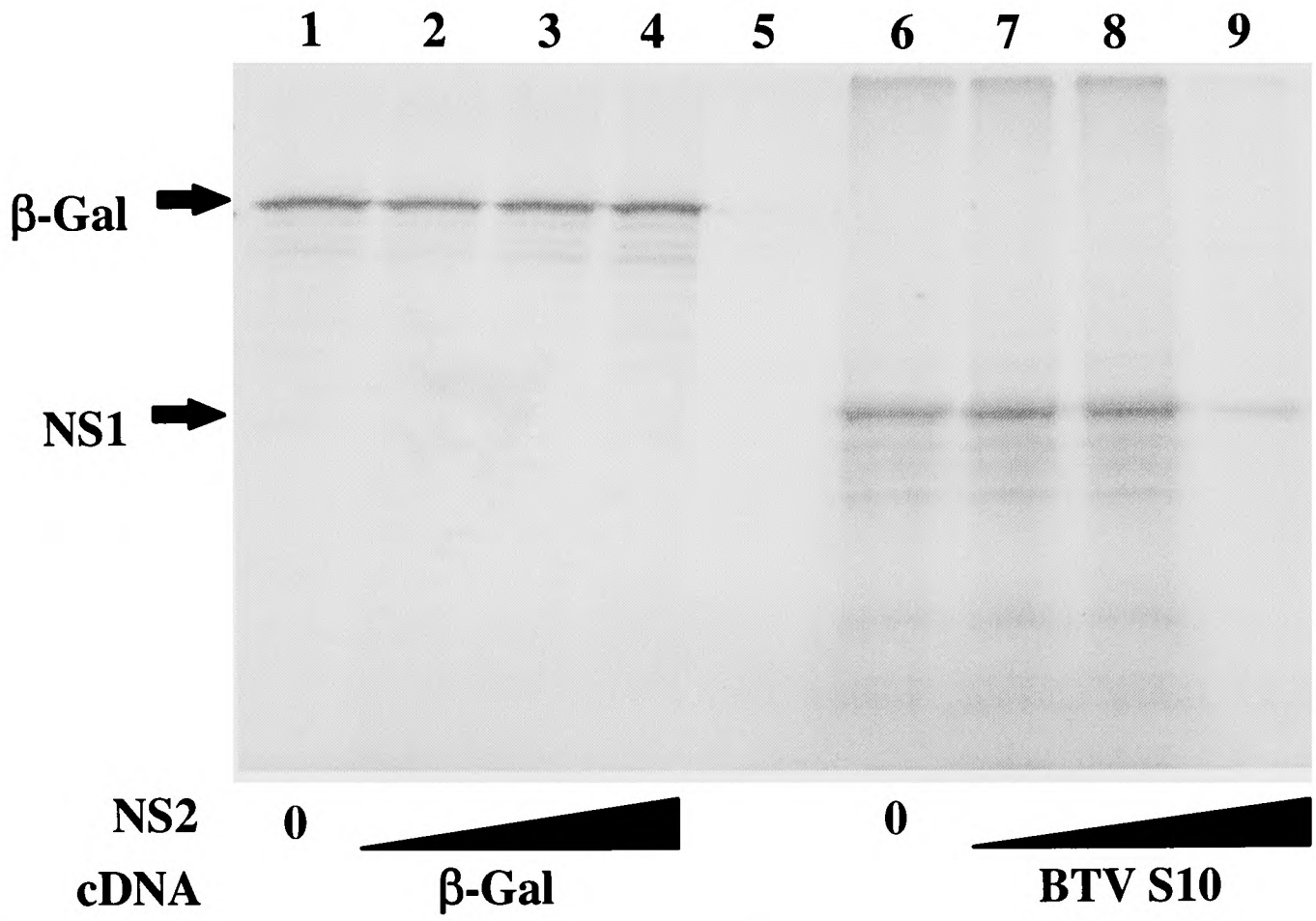

Fig 5.1: Effect of NS2 on transcription-translation. Reactions programmed with either an *E.coli* β-galactosidase gene or BTV segment 6 were incubated at 30°C with or without NS2. Lane 1-4: β-gal with 0, 10, 100, or 1000ng NS2, Lane 5: reaction with no DNA and 1000ng NS2. Lane 6-9: BTV segment M6 with 0, 10, 100 or 1000ng NS2. The production of NS1, the product of segment M6 was inhibited at the highest level of NS2 used (lane 9)

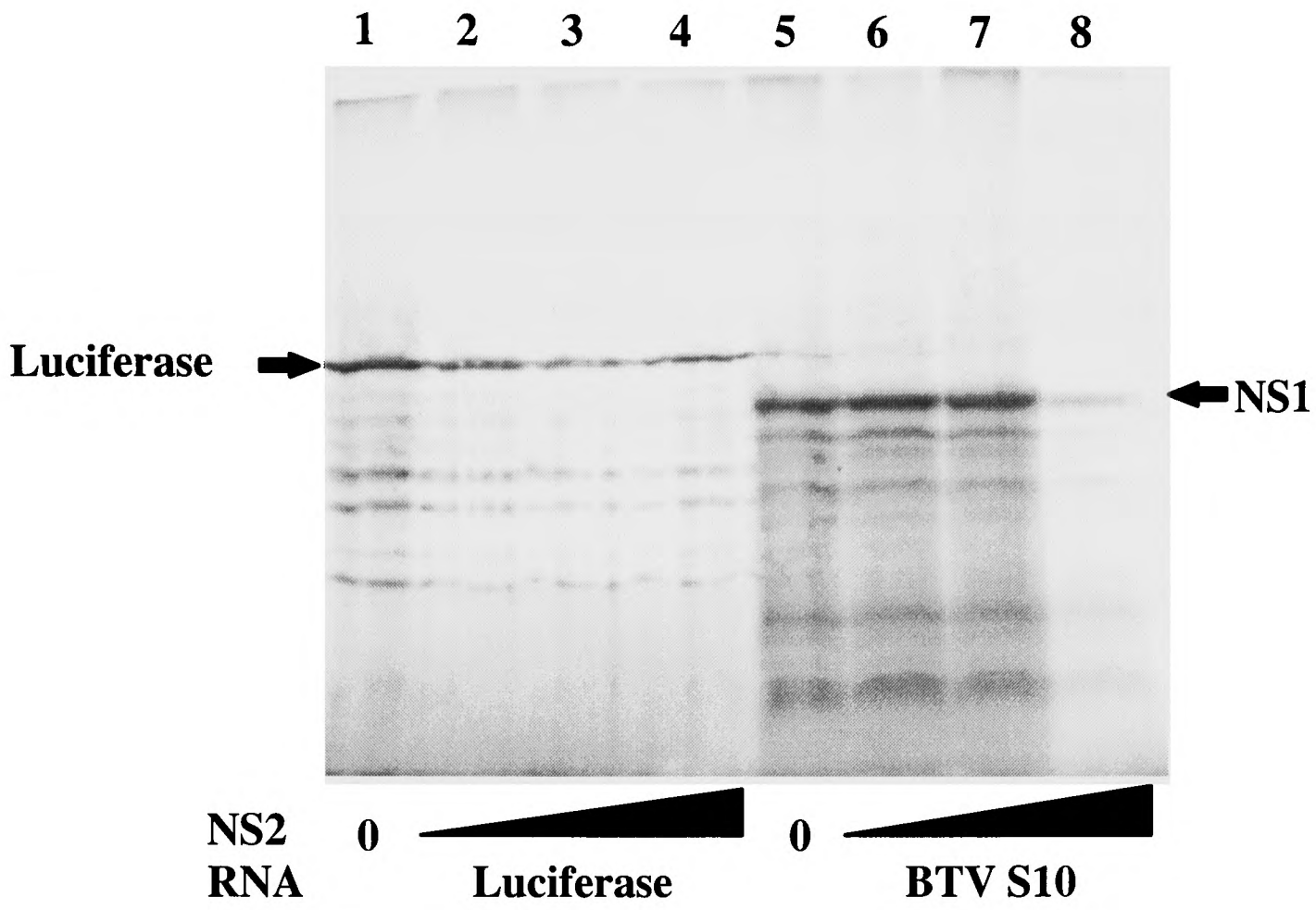

Fig 5.2: Effect of NS2 on translation. Rabbit reticulocyte lysate reactions were set up with either luciferase RNA and 0, 10, 100 or 1000 ng NS2 (lanes 1-4) or BTV segment M6 RNA and 0, 10, 100 or 1000 ng NS2. The production of NS1 was specifically inhibited (lane 8)

5.2.2 Conformational changes in NS2 on binding RNA

The multimerisation of NS2 is a critical step in the formation of VIBs and also appears to function as a switch between translation and packaging of BTV mRNA. NS2 can bind both BTV and non-BTV RNA but it is not known whether both types of RNA are present in VIBs. The data obtained in the previous experiments would suggest that only BTV RNA is internalised in VIBs. It may be possible that the specific interaction of BTV RNA with NS2 induces a conformational change that promotes the formation of VIBs.

CD spectroscopy was used to investigate the conformational changes in NS2 on binding RNA. This approach has been used to characterise conformational changes in both proteins and RNA on interacting with each other (van der Graaf & Hemminga, 1991, Tan & Frankel, 1994, Schultz *et al.*, 1996). RNA molecules absorb strongly above 250nm while the important wavelengths for the determination of protein structure are below 250nm. This makes it relatively easy to separate the contributions of RNA and protein to the overall spectra.

As mentioned in Chapter 3, CD is very sensitive to certain substances that absorb highly in the far UV region (Schmid, 1997). Tris buffers and chloride ions are generally avoided, while solutions containing phosphates, fluorides and perchlorates work well. Therefore the first step performed was to develop a buffer that would function in both RNA-binding and CD spectroscopy. These buffers were based on the RNA-binding buffer used throughout this thesis. Various components were replaced or included at different concentrations in an attempt to determine which were required for RNA-binding. The buffers used are presented in Table 5.1.

Table 5.1: Buffers used in gel-shift assay and for CD spectroscopy.

RNA-binding Buffers (1x)	
RNA-binding buffer A 10mM HEPES pH7.8 40mM KCl 1mM EDTA 1mM DTT 5% glycerol	**Buffer 1** 10mM HEPES pH7.8 70mM NaCl 0.1mM EDTA
Buffer 2 20mM HEPES pH7.8 150mM NaCl	**Buffer 3** 20mM HEPES pH7.8 50mM KCl 5mM $MgCl_2$
Buffer 4 5mM HEPES pH7.8 25mM KCl 2mM $MgCl_2$	**Buffer 5** 10mM HEPES pH7.8 40mM KCl 1mM EDTA
Buffer 6 10mM HEPES pH7.8 40mM KCl	**Buffer 7** 10mM HEPES pH7.8 40mM KF 1mM EDTA
Buffer 8 10mM HEPES pH7.8 40mM KF	**Buffer 9** 25mM NaPi pH7.8 40mM NaCl
Buffer 10 10mM NaPi pH7.8 40mM KF	**Buffer 11** 10mM NaPi pH7.8 200mM KF
Buffer 12 25mM NaPi pH7.8 40mM KF	**Buffer 13** 25mM KPi pH7.8 40mM KF
Buffer 14 10mM KPi pH7.8 200mM KF	**Buffer 15** 25mM KPi pH7.8 40mM KF

To test for RNA-binding, gel-shift analysis in 1% agarose gels was used as outlined in the materials and methods. Approximately 4μg of NS2 and 10,000 cpm of p10S10 RNA (see Fig 4.9) was mixed with 2μl of each buffer (10x conc.) in a total reaction volume of 20μl. The reactions were incubated at room temperature for 30 mins. The RNA-protein complexes were resolved by electrophoresis and the gels dried under vacuum. The complexes and free RNA were visualised by autoradiography. The best binding was obtained with buffer 3 (Fig 5.3). Buffers 5, 6, 7, 8, 10 and 13 also worked as RNA-binding buffers but with greatly reduced effectiveness.

These buffers were then tested to determine their suitability in CD spectroscopy. Spectra were obtained under the conditions used in Chapter 3 over a wavelength range of 200-250nm. As shown in from Fig 5.4A the only buffers that did not exceed a voltage of 500mV across the photovoltaic cell were buffers 10 and 13. These buffers were checked over the extended wavelength range of 190-250nm and again performed well (Fig 5.4B). However the voltage was expected to increase when all the reaction components were combined as every component contributes to the absorbance. This could be counteracted by restricting the wavelength range or lowering the concentration of reagents in the reaction.

Three spectra are required in order to detect a conformational change in an RNA-binding protein or peptide. The spectra of RNA only, protein only and RNA and protein together are obtained. The spectra of NS2 only was obtained in Chapter 3 but in a different buffer. Once all three spectra are available the spectra of the RNA only is subtracted from the spectra of the RNA-protein complex and the resultant spectra

compared with the protein only spectra. These manipulations were performed on the PC attached to the CD spectrophotometer with software supplied with the machine.

Spectra were obtained for NS2 complexed to p10S10 RNA by mixing 10μg NS2 and 10μg p10S10 RNA with 10x buffer 13 in a total volume of 200μl, incubating at room temperature for 30 mins and then measuring the CD spectra between 200 and 300nm. The amount of NS2 and RNA that could be used together was limited by the voltages generated across the detector when protein, RNA and buffer were combined. NS2 and S10 spectra were recorded in 1x buffer 13. Sixteen scans were performed for each spectrum. Figure 5.5A shows the spectra obtained for p10S10 RNA and NS2-p10S10. The molar ellipticities detected were quite small as the concentrations of protein and RNA used were low. Nevertheless some differences could be observed (Fig 5.5B) indicating that a conformational change does occur. However due to the small differences recorded it is not possible to conclusively interpret these changes. The poor results are most likely due to the low amount of RNA-binding obtained in buffer 13 combined with the use of low concentrations of NS2 and RNA in the determination of the CD spectra. The assay could be improved by making further buffer changes that would allow more protein and RNA to be used.

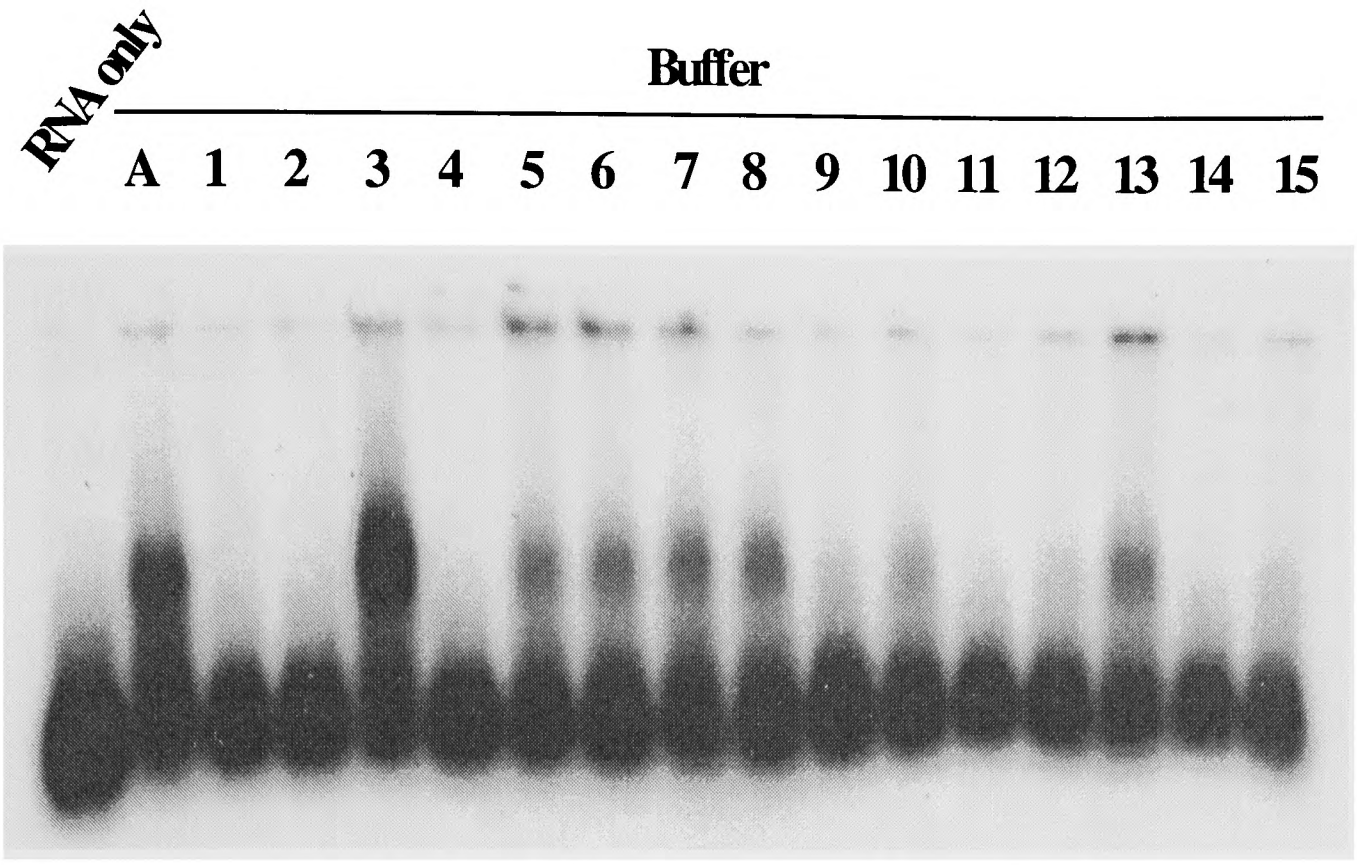

Fig 5.3: Gel-shift analysis of NS2 and p10S10 in various buffers. Approx. 4μg of NS2 and 10,000 cpm of p10S10 RNA was mixed with 2μl of each buffer (10x conc.) in a total reaction volume of 20μl. The reactions were incubated at room temperature for 30 mins and resolved on a 1% agarose gel.

A

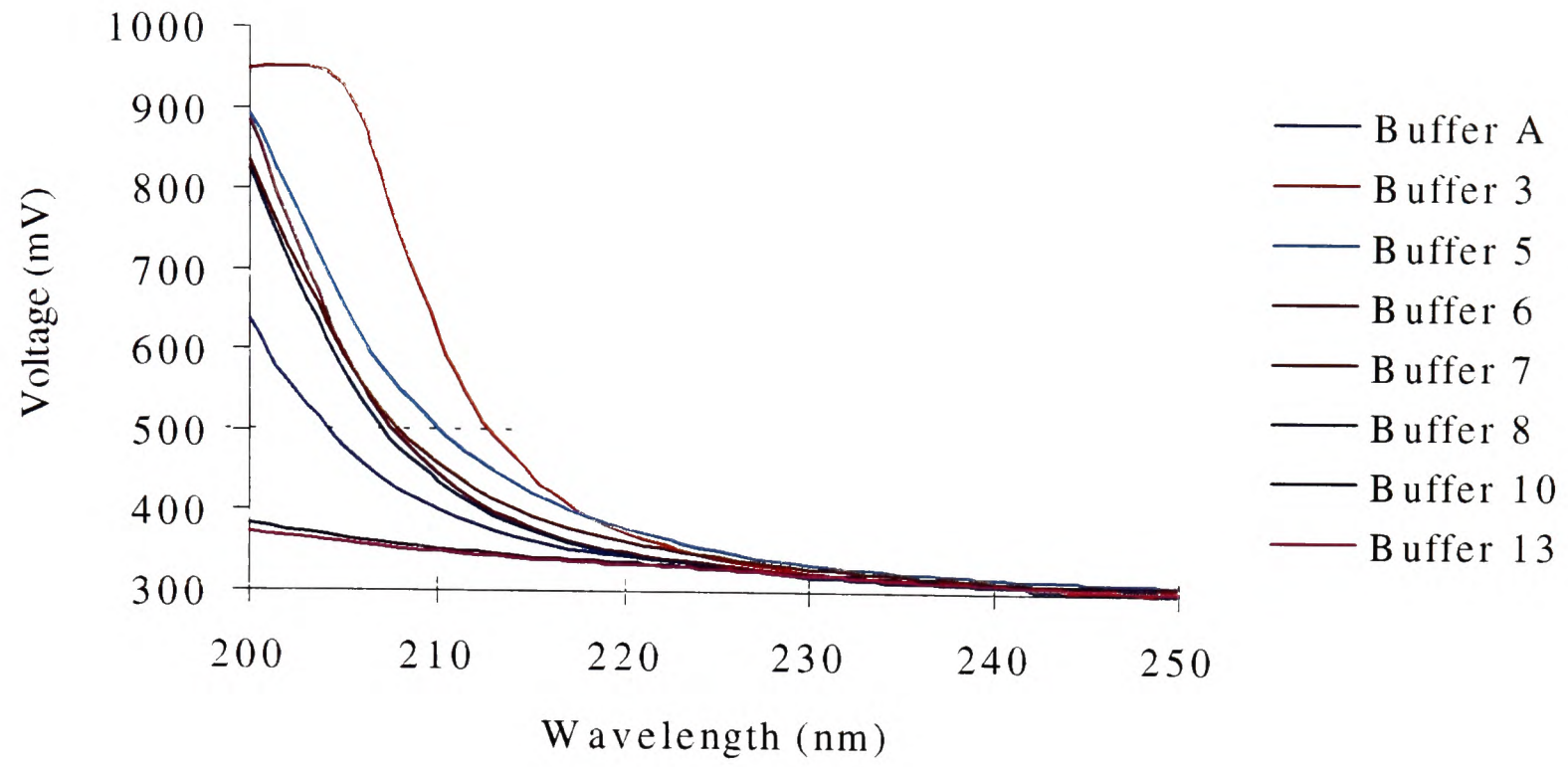

B

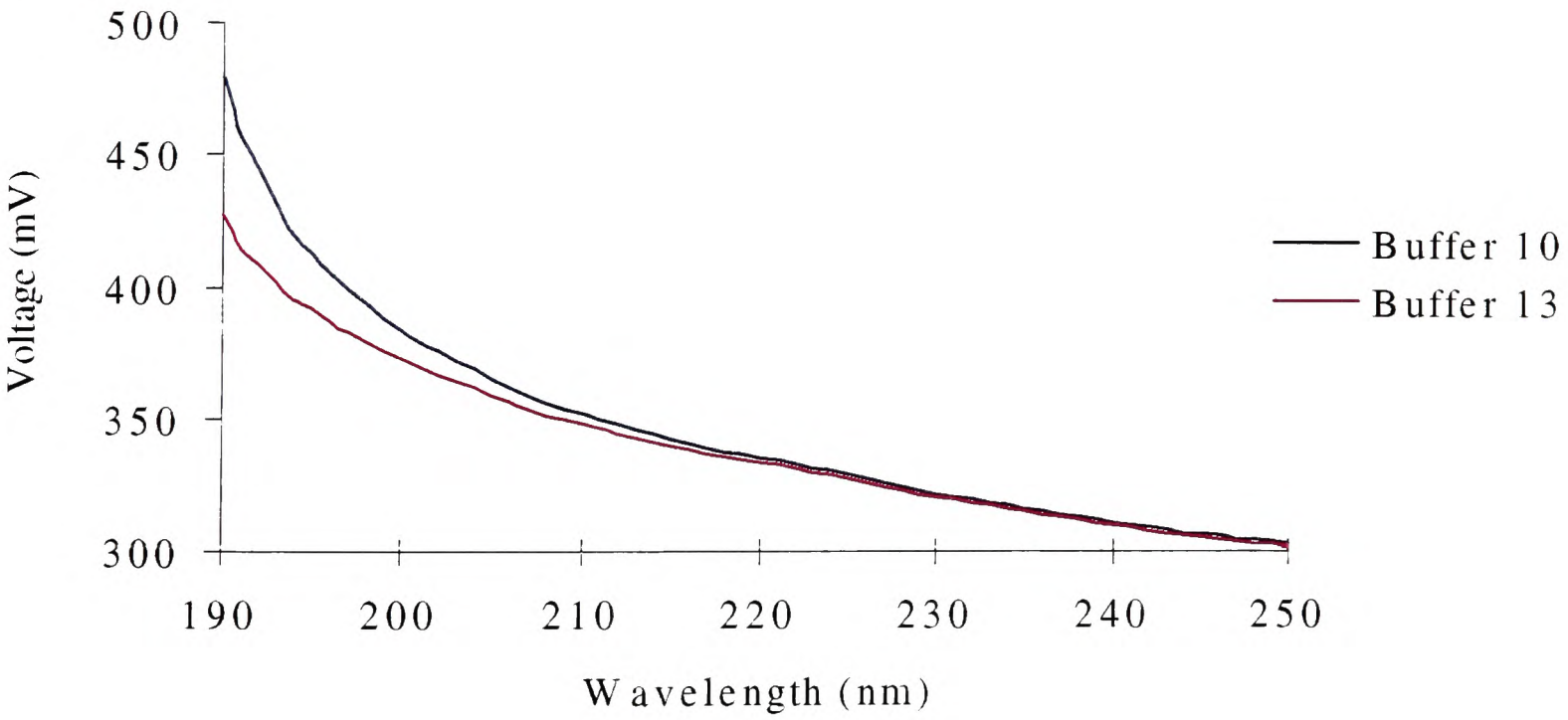

Fig 5.4: Absorbance of buffers. The voltage across the photomultiplier was monitored to determine the suitability of the buffers for use in CD spectroscopy. **A**: 200-250nm range. **B**: 190-250nm range.

A

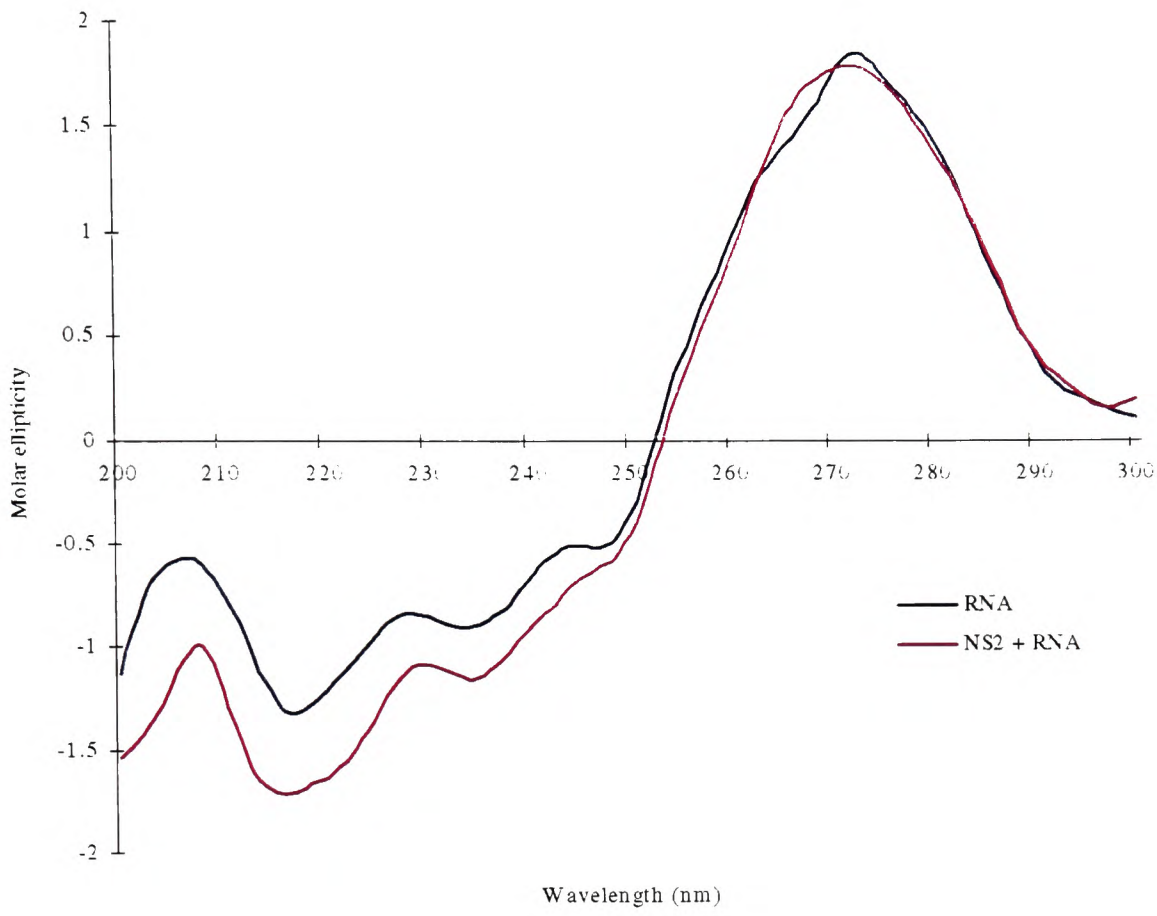

B

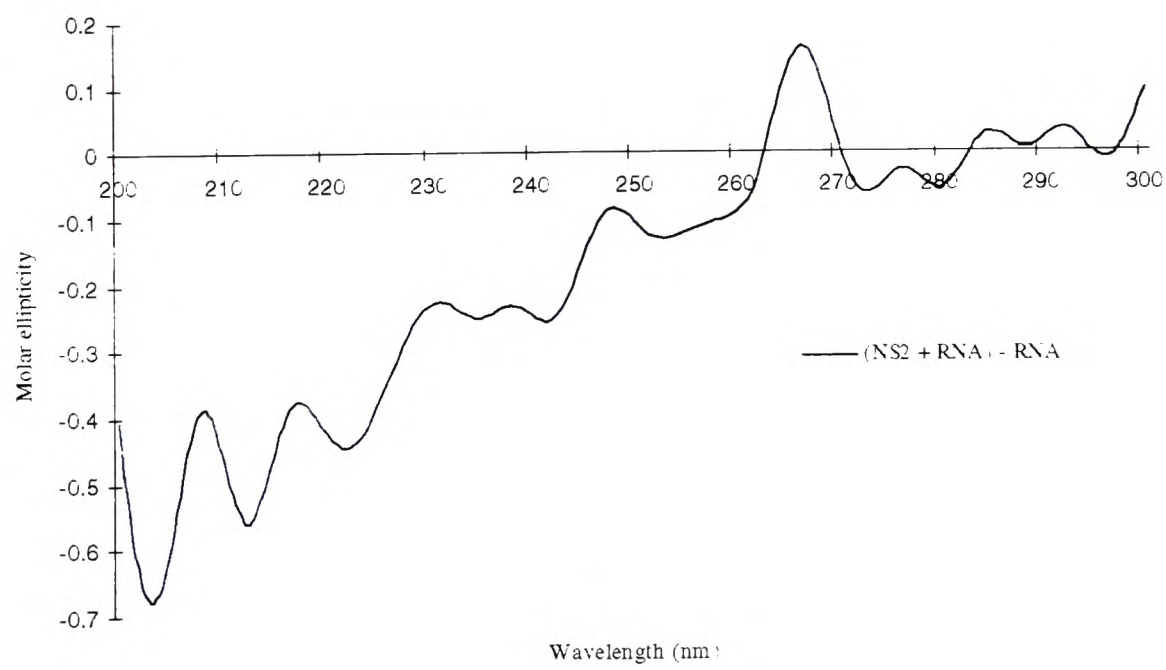

Fig 5.5: CD spectra of NS2 and p10S10 RNA. **A**: The spectra of p10S10 RNA either separately or complexed with NS2 was obtained by averaging over 16 scans from 200-300nm. **B**: Manipulation of spectra in A to give a spectrum for NS2 bound to RNA. Molar ellipticity (deg cm^2 $dmol^{-1}$) vs wavelength (nm) was plotted.

5.2.3 NS2 interacts with VP1

Another method by which NS2 could exert a functional effect in viral replication is through interaction with other proteins in infected cells. The approach selected to investigate the interaction of NS2 with other viral proteins was one that used chemical crosslinkers to stabilise protein-protein interactions (Mattson *et al.*, 1993). The crosslinkers used were cleavable, allowing proteins to be crosslinked, immunoprecipitated, cleaved and separated by SDS-PAGE. The methods used were modified from protocols supplied by the manufacturers of the crosslinkers, Pierce Chemical Company (Anon., 1992) and those found in Molecular Virology: A practical approach (Paterson & Lamb, 1993).

Initially the interaction of NS2 with the minor core protein and RNA polymerase VP1 and with the core protein VP3 was investigated. Recombinant baculoviruses expressing either VP1 or VP3 and VP7 were used to co-infect *Sf* cells with AcBTV10.8, the recombinant baculovirus expressing NS2. Cells were infected in the following combinations: mock, VP1 only, VP3 & VP7 only, NS2 only, NS2 & VP1 and NS2, VP3 & VP7, and labelled with ^{35}S-methionine. Cells were lysed in hypotonic buffer (3mM HEPES pH7.8, 3mM NaCl, 0.5mM $MgCl_2$) and clarified by centrifugation. Expression was checked by analysing a sample of the mock and co-infected cells on an SDS-PAGE gel followed by fluorography or autoradiography (Fig 5.6, lanes 1-4). Cross-reactivity with the NS2 polyclonal antisera was also checked by imunoprecipitating an aliquot of the lysates from mock-infected cells or cells infected with VP1, VP3 & VP7 or NS2 baculoviruses (Fig 5.6, lanes 5-8). Cross-reactivity was observed between the NS2 antisera and VP3 & VP7 proteins (lane 7). VP3 does not

remain in solution very well and this observation may also be due to VP3 & VP7 precipitating during the immunoprecipitation procedure.

The co-expressed proteins were crosslinked with dithiobis(succinimidylpropionate) (DSP), immunoprecipitated, cleaved and resolved by SDS-PAGE (Fig 5.7). Even without crosslinker, an interaction between VP1 and NS2 can be seen (lane 3). Due to the cross-reactivity of the antisera with VP3 & VP7 the detection of VP3 & VP7 in lane 6 is probably not representative of a co-immunoprecipitation. A band migrating at about 84kDa could possibly be a dimer of NS2 as a similar sized band has been reported previously when NS2 was analysed under non-denaturing conditions (Uitenweerde *et al.*, 1995).

Similar experiments were performed in BTV-infected BHK cells to determine whether the interaction of NS2 with VP1, or other proteins, could be detected. Tissue culture flasks ($80cm^2$) were infected with BTV-10 and labelled with 100μCi ^{35}S-methionine at 18 hpi. Cells were detached with 50mM EDTA in PBS, washed and lysed with 3ml hypotonic buffer. Expression was checked by SDS-PAGE and autoradiography. After crosslinking 100μl aliquots of the supernatants were immunoprecipitated with polyclonal antibodies against BTV VP1, VP3, VP4, VP6 and NS2, and against BLV-Gag. Following SDS-PAGE the labelled proteins were visualised by autoradiography or fluorography (data not shown). Fig 5.8 removed

The performance of the polyclonal antibodies in immunoprecipitation from BTV-infected BHK cells was poor. The only antibodies to immunoprecipitate their respective proteins were the antiVP3 and antiNS2 antibodies. No co-immunoprecipitation of other proteins was observed with these antibodies, with or without the use of DSP as a crosslinker.

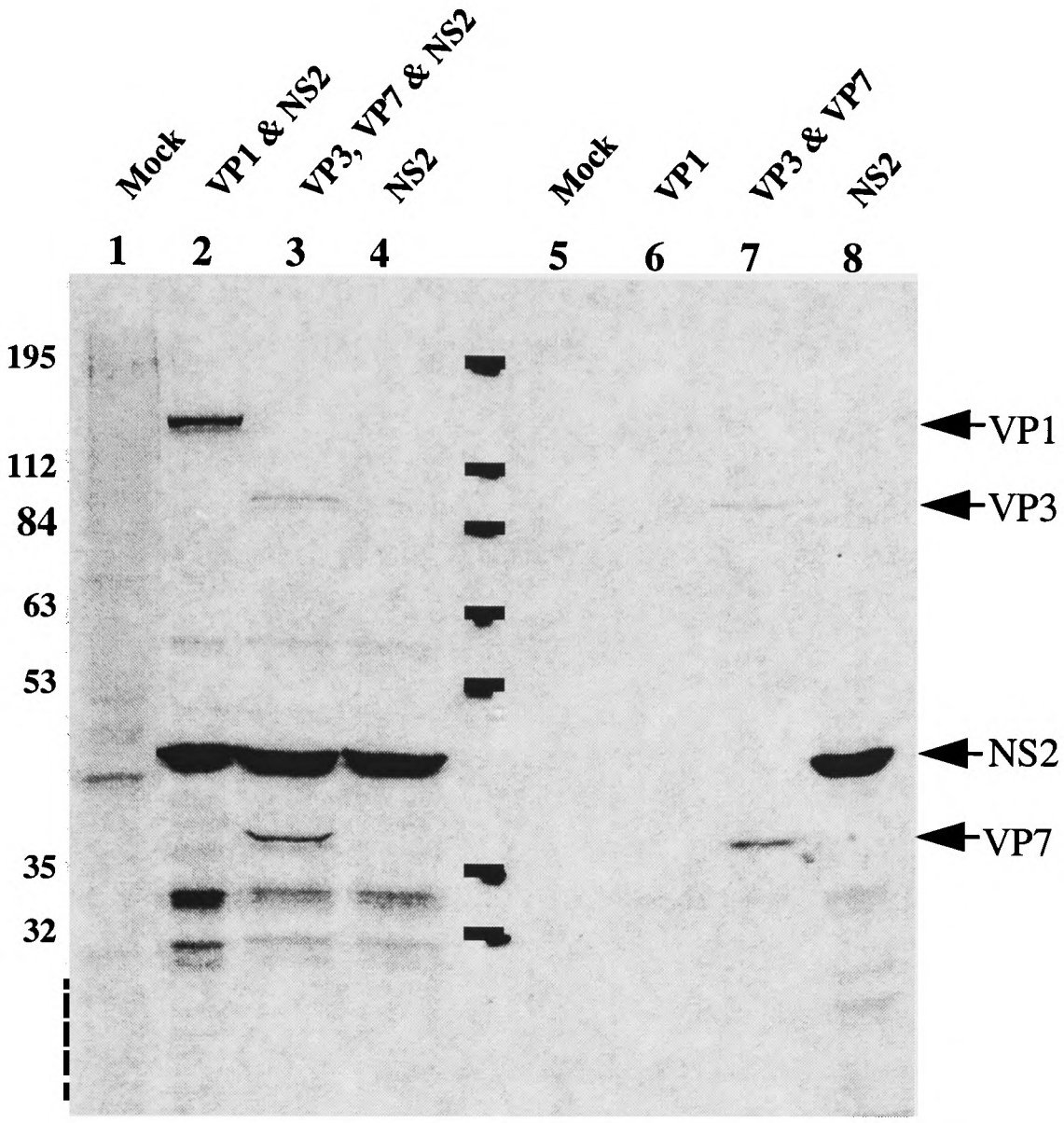

Fig 5.6: Expression and reactivity of baculovirus expressed VP1, VP3, VP7 and NS2 with NS2 antisera. Lanes 1-4: expression in mock infected , VP1 and NS2 co-infected, VP3, VP7 and NS2 co-infected and NS2 infected *Sf* cells respectively. Lanes 5-8: reactivity of mock infected, VP1 infected, VP3 & VP7 infected and NS2 infected cell lysates with rabbit-anti NS2 antisera by immunoprecipitation. The location of VP1, VP3, VP7 and NS2 is indicated.

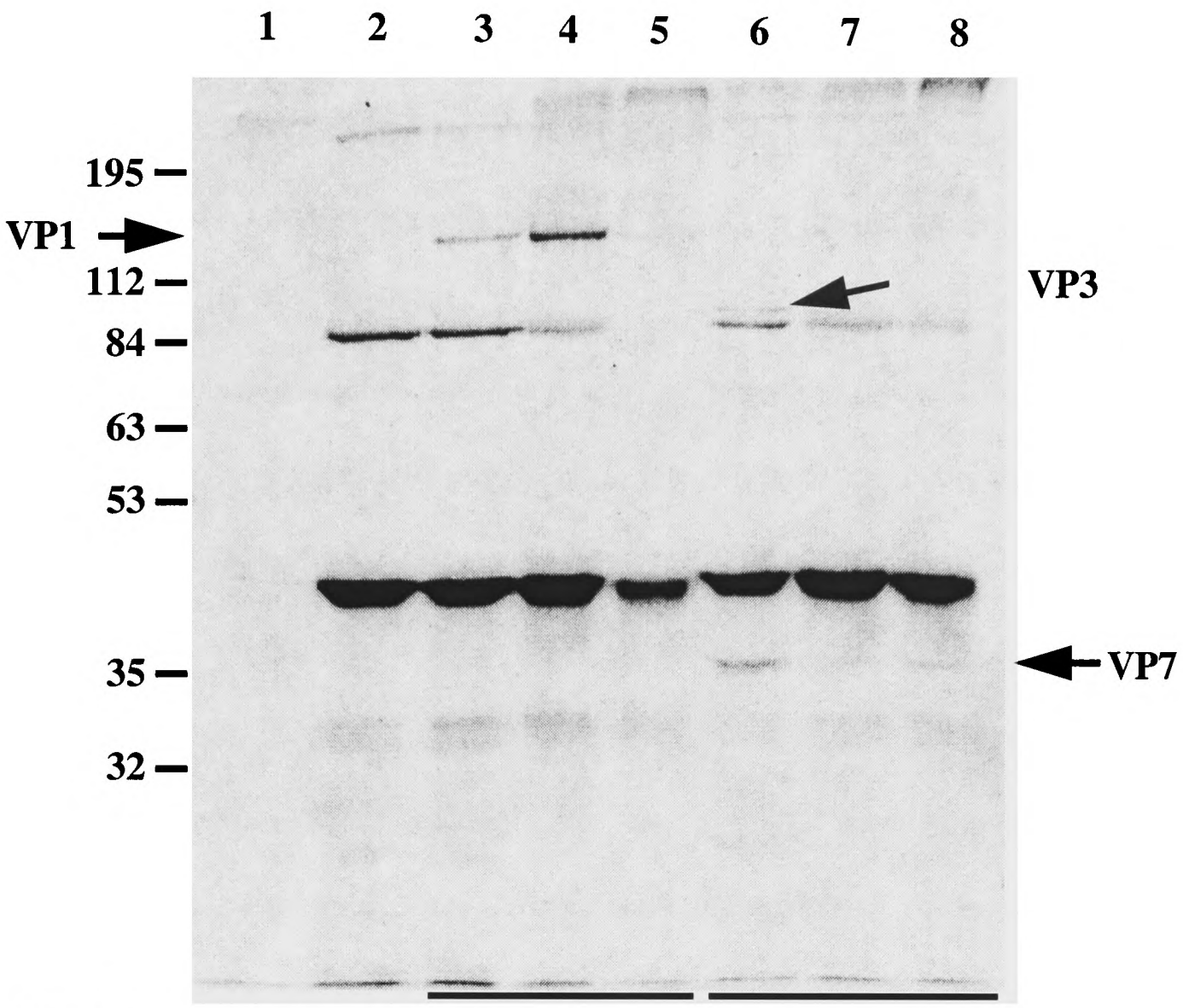

Fig 5.7: Co-immunoprecipitation of DSP-crosslinked cell lysates. Cells were lysed in hypotonic buffer and crosslinked with the indicated amounts of DSP for 30 mins at room temperature. The crosslinking reactions were stopped by the addition of glycine to 50mM, and protein-NS2 complexes were immunoprecipitated with NS2 antisera. The location of VP1, VP3 and VP7 is indicated.

5.3 Discussion

In this chapter the function of NS2 has been investigated. Molecular biology, biophysical and biochemical techniques were used to characterise various facets of NS2 function in the BTV lifecycle.

It is apparent that NS2 can down regulate translation in a manner similar to translational masking during gametogenesis by members of the y-box family of nucleic acid binding proteins (Standart & Jackson, 1994, Sommerville & Ladomery, 1996a). These phosphoproteins bind to mRNA (Marello *et al.*, 1992) and can inhibit *in vitro* translation (Richter & Smith, 1984). In infected cells BTV cores produce mRNA which extrudes from the cores into the cytoplasm where translation occurs. VIBs are formed by the multimerization of NS2 and ssRNA is packaged along with VP1, VP4 and VP6, within a core of VP3. Second-strand synthesis occurs within these cores. As translation progresses in the cytoplasm the levels of NS2 increase. It is possible that by binding to ssRNA and multimerizing to form a VIB NS2 makes an RNA molecule unavailable for translation. It may therefore act as a control mechanism, determining whether an RNA molecule is translated or packaged depending on the amount of NS2 in the cytoplasm. This seems to be an "all or nothing" response as opposed to a gradual change. VIBs are formed by baculovirus expressed NS2 in insect cells suggesting that no other viral proteins are necessary for multimerization of NS2. The effect of the presence of a full complement of BTV RNA on the assembly efficiency or stability of VIBs is not known.

It is not known whether mRNA localisation plays a role in BTV replication. There are no reports in the literature of BTV structural proteins found free in the cytoplasm of infected cells although VP3, VP5, VP6 and VP7 have been found to be

associated with the matrix of virus inclusion bodies (Hyatt & Eaton, 1988, Roy *et al.*, 1990a, Brookes *et al.*, 1993). VP2, VP5, VP6 and VP7 were also found in virions associated with the periphery of VIBs. NS2 directed mRNA localisation could possibly be responsible for lack of free structural proteins.

A conformational change in NS2 on binding RNA remains a possibility, although further work is required to develop methods with which to characterise this. In other studies where CD has been used to study conformational changes peptides were used (van der Graaf & Hemminga, 1991, Tan & Frankel, 1994). This meant there was an effective amplification of the signals produced as only a small region of the protein was being observed. The key to using such a system to study changes in NS2 is to identify a buffer that will allow both a high degree of RNA-protein interaction and have a low absorbance in the far UV region. A similar approach could be used to detect conformational changes in proteins that interact with other molecules, for example the binding of nucleosides.

While interaction between VP1 and NS2 was observed when both proteins were expressed in insect cells, it remains to be seen whether they interact *in vivo,* i.e. in BTV-infected cells. This confirmation has been hampered by the poor performance of the available polyclonal antibodies. The production of monoclonal antibodies against purified NS2 is at an advanced stage and should be of high enough affinity to immunoprecipitate a wider range of complexes from infected cells. Nevertheless, the finding that NS2 can interact with VP1 is important. It provides further evidence that NS2 is similar to the rotavirus protein NSP2 (Kattoura *et al.*, 1992, Kattoura *et al.*, 1994) and suggests that NS2 may be a component of the replicase complex (Patton & Gallegos, 1988, Aponte *et al.*, 1996).

Although a definitive function for NS2 remains elusive, the data presented in this chapter suggests that it is involved in more than just the formation of VIBs for viral assembly. Through protein-RNA and protein-protein interactions NS2 appears to have a central role in the movement of RNA from the cytoplasm into assembling virions. This would make NS2 an essential component of any reverse genetic system, the holy grail of *Reoviridae* research.

Chapter 6

NUCLEOSIDE BINDING, PHOSPHOHYDROLASE ACTIVITY AND PHOSPHORYLATION OF NS2

6.1 INTRODUCTION

The phosphorylation and dephosphorylation of proteins is essential for cellular signal transduction. These processes are catalysed by protein kinases and protein phosphatases respectively, two groups of enzymes that have generated much interest. Kinases function by transferring a phosphate molecule from organic phosphate or a nucleoside triphosphate to either a serine, threonine or tyrosine residue. They can be conveniently divided into two groups: serine/threonine kinases and tyrosine kinases. The nucleotide donor can be either ATP or GTP. These nucleosides are bound by the nucleoside binding site of the kinase, making NTP binding absolutely necessary for kinase activity (Colburn *et al.*, 1987). Motifs for NTP binding can be identified in a variety of proteins including kinases, guanylyltransferases and helicases but there is much variation in sequence with some nucleotide binding proteins not containing a recognisable motif. A larger catalytic domain encompassing the NTP binding site has been well characterised in a number of different kinases (Hanks & Quinn, 1991). This domain is 250-300 amino acids in size and is further divided into 12 catalytic subdomains. Autophosphorylation by intramolecular reaction is also observed with protein kinases (Boni Schnetzler & Pilch, 1987). This appears to be a self-activation process where two (or more) kinase molecules interact to phosphorylate each other, leading to an increase in phosphorylating activity.

Protein kinases phosphorylate specific sites in substrate proteins and these sites can also be identified by characteristic motifs (Pearson *et al.*, 1993). These motifs are usually quite short (3-6 residues). As with NTP binding domains and kinase catalytic regions, there is no single definite phosphorylation site sequence for any specific protein kinase. Also, the identification of a phosphorylation motif is certainly

not evidence that a particular residue is phosphorylated. As more and more protein kinase sequences are studied a clearer picture may emerge of the requirements for particular kinases.

NTP binding and phosphohydrolase activity is a key feature of various enzymes. ATPase activity is required for the splicing of RNA (Schwer & Guthrie, 1992a, Schwer & Guthrie, 1992b), in transcription (Lowery & Richardson, 1977a, Lowery & Richardson, 1977b) and in helicases (Bisaillon *et al.*, 1997, Staeuber *et al.*, 1997). The capping of viral RNA transcripts is performed by a guanylyltransferase which binds and hydrolyses GTP (Mertens *et al.*, 1991, Pizarro *et al.*, 1991, Liu *et al.*, 1992, Martinez-Costas *et al.*, 1997). Apart from these enzymatic activities, NTP hydrolysis, especially ATP and GTP hydrolysis, can serve as a crucial source of energy to enable movement or conformational change in proteins or nucleic acids (Palacios *et al.*, 1996, Rodnina *et al.*, 1997). Two separate ATPase activities have been identified in reovirus cores in addition to the GTPase activity associated with the guanylyltransferase λ2 (Cleveland *et al.*, 1986, Noble & Nibert, 1997a, Noble & Nibert, 1997b). They map to the λ1 and μ2 proteins and the λ1 activity has since been shown to be associated with an RNA helicase activity (Bisaillon *et al.*, 1997).

Phosphoproteins have been identified in a wide variety of viruses (Leader & Katan, 1988). These include both structural and non-structural proteins, and their phosphorylation state has been linked to various functions including multimerisation and the assembly of transcription complexes (Montenarh & Muller, 1987, Gao & Lenard, 1995a, Gao & Lenard, 1995b). In rotavirus, the non-structural protein NSP5 is the only phosphoprotein (Welch *et al.*, 1989). Phosphoamino acid analysis of tryptic peptides revealed that it is phosphorylated at serine residues (Blackhall *et al.*, 1997).

Immunoprecipitated NSP5 was labelled after incubation with [γ^{32}P]-ATP as was recombinant NSP5 expressed in *E.coli*. Poncet and colleagues also demonstrated that NSP5 exists in multiple phosphorylated forms and can be phosphorylated after immunoprecipitation or expression in *E.coli* (Poncet *et al.*, 1997a) indicating that NSP5 is autophosphorylated. They also showed NSP5 forms dimers and interacts with NSP2. Multiple phosphorylation appears only to occur during rotavirus infection. This correlates with the localisation of NSP5 to viroplasms.

Whilst it is clear that orbivirus NS2 is a phosphoprotein (Devaney *et al.*, 1988, Thomas *et al.*, 1990), it is not entirely clear how it is phosphorylated. Autophosphorylation appears unlikely as recombinant EHDV NS2 expressed in *E.coli* is not labelled when incubated with a ^{32}P labelled phosphate donor, although it could be subsequently labelled by incubation with an insect cell extract (Theron *et al.*, 1994). This non-phosphorylated NS2 appears to have a lower affinity for ssRNA, in contrast to the findings of Thomas and colleagues who showed that *in vitro* dephosphorylated BTV NS2 can still bind NS2 with the same affinity as phosphorylated NS2 (Thomas *et al.*, 1990). Both authors show that immunoprecipitated NS2 can also become phosphorylated but speculate that this may be the result of a cellular kinase co-immunoprecipitating. In support of this hypothesis it has been demonstrated that the anti BTV-10 polyclonal antibody used by Thomas and colleagues can immunoprecipitate a protein from uninfected cell lysates that phosphorylates casein and phosvitin, two proteins used in *in vitro* kinase assays (Thomas, 1990).

During some of the early *in vivo* RNA binding studies performed by myself and Dr Norbert Staeuber we observed anomalous results when we attempted to 5'

end-label digested RNA UV-crosslinked to NS2. As both UV-crosslinked and non-crosslinked controls were becoming labelled, the most obvious explanation seemed to be that NS2 was becoming phosphorylated by the kinase. However, upon further investigation it became apparent that a simple phosphorylation of NS2 was not the answer. In this chapter I shall present results that demonstrate that NS2 binds nucleoside triphosphates and can hydrolyse them. In addition I shall present data suggesting that the cellular kinase responsible for the phosphorylation of NS2 is casein kinase II (CKII).

6.2 RESULTS

6.2.1 NS2 binds ATP

During the study of RNA-protein interactions, attempts were made to demonstrate that NS2 binds RNA *in vivo*. The method used employed UV-crosslinking to bind RNA to protein in BTV infected cells. The cells were then lysed, NS2 immunoprecipitated, excess RNA digested with T1 RNAse, and the 5' ends of the RNA labelled with polynucleotide kinase and [γ^{32}P]-ATP. This method has been successfully used in the study of rotavirus RNA binding proteins (Poncet *et al.*, 1993, Aponte *et al.*, 1996). However, the results obtained were inconclusive as non-crosslinked control samples also became labelled (Staeuber, Horscroft and Roy, unpublished results). As a kinase activity was suspected of being closely associated with NS2 even after immunoprecipitation, it was thought to be the most probable cause of the results observed.

Another possibility was that NS2 could directly bind the ATP used in the labelling reaction. To investigate this possibility an *in vitro* kinase assay was set up where partially purified NS2 (Q-sepharose column only) was immunoprecipitated with an antibody against purified recombinant NS2 and then incubated with either [γ^{32}P]-ATP or [α^{32}P]-ATP in kinase buffer. With [α^{32}P]-ATP the labelled phosphate is in the first or α position and cannot be transferred to a substrate molecule or cleaved. Following incubation of immunoprecipitated NS2 with labelled ATP, the samples were heated in sample buffer and separated on a 10% SDS-PAGE gel (Fig 6.1, lanes 1 & 2). When NS2 was incubated with [γ^{32}P]-ATP (lane 1) it became labelled, probably mainly due to phosphorylation by a co-immunoprecipitating

cellular kinase. However NS2 also became labelled, albeit to a lesser extent, when incubated with [α^{32}P]-ATP (lane 2) suggesting that NS2 can bind ATP. The fact that the protein remains labelled even after heating in sample buffer and separation on an SDS gel indicates that the interaction is stable and involves a covalent linkage (Martinez-Costas *et al.*, 1997).

To compare the amount of kinase activity associated with either partially purified or purified NS2 (three column procedure) both types of protein were incubated with [γ^{32}P]-ATP in a similar experiment (Fig 6.1, lanes 3 &4). The amount of labelling seen with purified NS2 was much less than that with partially purified NS2. There was, however, some labelling of purified NS2 which is due to NS2 binding the labelled ATP as opposed to being labelled with it. Some higher molecular weight bands were also observed (lanes 1, 3 & 4) and may be dimers of NS2. These, along with larger multimers, are occasionally seen on SDS-PAGE analysis of NS2 and their appearance may be related to the freshness of the reducing agent (β-mercaptoethanol) used in the sample buffer.

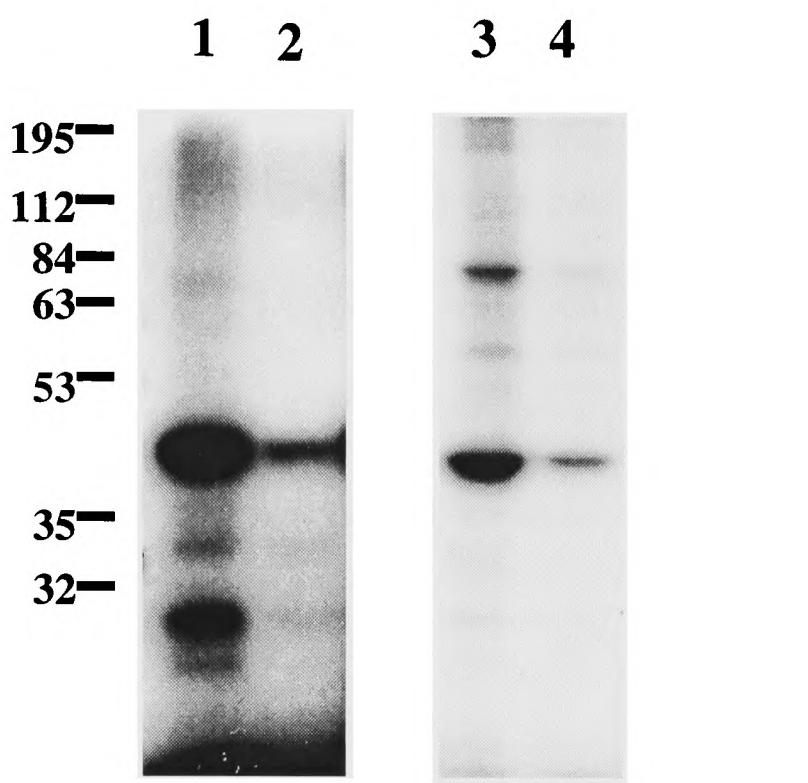

Fig 6.1: Labelling of NS2 with [α] and [γ ^{32}P] ATP. NS2 (5μg) was immunoprecipitated with anti-NS2 polyclonal antibody and incubated for 30 mins at 37°C with 1μCi [α] or [γ ^{32}P] ATP as indicated in the figure. Lanes 1-3 contained NS2 partially purified on a Q-sepharose column and lane 4 contained NS2 purified by the three column procedure described in Chapter 3.

6.2.2 NS2 has an NTPase activity

Both the helicase and guanylyltransferase activities of BTV have been localised to specific proteins so the significance of ATP binding by NS2 was not immediately apparent. Phosphohydrolase activity is one activity that relies on the ability of a protein to bind NTPs. To test for phosphohydrolase activity with NS2 a thin layer chromatography (TLC) assay was used. NS2 (1μg) was incubated at 37°C for 30 mins with 1μCi [α^{32}P]-ATP and buffers and salts as indicated in Fig 6.2. The reaction was stopped by the addition of an equal volume (10μl) 10% TCA, mixing and placing on ice. The products were separated by TLC by spotting 2.5μl of the reaction onto a PEI-cellulose plate (Merck) along with known standards and developing in a TLC tank with 0.75M KH_2PO_4 (Martinez-Costas *et al*, 1997). As indicated in Fig 6.2 NS2 can hydrolyse ATP to ADP and AMP. As observed for all other NTPases the reaction requires a divalent cation, in this case Mg^{2+}. The reducing agent DTT did not appear to influence the reaction.

This experiment was repeated using [α^{32}P]-GTP to investigate the specificity of the NTP hydrolysis. Fig 6.3 shows that NS2 can also hydrolyse GTP but only as far as GDP. Overexposure of x-ray film showed that a small amount of GMP could be detected (data not shown). These two experiments suggest that NS2 binds and hydrolyses both ATP and GTP but that there appears to be a difference in the hydrolysis of the two nucleotides.

To further characterise the binding of ATP and GTP by NS2 aliquots from the two previous experiments were analysed by SDS-PAGE. The gels were transferred to Immobilon membranes before exposure to x-ray film to reduce the excess of

background radiation observed in preliminary experiments. The results (Fig 6.4) show that NS2 binds both ATP and GTP (lanes 3, 4, 7 & 8). Without Mg^{2+} it appears that NS2 is not able to bind the nucleosides (lanes 2 &6) explaining the lack of hydrolysis seen in the TLC assays (Figs 6.2 and 6.3). It also seems as if the inclusion of DTT may have an effect on ATP binding as there seems to be an increase in binding when it is included (lane 4). However on repetition such a large difference was not always observed. The apparent difference in binding of ATP when compared with GTP was consistent when repeated and suggests that the decreased hydrolysis of GTP (Fig 6.3) as compared to ATP (Fig 6.2) may be due to a lower affinity of NS2 for GTP. In other experiments the binding of UTP by NS2 was also investigated but the level of binding was very low compared with ATP and GTP binding, even after excessively long exposure to x-ray film.

A TLC assay was also used to determine if NS2 had a preference for the divalent cation in the phosphohydrolase reaction. Identical assays were set up differing only in their divalent cation content, with either [α^{32}P]-ATP (Fig 6.5) or [α^{32}P-GTP] (Fig 6.6) as the phosphate donor. The reactions contained either $MgCl_2$, $MnCl_2$ or $CaCl_2$ at a concentration of 10mM (Fig 6.5 and 6.6, lanes 2, 3, and 4 respectively) or no divalent cation (Fig 6.5 and 6.6, lane 1). For the ATPase activity, Mn^{2+} ions gave the greatest hydrolysis of ATP (Fig 6.5, lane 3). In terms of hydrolysis to ADP, calcium and magnesium appeared to give equal results. However there seemed to be less hydrolysis to AMP with calcium than with magnesium (lanes 2 and 4). With GTP both manganese and calcium gave better results than magnesium with little difference in the low levels of GMP hydrolysed (Fig 6.6).

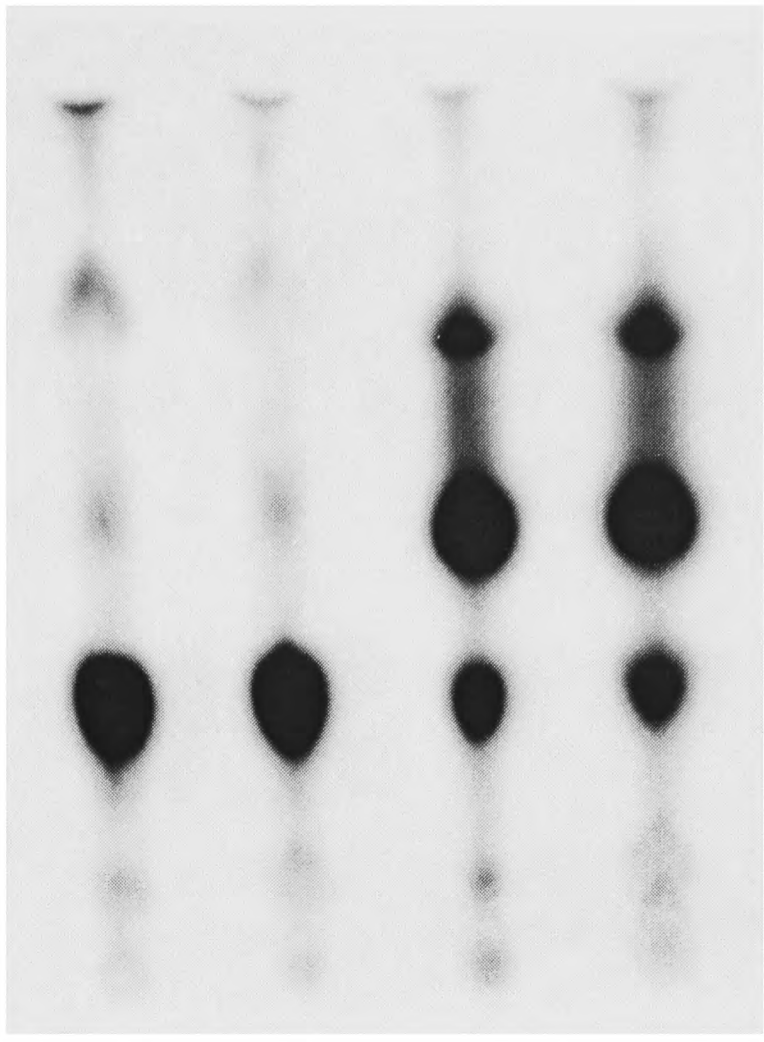

NS2 (1µg)	-	+	+	+
50mM Tris pH 8.0	+	+	+	+
10mM $MgCl_2$	+	-	+	+
1mM DTT	+	-	-	+

Fig 6.2: ATPase activity of NS2. Purified NS2 was incubated 1µCi [α^{32}P]-ATP and various reaction components as described in the figure. Reactions were performed at 37°C for 30 mins and stopped by the addition of 1 vol. 10% TCA. The products were resolved by PEI-cellulose TLC (Martinez-Costas *et al.*, 1997).

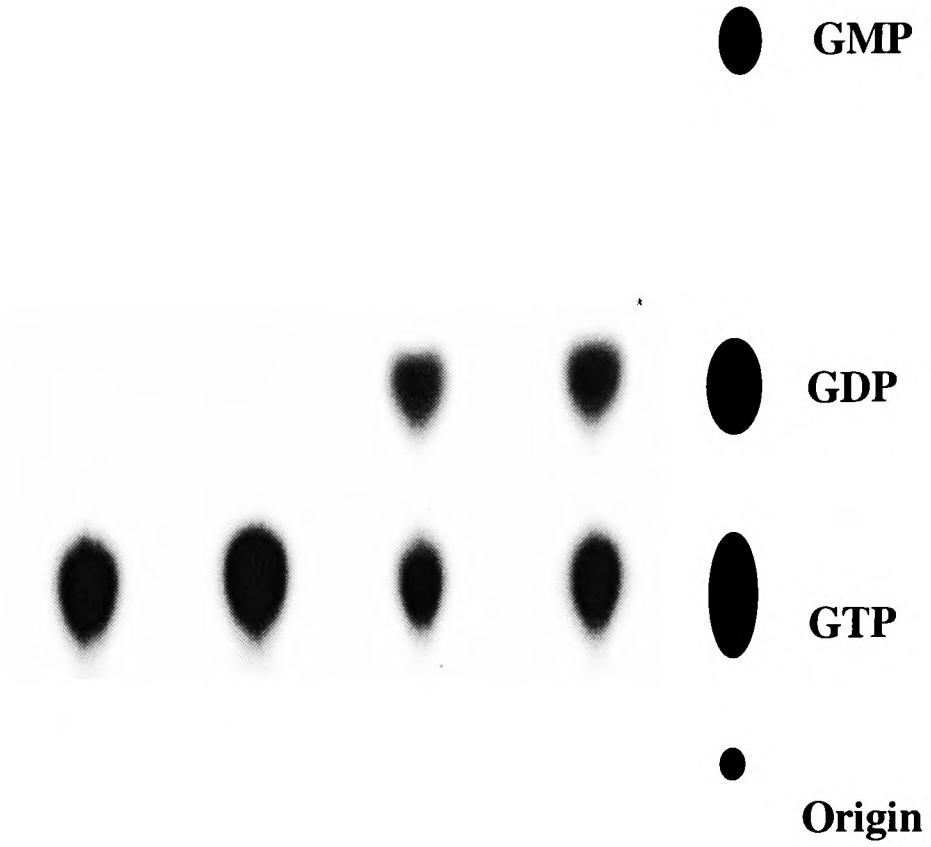

NS2 (1μg)	-	+	+	+
50mM Tris pH 8.0	+	+	+	+
10mM $MgCl_2$	+	-	+	+
1mM DTT	+	-	-	+

Fig 6.3: GTPase activity of NS2. Purified NS2 was incubated 1μCi [α^{32}P]-GTP as described in the previous figure.

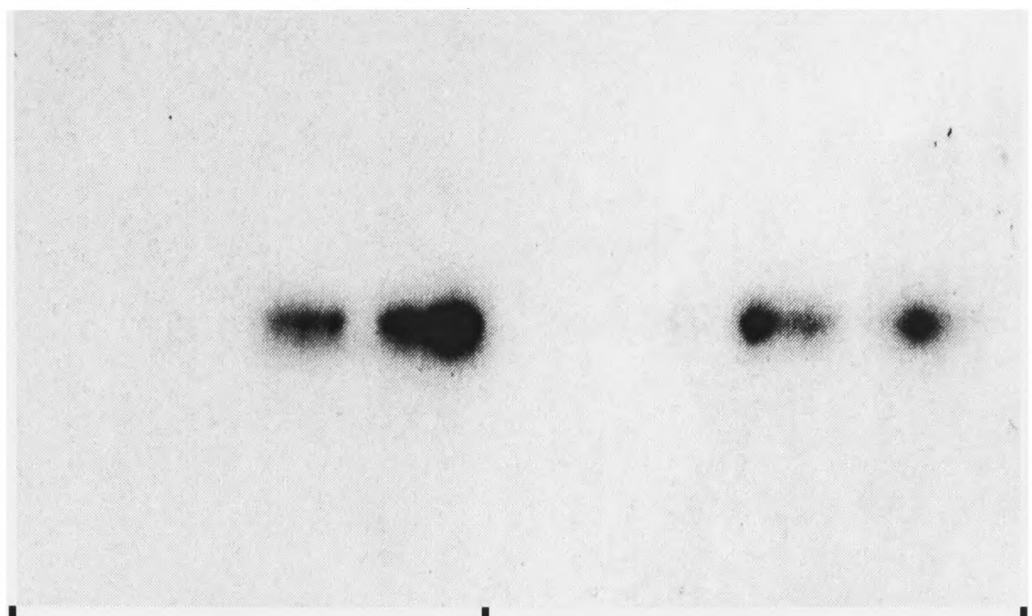

	ATP				GTP			
NS2	-	+	+	+	-	+	+	+
Tris pH 8.0	+	+	+	+	+	+	+	+
$MgCl_2$	+	-	+	+	+	-	+	+
DTT	+	-	-	+	+	-	-	+

Fig 6.4: NTP-binding by NS2. Aliquots of the stopped reactions described in Fig 6.2 and 6.3 were separated by 10% SDS-PAGE, blotted onto PVDF-immobilon membranes and labelled proteins detected by autoradiography. The concentration of added reagents is the same as in Fig 6.2 and 6.3.

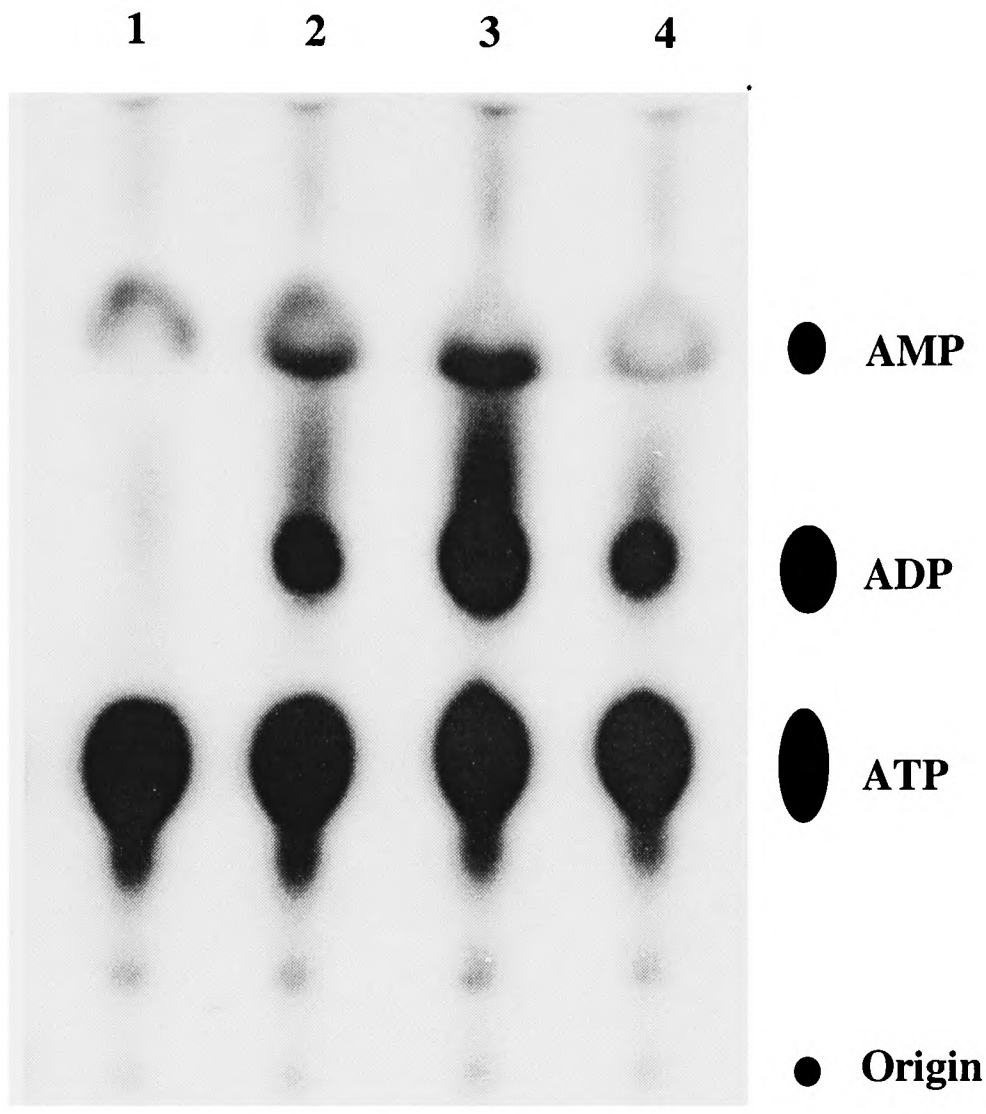

Fig 6.5: Effect of different divalent cations on the ATPase activity of NS2. Each reaction contained 0.9μg NS2, 50mM Tris pH8.0, 3μCi [α^{32}P]-ATP and 10mM $MgCl_2$ (lane 2), $MnCl_2$ (lane 3) or $CaCl_2$ (lane 4). Lane 1: no divalent cation. 1.5μl was spotted onto the TLC plate.

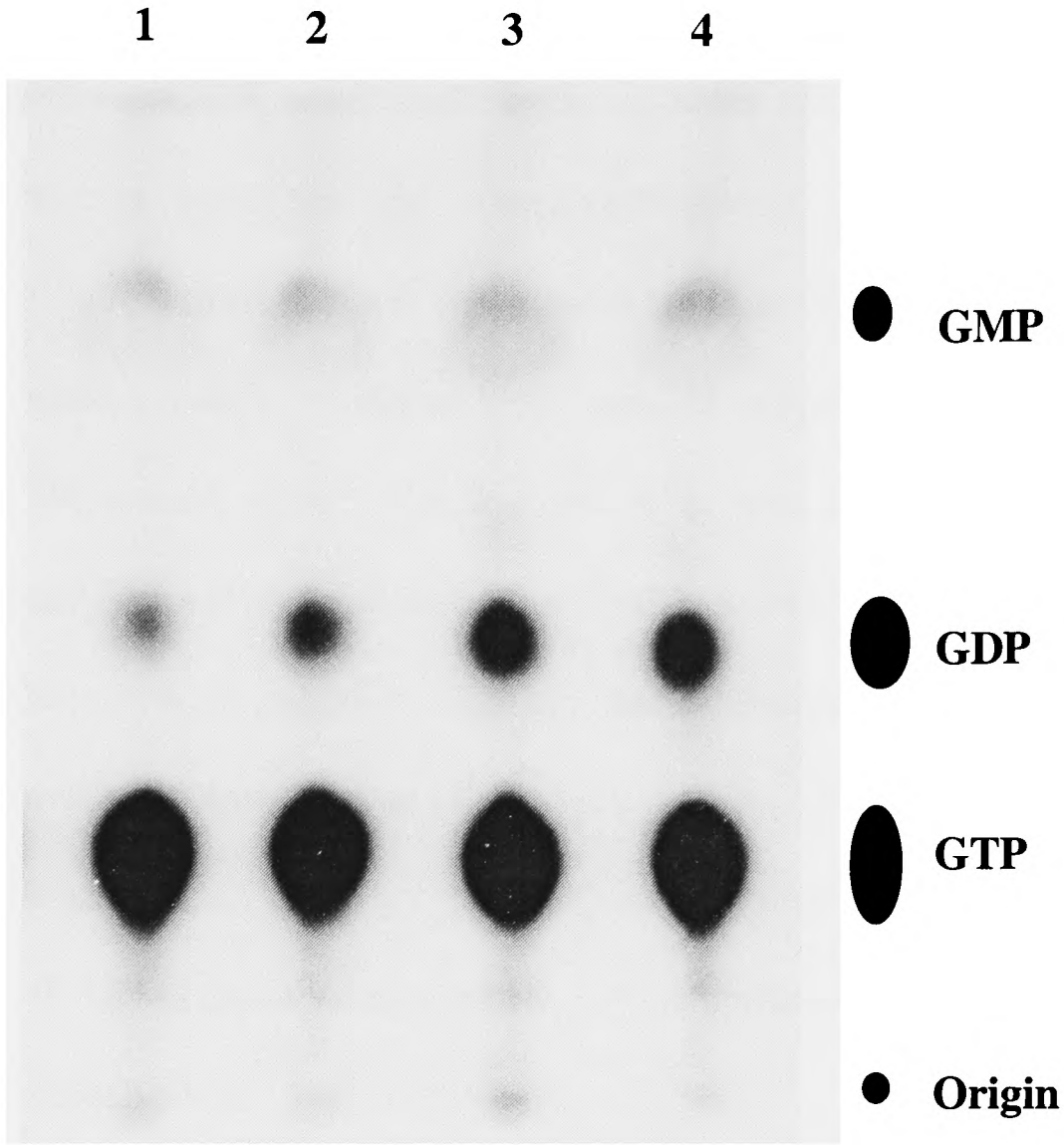

Divalent cation	**-**	**Mg^{2+}**	**Mn^{2+}**	**Ca^{2+}**

Fig 6.6: Effect of different divalent cations on the GTPase activity of NS2. Each reaction contained 0.9µg NS2, 50mM Tris pH8.0, 3µCi [α^{32}P]-GTP and 10mM $MgCl_2$ (lane 2), $MnCl_2$ (lane 3) or $CaCl_2$ (lane 4). Lane 1: no divalent cation. 1.5µl was spotted onto the TLC plate.

6.2.3 *In vivo* phosphorylation of NS2 by casein kinase II

The published evidence pointing to a cellular kinase as being responsible for the phosphorylation of NS2 is significant and autophosphorylation now seems unlikely. To determine which cellular kinase or kinases are involved in the phosphorylation of NS2 various kinase inhibitors were used in conjunction with metabolic labelling with [^{32}P] orthophosphate. This is a commonly used technique in the study of protein phosphorylation (Hidaka & Kobayashi, 1993, Schwemmle *et al.*, 1997). Three kinase inhibitors were selected, each having differences in their inhibition constants (K_i) towards different kinases (Table 6.1). A3 (N-(2-aminoethyl)-5-chloronaphthalene-1-sulfonamide), H7 (1-(5-isoquinolinesulfonyl)-2-methylpiperazine) and H8 (N-(2-(methylamino)ethyl)-5-isoquinolinesulfonamide) were all purchased from Calbiochem.

Insect cells (*Sf*9) were grown in monolayer culture in 35mm tissue culture dishes and infected with an NS2 expressing baculovirus, AcBTV10.8. The cells were incubated at 28°C for 48 hrs, washed with TC100 media lacking phosphate and then incubated for 30 mins in the same media. Various amounts of kinase inhibitor were added when the phosphate free TC100 was added to the cells. To each well, 100μCi of [^{32}P] orthophosphate was added and the cells incubated for a further hour. The cells were lysed and NS2 immunoprecipitated with anti-NS2 polyclonal antibody. The labelled products were identified by SDS-PAGE and autoradiography. Figure 6.7 shows that inhibitors H7 and H8 have no effect on the phosphorylation of NS2 at concentrations of up to 100μM in the cell culture fluid (lanes 5-10). A3 on the other hand clearly has an inhibitory affect on the phosphorylation of NS2 (lanes 2-4). This

inhibitory affect is apparent at concentrations of 10-100μM. In a similar experiment (Fig 6.8) a wider range of A3 concentrations was used along with H7 and H8 concentrations of up to 200μM. The inhibition of the cellular kinase by A3 is still apparent (lanes 2-6), as is the ineffectiveness of H7 and H8 (lanes 7- 10), even with overexposure of the film.

When the original experiment was repeated with BTV-10 infected BHK cells an identical pattern of inhibition was observed (Fig 6.9). Despite the high level of background radioactivity, NS2 is the major protein precipitated and shows clear inhibition by the kinase inhibitor A3. H7 and H8 appear to have little effect on the kinase, as was the case with *Sf*9 cells.

By referring to the table of K_i values in Table 6.1 it is possible to interpret the above data in terms of the kinases inhibited. The only kinase that is sensitive to A3 but relatively insensitive to both H7 and H8 is casein kinase II. By using an excess of H7 and H8 in Fig 6.x the only other kinase that has a low A3 Ki value and higher H7 and H8 values, myosin light chain kinase, can be ruled out. A search of NS2 sequences in the Prosite database (Bairoch *et al.*, 1997) identified four CKII serine phosphorylation sites in BTV serogroups 1 and 10, four in AHSV-9 and three in EHDV-2 (Fig 6.10). Only one other serine residue in BTV-10 is found in a kinase consensus sequence. The serine at position 323 is in a protein kinase C consensus sequence.

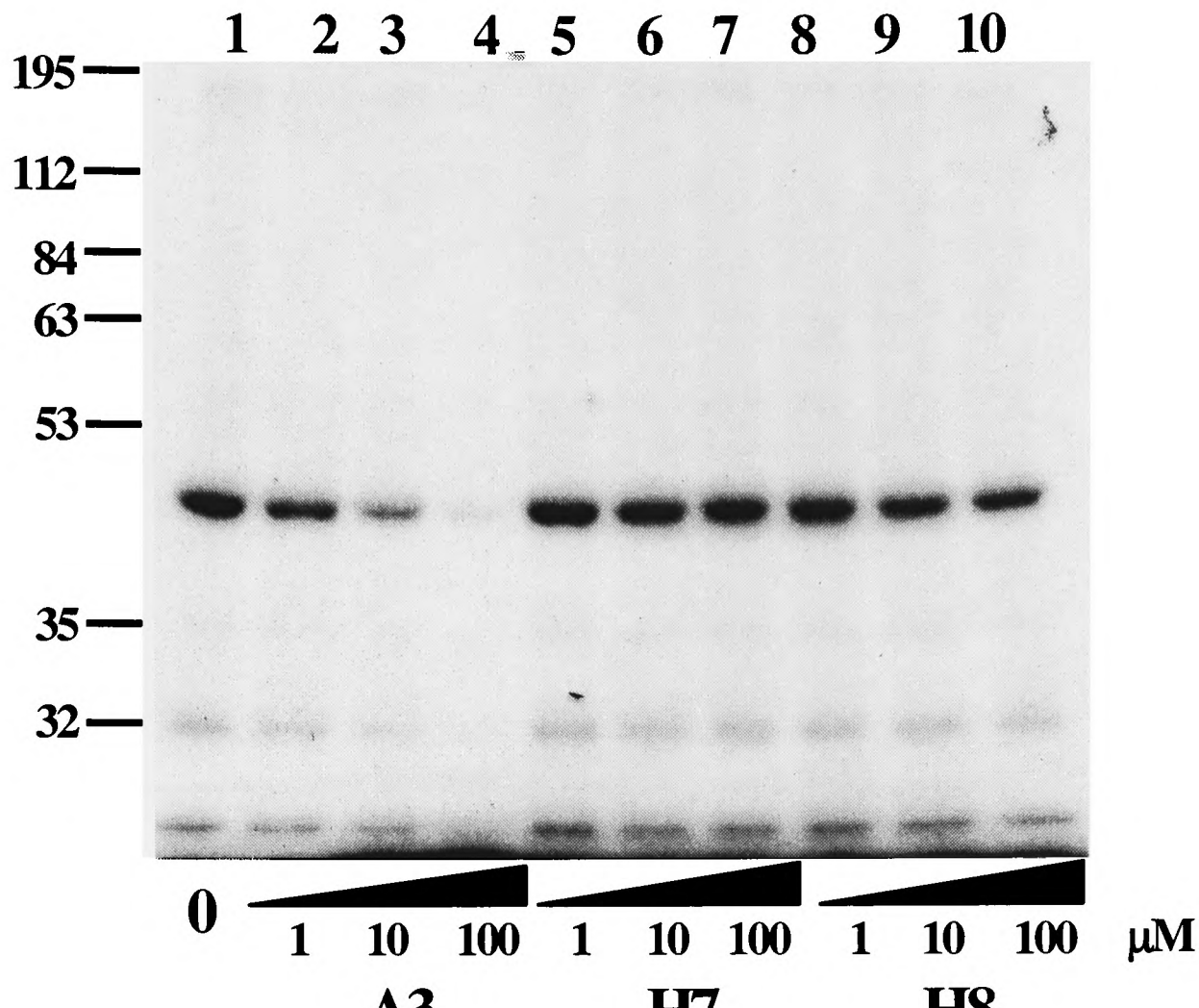

Fig 6.7: Inhibition of NS2 phosphorylation in *Sf*9 cells. *Sf*9 monolayers (35mm dishes) were infected with AcBTV10.8 and labelled 48 hpi in the presence or absence of kinase inhibitors as indicated in the figure. Following labelling the cells were lysed and NS2 immunoprecipitated with anti-NS2 polyclonal antibody and resolved by 10% SDS-PAGE. The gels were dried and NS2 detected by autoradiography.

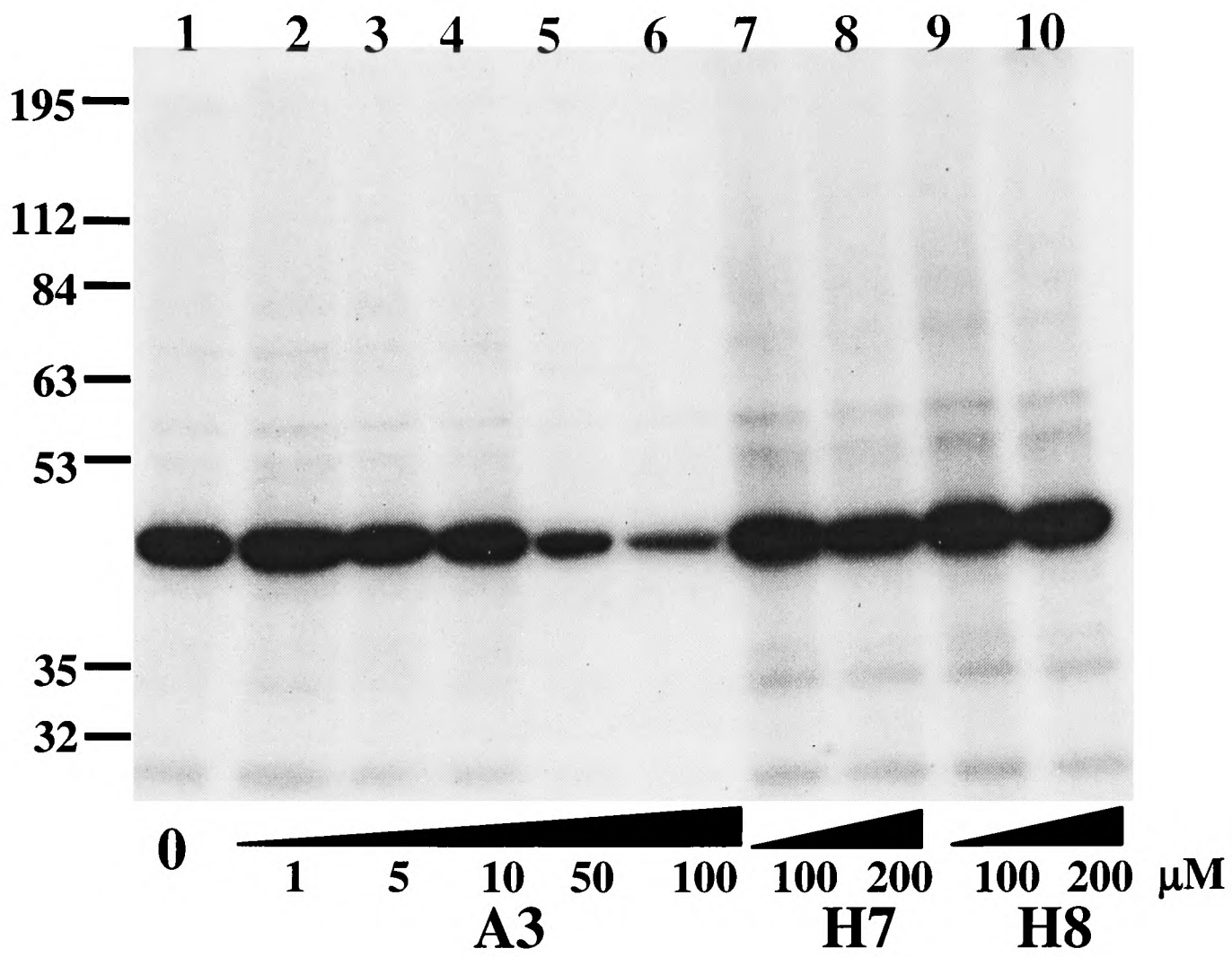

Fig 6.8: Inhibition of NS2 phosphorylation in *Sf*9 cells. The conditions employed were identical to Fig 6.5 except that a wider range of A3 inhibitor concentrations and higher H7 and H8 inhibitor concentrations were used.

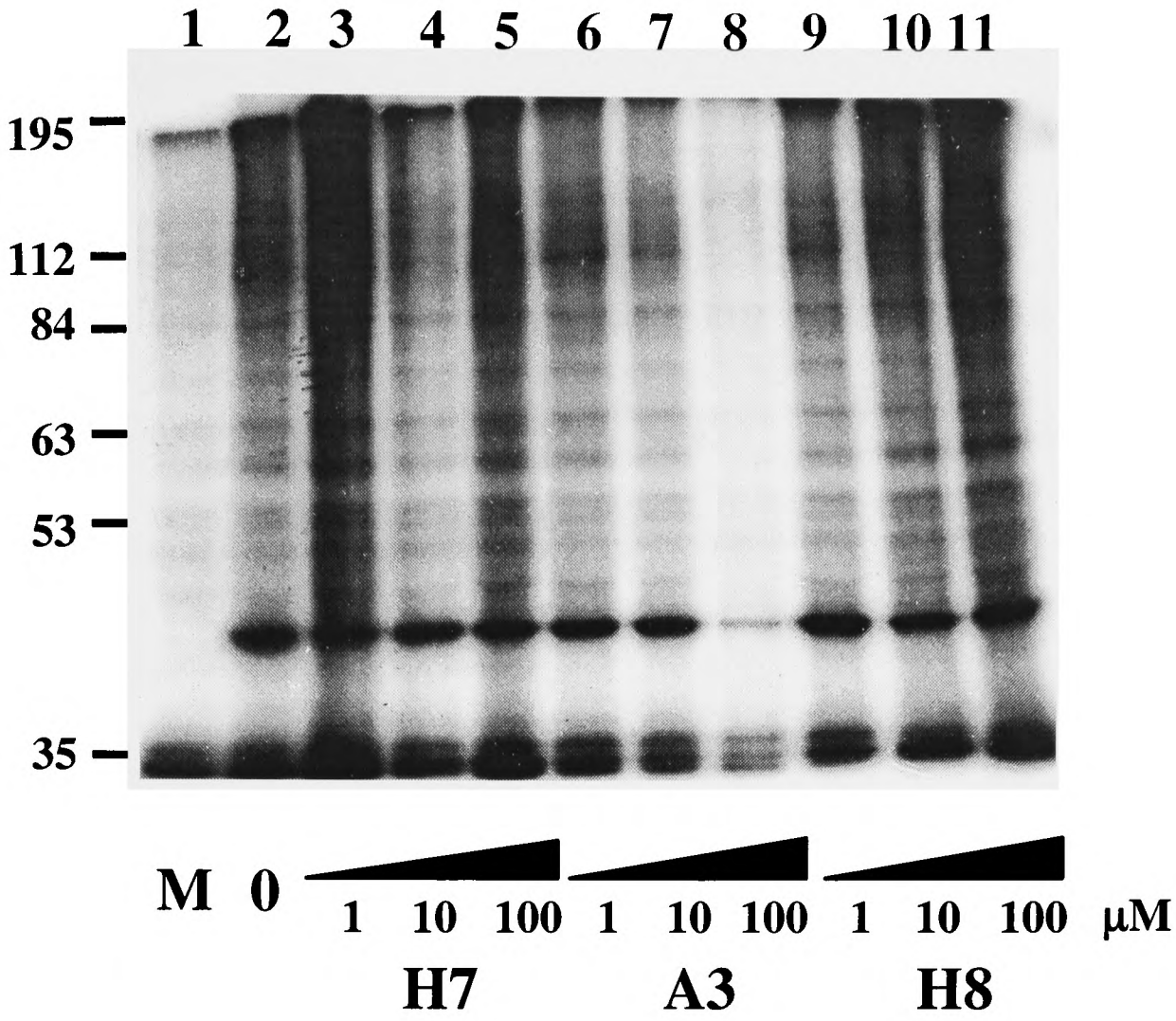

Fig 6.9: Inhibition of NS2 phosphorylation in BHK cells. BHK monolayers (35mm dishes) were either mock-infected (M) or infected with BTV-10 and labelled 18 hpi in the presence or absence of kinase inhibitors as indicated in the figure. Following labelling the cells were lysed and NS2 immunoprecipitated with anti-NS2 polyclonal antibody and resolved by 10% SDS-PAGE.

Table 6.1: Protein kinase inhibitors and their K_i values (μM) to various cellular kinases. Data from Calbiochem Signal Transduction Catalogue and Technical Resource (Anon., 1996).

	A3	H7	H8
Casein Kinase-I	80.0	100.0	133.0
Casein Kinase-II	5.1	780.0	950.0
Myosin Light Chain Kinase	7.4	97.0	68.0
cAMP-dependent Protein Kinase	4.3	3.0	1.2
cGMP-dependent Protein Kinase	3.8	5.8	0.5
Protein Kinase C	47.0	6.0	15.0
Protein Kinase C-β_1 Isotype	-	10.0	-

BTV-10

PGVMR **S^{150}**NY**D** IRELR

IVPGT **S^{204}**GL**E** KLREA

QVKTL **S^{249}DDD** DQGEDA **S^{259}DDE** HPKTH

BTV-1

PGVMR **S^{150}**NY**D** VRELR

QVQSV **S^{177}**PR**E** ESRWM

QVKTL **S^{249}DDD** EQGEDA **S^{259}DDE** HPKTH

EHDV-2

PGVQR **S^{150}**KY**D** IRELR

MNRPD **S^{189}DE**D QNPAG

EDDED S^{276}EEE EGARA

AHSV-9

LMITE **S^{84}**GI**E** VTQNR

SLPGI **T^{150}**TL**D** VGVRD

VQSNE **S^{221}**RS**D DV**ARR

SMWCQ **S^{256}DSD** DQ **S^{262}DED** HEVGG

Fig 6.10: Possible CKII serine phosphorylation sites in Orbiviral NS2. Phosphorylated residues are shown in large bold font with the critical acidic +3 residue in bold and underlined. Other acidic residues in the vicinity are also shown in bold.

6.3 DISCUSSION

The results presented in this chapter identify enzymatic activity associated with NS2. While the RNA binding capability of NS2 has been long known, NTP binding and hydrolysis represents a novel finding. The results indicate that NS2 can bind and hydrolyse ATP and GTP but with a higher binding affinity for the former.

NTP binding is indicative of a number of enzymatic activities including the mRNA capping and dsRNA helicase activities already identified in BTV. Of particular interest however, is the role of the bacteriophage ϕ6 P4 protein and its associated NTPase activity in packaging and condensation of the positive-sense RNA genome of ϕ6 (Gottlieb *et al.*, 1992, Paatero *et al.*, 1995). ϕ6 is a bacteriophage with a segmented dsRNA genome. This genome consists of three segments that are precisely packaged within assembled procapsids in a specific order. Energy is required for this packaging and the NTPase activity of P4, a component of the polymerase complex, is thought to provide that energy (Paatero *et al.*, 1995). The NTPase activity described for NS2 may play a role in providing energy for the assortment, movement, packaging or condensation of the ssRNA that it binds.

The different amounts of phosphohydrolase activity observed when different divalent cations were used may indicate slightly different structural conformations of NS2 in the presence of different cations. This might allow the different nucleosides to be bound more tightly depending on the cation species present.

A note of caution must be added here. While the purified NS2 used in these experiments appears pure by SDS-PAGE, even a small amount of a co-purifying NTPase could result in the observed hydrolysis of nucleosides. However, the NTP binding activity localises to a protein the same size as NS2 suggesting that NS2 is at

least responsible for NTP binding. Further work, including peptide sequencing of the NTP binding fragments of NS2 should confirm that NS2 is indeed an NTP binding protein.

Phosphorylation controls the activity of a number of proteins *in vivo* and *in vitro*. The interaction of a number of viral proteins with nucleic acid is determined by the phosphorylation state of the protein. Phosphorylation of the large T antigen of SV40 reduces its binding to DNA (Simmons *et al.*, 1986). In HTLV however, dephosphorylation of the Rex protein caused a decrease in RNA binding (Green *et al.*, 1992). EHDV NS2 has been reported to bind RNA with a lower affinity when unphosphorylated (Theron *et al.*, 1994) but BTV NS2 does not show a similar phosphorylation dependant binding (Thomas, 1990).

The range of proteins phosphorylated by casein kinase II is vast. Even the number of viral proteins phosphorylated by CKII is large and continually growing, and already includes proteins of vesicular stomatitis virus (Gao & Lenard, 1995b, Gao & Lenard, 1995a), Borna disease virus (Schwemmle *et al.*, 1997), influenza virus (Tucker *et al.*, 1991), human immunodeficiency virus (Schubert *et al.*, 1992, Meggio *et al.*, 1996) and herpes simplex virus (Mitchell *et al.*, 1994) to name a few. The results presented in this chapter strongly suggest that CKII is the cellular kinase responsible for the phosphorylation of NS2 *in vivo*. NS2 encodes for a number of potential CKII phosphorylation sites. The consensus sequence for CKII phosphorylation is S/TxxD/E with serine favoured over threonine (Pinna & Ruzzene, 1996). Acidic residues around the phosphorylated residue (position -2 to +7), but particularly in the +1, +2, +4 and +5 positions increase the phosphorylation rate (Pinna, 1990).

The nature of the residues phosphorylated in orbivirus NS2 has only been determined for BTV and AHSV and was shown to be exclusively serine residues (Devaney *et al.*, 1988, Thomas *et al.*, 1990). In the previous work of Thomas (1990), five possible phosphorylated serine residues were identified by peptide sequencing of tryptic peptides separated by HPLC (Fig 6.11). None of these residues were found as part of the consensus sequence for any kinase. Her conclusions were that S^{175} and S^{298} are likely to be phosphorylated with serines at positions 289, 291 and 292 also possibly phosphorylated (Thomas, 1990). Devaney and coworkers used 2-D electrophoresis of NS2 obtained from BTV and AHSV infected cells to identify two different phosphorylated forms of BTV NS2 and four different forms of AHSV NS2 (Devaney *et al.*, 1988). No non-phosphorylated forms of NS2 were identified and the serine residues were not identified. The serine residues identified here as possible sites for CKII phosphorylation are not conserved throughout the orbiviruses (Fig 6.10). However the serine at position 150 in BTV and EHDV appears to be replaced by a threonine in AHSV. Further evidence pointing to CKII as the cellular kinase involved in BTV NS2 phosphorylation was obtained by Thomas, although the significance was not recognised at the time. She showed that the polyclonal antibody used to immunoprecpitate NS2 from BTV infected cells also immunoprecipitated a kinase from uninfected cells. This kinase was able to phosphorylate casein and phosvitin *in vitro*, two CKII substrates often used in *in vitro* kinase assays (Thomas, 1990).

Based on the data of Thomas (1990) and the results presented in this Chapter, a site-directed mutagenesis programme has been initiated in order to accurately determine which BTV residues are phosphorylated and the possible significance of the phosphorylation. Further work will also be required to investigate how similar the

phosphorylation of EHDV and AHSV is to BTV and to fully characterise NTP binding and hydrolysis of NS2 from BTV, AHSV and EHDV.

Fig 6.11: Phosphorylated peptides in BTV-10 NS2 as determined by peptide sequencing of tryptic peptides by Thomas (1990). Possibly phosphorylated residues are shown in large, bold type.

LQVH**S**^{175}VAPR

A**S**^{298}GGFDR

FM**S**^{289}L**S**^{291}**S**^{292}AMPQA**S**^{298}GGFDR

Chapter 7

GENERAL DISCUSSION

Of the three non-structural proteins found in BTV-infected cells NS2 is the only one that can bind RNA. It is also the only phosphorylated BTV protein. These two features along with the knowledge that NS2 binds ssRNA but not dsRNA suggests that it might play an important role in the viral lifecycle, particularly with respect to the packaging of the RNA subgenome and its replication. This thesis presents research that leads to a better understanding of the structure-function relationship of BTV NS2, and has implications for the role of this protein in virus replication and assembly.

The biochemical and biophysical characterisation of a protein requires pure protein, and with this in mind a procedure to produce highly purified NS2 in large amounts was developed. This procedure exploited both the charge and functional characteristics of the protein in a purification scheme that employed three separate columns. The final product was free of other proteins as determined by SDS-PAGE and gave a yield 5mg per 500ml of culture fluid. The amounts of NS2 degradation products were reduced to a minimum by varying buffer components. Structural studies on NS2 were initiated, and crystallography was the first method attempted.

A wide range of crystallisation conditions were tested but no crystals were formed. As discussed in Chapter 3, this is probably due to the multimeric nature of NS2 even when purified. VIBs of various sizes and shapes can be identified in infected cells and it does not seem that there is any regular structure, essential for crystal formation, in multimeric NS2. Results obtained by size-exclusion chromatography confirmed the purified NS2 forms large multimers and data obtained in Chapter 5 on the inhibition of translation of BTV transcripts by NS2 suggest that multimerisation is possible at relatively low concentrations of NS2. One attempt

considered was to collect the monomeric form of NS2 from the size-exclusion column and use this for structural studies. However this material was of a low concentration and in small amounts making it unsuitable for use in crystallography.

In a previous study on the multimerisation of BTV-10 NS2 deletions of up to 130 residues from the carboxy terminal or 92 residues from the amino terminal did not abrogate VIB formation (Zhao *et al.*, 1994). It therefore appears likely that the residues required for the multimerisation of NS2 into VIBs lie between aa 92 and aa 227. This region is predicted to encode for two α-helices conserved within the orbiviruses (see Appendix, BTV helices α1 and α2). These helices may play a role in the formation of VIBs. However, in terms of determining the correct structure of NS2, mutations within this region are likely to yield NS2 mutants significantly different from the wild type.

NS2 is predicted to have a high α-helical content (van Staden *et al.*, 1991) and the CD data presented confirm this. A high α-helical content is a feature shared with reovirus σ-NS (Wiener & Joklik, 1987) and rotavirus NSP3 (Both *et al.*, 1984). Reovirus σ-NS is predicted to contain an α-helical content of up to 50% (Wiener & Joklik, 1987), a figure in agreement with that obtained for BTV-10 NS2.

Reovirus σ-NS, rotavirus NSP3 and orbivirus NS2 also share a short motif that has been shown to be involved in RNA-binding in EHDV (Uitenweerde *et al.*, 1995). However, σ-NS and NS2 also share an acidic region at their amino termini important for RNA-binding (Zhao *et al.*, 1994, Gillian & Nibert, 1997) but do not exhibit a specificity for the 3' end of their respective RNAs as NSP3 does (Poncet *et al.*, 1993). The significance of this motif is therefore unclear.

NS2 binds ssRNA and has a higher affinity for a short sequence found in all ten segments. The protein can bind both BTV and non-BTV RNA and may have two distinct RNA-binding activities. The identification of this aptamer in all segments suggests that it may be involved in the identification or packaging of the RNA genome into assembling virions within VIBs. The fact that the sequence is found in different locations in each segment could be indicative of a mechanism whereby NS2 is able, not only to differentiate between BTV and non-BTV RNA, but also between segments. This would allow for the packaging of only one of each RNA segment. RNA-RNA interactions are also thought to occur in BTV replication (P.Wang and P.Roy, unpublished data) and these interactions have been proposed as a possible mechanism of genome assortment in rotaviruses (Patton, 1995). If not directly involved in assortment, NS2 could possibly serve as a site for RNA condensation allowing RNA-RNA interactions to form.

The data indicating that NS2 down regulates the translation of BTV mRNA but not non-BTV mRNA supports the findings that NS2 can specifically bind BTV RNA. In both the transcription-translation and rabbit reticulocyte lysate assays the only difference was the inclusion of either BTV or non-BTV RNA. This suggests that NS2 is acting by interacting with the RNA and not some other component of the reactions. As no other BTV proteins were present, except for the NS1 produced in the reaction, it appears that NS2 on its own is responsible for the down-regulation. This effect is concentration dependent and does not appear as a gradual reduction in translation, suggesting that a certain minimum concentration of NS2 is required for activity. In infected cells it is likely that NS2 associated with BTV RNA can be displaced by the movement of the ribosome along the RNA. However, when the

concentration of NS2 is high enough, i.e. later in infection, it can multimerise into a VIB thereby making the BTV RNA inaccessible by the translational machinery. By immunoflourescence NS2 can be observed, not only in the characteristically dense VIBs, but also spread relatively evenly throughout the cytoplasm (Thomas, 1990, Brookes *et al.*, 1993).

The interaction of NS2 with VP1 is one more strand of evidence pointing to the similarity of BTV NS2 and rotavirus NSP2. NSP2 has been shown to interact with VP1 in rotavirus infected cells (Kattoura *et al.*, 1994). However, unlike Aponte and colleagues (Aponte *et al.*, 1996), it has not been possible to isolate replicase complexes by using an antibody against NS2. This may be due to the use of a polyclonal antibody instead of a monoclonal antibody with higher affinity. The NS2 purification methods described in Chapter 1 have been used to produce monoclonal antibodies that are now being characterised and the isolation of a replicase complex may be possible in the future.

Although no other interactions between NS2 and viral proteins were detected it is possible that such interactions do occur. A number of viral proteins have been found associated with VIBs in BTV-infected cells (Brookes *et al.*, 1993). This association may not represent protein-protein interactions particularly with the capsid proteins. However if the interaction of NS2 with VP1 is related to the formation of a replicase complex it seems likely that there may be other proteins involved.

NS2 also has enzymatic activity. The hydrolysis of nucleosides has been shown to be important for the movement of RNA (Rodnina *et al.*, 1997) and NTP binding and hydrolysis is believed to be important in the packaging of the dsRNA bacteriophage ϕ6 (Gottlieb *et al.*, 1992, Ojala *et al.*, 1994). Protein P4 of ϕ6 undergoes

a conformational change on binding NTPs and the hydrolysis of these NTPs is thought to provide the energy for the packaging of its ssRNA sub-genome into procapsids. Whether the NTP binding and hydrolysis observed in NS2 is related to packaging or moving RNA is not certain. NTP hydrolysis by non-structural proteins of other members of the *Reoviridae* has not been reported but rotavirus NSP5 has been shown to have an autophosphorylating kinase activity and would therefore be able to bind nucleosides (Blackhall *et al.*, 1997, Poncet *et al.*, 1997a). A putative nucleoside binding site has been identified in NSP5 (Mattion *et al.*, 1994). If NS2 can move RNA it may be possible that RNA is packaged into partially assembled cores rather than the core proteins assembling around the RNA.

Another alternative is that NS2 uses the energy from NTP hydrolysis to move along the BTV RNA segments so that it can locate the NS2 target sequence. If this were the case then the non-specific RNA-binding observed could be the result of NS2 being crosslinked to RNA before it located its target site. Exactly how proteins locate their specific binding site is unclear. This could be via a random interaction between protein and RNA, similar to enzyme substrate interactions, with high affinity interactions persisting. The other possibility is a scanning process where the protein binds the RNA with low affinity and scans the RNA until it is held in place by a high affinity binding site. The latter option would require energy that could be provided by NTP hydrolysis.

The phosphohydrolase activity of NS2 appears to have a preference for ATP over GTP, and this may be related to the relative affinity of the protein for various nucleosides. Phosphohydrolase activity was possible with all of the divalent cations tested but a higher amount of hydrolysis was observed with manganese. Manganese

may help provide the optimal structure for NTP binding. The identification of the NTP binding site by peptide sequencing is in progress and should provide further information on the region of NS2 involved.

NSP5 is the only phosphorylated rotavirus protein and, as mentioned above, it has the ability to autophosphorylate (Blackhall *et al.*, 1997, Poncet *et al.*, 1997a). NS2 is also the only phosphorylated BTV protein but does not appear to be able to autophosphorylate (Thomas, 1990, Theron *et al.*, 1994). Instead it appears to rely on a ubiquitous cellular kinase, casein kinase II for phosphorylation. This was demonstrated in both insect and mammalian cells. Up to four residues in NS2 can possibly be phosphorylated in different serotypes of BTV. The significance of this phosphorylation is not known but phosphorylation has been shown to play an important role in multimerisation (Montenarh & Muller, 1987). In the mutagenesis studies of Zhao and colleagues (1994) one particular mutant form of NS2 lacking 130 residues from the carboxy terminus was still able to form VIBs when expressed by recombinant baculovirus in insect cells. This mutant lacked S^{249} and S^{259} identified in Chapter 6 as possible sites for CKII phosphorylation and S^{289}, S^{291}, S^{292} and S^{298} identified as likely phosphorylation sites by Thomas (1990). If these residues are indeed phosphorylated then it is unlikely that they are critical for the formation of VIBs.

Similarities and differences between BTV and rotavirus proteins have been noted throughout this thesis. While there is broad similarity between the structural proteins that make up the capsid structures (see Fig 1.4) there is more variability between the non-structural proteins. BTV encodes for four non-structural proteins

while rotavirus encodes for six. BTV NS3/3A appears to be similar in function to rotavirus NSP4 but there is no equivalent in rotavirus to tubule-forming NS1 of BTV.

NS2 is broadly similar to rotavirus NSP2 but differs in a some significant respects (Fig 7.1). Both proteins bind ssRNA and, until this thesis, were thought to do so in a non-specific manner. NS2 forms 7S multimers (Uitenweerde *et al.*, 1995) while NSP2 forms 10S multimers and both proteins are now known to interact with their respective viral polymerases (Kattoura *et al.*, 1994). However, unlike NSP2, NS2 is phosphorylated. Nucleoside binding and phosphohydrolase activity has not been reported for NSP2.

Although NS2 expressed by itself can form VIBs, NSP2 assembles into viroplasms only in infected cells. NSP5 localises to viroplasms in infected cells but not when transfected, a feature that it shares with NSP2 (Kattoura *et al.*, 1994, Poncet *et al.*, 1997a). NSP2 and NSP5 interact with each other and the detection of multiphosphorylated forms of NSP5 have been shown to correlate with localisation to viroplasms (Poncet *et al.*, 1997a). It has not been reported whether the co-expression of NSP2 and NSP5 can lead to the formation of viroplasms or the detection of multiphosphorylated forms of NSP5.

	NS2	NSP1	NSP2	NSP3	NSP5
ssRNA binding	☑	☑	☑	☑	?
Phosphorylated	☑	☒	☒	☒	☑
VIBs	☑	☒	☑#	☒	☑#
Multimerisation	☑ 7S	☒	☑ 10S	☑	☑ dimers

 # Only in infected cells, not transfected cells

Fig 7.1: Functional similarities between orbivirus NS2 and rotavirus non-structural proteins NSP1, NSP2, NSP3 and NSP5. Data from Kattoura *et al.*, (1994), Patton, (1995), Uitenweerde *et al.*, (1995), Aponte *et al.*, (1996), Roy, (1996a), Poncet *et al.*, (1997a).

Taken together it appears that BTV NS2 combines most of the features of both rotavirus NSP2 and NSP5. NSP2 binds ssRNA and forms large multimers. NSP5 is phosphorylated but neither NSP2 nor NSP5 is able to form viroplasms when expressed on their own. Referring to unpublished data, Mattion and colleagues report that NSP5 can bind poly-U and ssRNA, with this binding being enhanced by the presence of NSP2 (Mattion *et al.*, 1994). NS2 binds ssRNA, forms large multimers, is phosphorylated and can form VIBs when expressed by itself.

Poncet and colleagues (1997) conclude that the reason they are unable to identify fully phosphorylated NSP5 when the protein is expressed *in vitro* is because a cofactor linked to viral infection is missing. This viral co-factor may be NSP2 and would suggest that it is required for the full phosphorylation of NSP5 and for both proteins to assemble into viroplasms. The interaction of NSP2 with NSP5 could induce a conformational change in the latter allowing the kinase domain of NSP5 to phosphorylate additional residues previously inaccessible.

This NSP2-NSP5 complex would therefore contain most of the features of BTV NS2. There are two significant differences though. First, NSP5 is autophosphorylated and NS2 is phosphorylated by a cellular kinase. However, if the phosphorylation state is what is important and not how phosphorylation is achieved then NS2 would be very similar to an NSP2-NSP5 viroplasm complex. The second difference is that NSP5 is also glycosylated while NS2 is not (Gonzalez & Burrone, 1991). Whether glycosylation of NSP5 has a functional role in the proposed NSP2-NSP5 complex is not known.

Although the precise function of NS2 is still not known, the new features described in this thesis along with the previously identified ones would strongly

suggest a role in RNA packaging. The protein appears to act as a switch, determining when RNA should no longer be translated and shifting those RNA molecules towards a packaging pathway. How the characteristics of NS2 each contribute to its function would best be resolved by the use of a reverse genetics system. In the absence of such a system for the *Reoviridae* family traditional *in vitro* molecular biology approaches will continue to be used. Future work involving site-directed mutagenesis of residues that are likely to be phosphorylated or located within the nucleoside binding site should be able to demonstrate the significance of phosphorylation, NTP binding and phosphohydrolase activity.

REFERENCES

Altenburg, B. C., Graham, D. Y. & Estes, M. K. (1980). Ultrastructural study of rotavirus replication in cultured cells. *J Gen Virol* **46**, 75-85.

Anon. (1992). Homobifunctional NHS-ester crosslinkers: Pierce Chemical Company.

Anon. (1996). Calbiochem Signal Transduction & Technical Resource 1996/97.

Anthony, I. D., Bullivant, S., Dayal, S., Bellamy, A. R. & Berriman, J. A. (1991). Rotavirus spike structure and polypeptide composition. *J Virol* **65**, 4334-4340.

Anzola, J. V., Xu, Z. K., Asamizu, T. & Nuss, D. L. (1987). Segment-specific inverted repeats found adjacent to conserved terminal sequences in wound tumor virus genome and defective interfering RNAs. *Proc Natl Acad Sci U S A* **84**, 8301-8305.

Aponte, C., Poncet, D. & Cohen, J. (1996). Recovery and characterization of a replicase complex in rotavirus-infected cells by using a monoclonal antibody against NSP2. *J Virol* **70**, 985-991.

Au, K. S., Mattion, N. M. & Estes, M. K. (1993). A subviral particle binding domain on the rotavirus nonstructural glycoprotein NS28. *Virology* **194**, 665-673.

Bairoch, A., Bucher, P. & Hofmann, K. (1997). The PROSITE database, its status in 1997. *Nucleic Acids Res* **25**, 217-221.

Ball, J. M., Tian, P., Zeng, C. Q., Morris, A. P. & Estes, M. K. (1996). Age-dependent diarrhea induced by a rotaviral nonstructural glycoprotein [see comments]. *Science* **272**, 101-104.

Basak, A. K., Gouet, P., Grimes, J., Roy, P. & Stuart, D. (1996). Crystal structure of the top domain of African horse sickness virus VP7: comparisons with bluetongue virus VP7. *J Virol* **70**, 3797-3806.

Basak, A. K., Stuart, D. I. & Roy, P. (1992). Preliminary crystallographic study of bluetongue virus capsid protein, VP7. *J Mol Biol* **228**, 687-689.

Belyaev, A. S. & Roy, P. (1993). Development of baculovirus triple and quadruple expression vectors: co-expression of three or four bluetongue virus proteins and the synthesis of bluetongue virus-like particles in insect cells. *Nucleic Acids Res* **21**, 1219-1223.

Belyaev, A. S., Stuart, D., Sutton, G. & Roy, P. (1994). Crystallization and preliminary X-ray investigation of recombinant simian immunodeficiency virus matrix protein. *J Mol Biol* **241**, 744-746.

Bergmann, C. C., Maass, D., Poruchynsky, M. S., Atkinson, P. H. & Bellamy, A. R. (1989). Topology of the non-structural rotavirus receptor glycoprotein NS28 in the rough endoplasmic reticulum. *Embo J* **8**, 1695-1703.

Bican, P., Cohen, J., Charpilienne, A. & Scherrer, R. (1982). Purification and characterization of bovine rotavirus cores. *J Virol* **43**, 1113-1117.

Bisaillon, M., Bergeron, J. & Lemay, G. (1997). Characterization of the nucleoside triphosphate phosphohydrolase and helicase activities of the reovirus lambda1 protein. *J Biol Chem* **272**, 18298-18303.

Blackhall, J., Fuentes, A., Hansen, K. & Magnusson, G. (1997). Serine protein kinase activity associated with rotavirus phosphoprotein NSP5. *J Virol* **71**, 138-144.

Boni Schnetzler, M. & Pilch, P. F. (1987). Mechanism of epidermal growth factor receptor autophosphorylation and high-affinity binding. *Proc Natl Acad Sci U S A* **84**, 7832-7836.

Both, G. W., Bellamy, A. R. & Siegman, L. J. (1984). Nucleotide sequence of the dsRNA genomic segment 7 of Simian 11 rotavirus. *Nucleic Acids Res* **12**, 1621-1626.

Both, G. W., Siegman, L. J., Bellamy, A. R. & Atkinson, P. H. (1983). Coding assignment and nucleotide sequence of simian rotavirus SA11 gene segment 10: location of glycosylation sites suggests that the signal peptide is not cleaved. *J Virol* **48**, 335-339.

Boyle, J. F. & Holmes, K. V. (1986). RNA-binding proteins of bovine rotavirus. *J Virol* **58**, 561-568.

Bresnahan, W. A., Boldogh, I., Thompson, E. A. & Albrecht, T. (1996). Human cytomegalovirus inhibits cellular DNA synthesis and arrests productively infected cells in late G1. *Virology* **224**, 150-160.

Brimacombe, R., Stiege, W., Kyriatsoulis, A. & Maly, P. (1988). Intra-RNA and RNA-protein cross-linking techniques in Escherichia coli ribosomes. *Methods Enzymol* **164**, 287-309.

Bringas, R. (1997). Folding and assembly of hepatitis B virus core protein: a new model proposal. *J Struct Biol* **118**, 189-196.

Brookes, S. M., Hyatt, A. D. & Eaton, B. T. (1993). Characterization of virus inclusion bodies in bluetongue virus-infected cells. *J Gen Virol* **74**, 525-530.

Brottier, P., Nandi, P., Bremont, M. & Cohen, J. (1992). Bovine rotavirus segment 5 protein expressed in the baculovirus system interacts with zinc and RNA. *J Gen Virol* **73**, 1931-1938.

Budowsky, E. I. & Abdurashidova, G. G. (1989). Polynucleotide-protein cross-links induced by ultraviolet light and their use for structural investigation of nucleoproteins. *Prog Nucleic Acid Res Mol Biol* **37**, 1-65.

Burnette, W. N. (1981). "Western blotting": electrophoretic transfer of proteins from sodium dodecyl sulfate--polyacrylamide gels to unmodified nitrocellulose and radiographic detection with antibody and radioiodinated protein A. *Anal Biochem* **112**, 195-203.

Burns, J. W., Greenberg, H. B., Shaw, R. D. & Estes, M. K. (1988). Functional and topographical analyses of epitopes on the hemagglutinin (VP4) of the simian rotavirus SA11. *J Virol* **62**, 2164-2172.

Chan, W. K., Au, K. S. & Estes, M. K. (1988). Topography of the simian rotavirus nonstructural glycoprotein (NS28) in the endoplasmic reticulum membrane. *Virology* **164**, 435-442.

Chang, D. K., Chien, W. J., Cheng, S. F. & Chen, S. T. (1997). NMR and circular dichroism studies on the conformation of a 44-mer peptide from a CD4-binding domain of human immunodeficiency virus envelope glycoprotein. *J Pept Res* **49**, 432-443.

Charpilienne, A., Abad, M. J., Michelangeli, F., Alvarado, F., Vasseur, M., Cohen, J. & Ruiz, M. C. (1997). Solubilized and cleaved VP7, the outer glycoprotein of rotavirus, induces permeabilization of cell membrane vesicles. *J Gen Virol* **78**, 1367-1371.

Chen, D., Gombold, J. L. & Ramig, R. F. (1990). Intracellular RNA synthesis directed by temperature-sensitive mutants of simian rotavirus SA11. *Virology* **178**, 143-151.

Cheng, J. W., Cheng, C. C., Lyu, P. C., Chen, S. T. & Lin, T. H. (1996). Solution conformation of a peptide corresponding to residues 151-172 of HIV-1 integrase using NMR and CD spectroscopy. *Int J Pept Protein Res* **47**, 117-122.

Clapp, L. L. & Patton, J. T. (1991). Rotavirus morphogenesis: domains in the major inner capsid protein essential for binding to single-shelled particles and for trimerization. *Virology* **180**, 697-708.

Clark, B. & Desselberger, U. (1988). Myristylation of rotavirus proteins. *J Gen Virol* **69**, 2681-2686.

Cleveland, D. R., Zarbl, H. & Millward, S. (1986). Reovirus guanylyltransferase is L2 gene product lambda 2. *J Virol* **60**, 307-311.

Clever, J., Sassetti, C. & Parslow, T. G. (1995). RNA secondary structure and binding sites for gag gene products in the 5' packaging signal of human immunodeficiency virus type 1. *J Virol* **69**, 2101-2109.

Cohen, J. (1977). Ribonucleic acid polymerase activity associated with purified calf rotavirus. *J Gen Virol* **36**, 395-402.

Cohen, J., Charpilienne, A., Chilmonczyk, S. & Estes, M. K. (1989). Nucleotide sequence of bovine rotavirus gene 1 and expression of the gene product in baculovirus. *Virology* **171**, 131-140.

Colburn, J. C., Kennelly, P. J., Krebs, E. G. & Stull, J. T. (1987). Affinity labeling of the nucleotide-binding site of myosin light chain kinases. *Methods Enzymol* **139**, 188-196.

Consonni, R., Limiroli, R., Longhi, R., Manera, E., Vecchio, G., Ragona, L., Siccardi, A. G. & Zetta, L. (1996). NMR and CD studies on the conformation of a synthetic peptide containing epitopes of the human immunodeficiency virus 1 transmembrane protein gp41. *Biopolymers* **38**, 423-435.

Cowley, J. A. & Gorman, B. M. (1987). Genetic reassortants for identification of the genome segment coding for the bluetongue virus hemagglutinin. *J Virol* **61**, 2304-2306.

Cowley, J. A., Walker, P. J. & Gorman, B. M. (1991). Recognition sites in assembly of bluetongue virus. In *Bluetongue, African Horse-Sickness, and related Orbiviruses*, pp. 423-432. Edited by T. E. Walton & B. I. Osburn. Paris, France: CRC Press.

Davies, F. G., Mungai, J. N. & Pini, A. (1992). A new bluetongue virus serotype isolated in Kenya. *Vet Microbiol* **31**, 25-32.

Deleage, G. & Geourjon, C. (1993). An interactive graphic program for calculating the secondary structure content of proteins from circular dichroism spectrum. *Comput Appl Biosci* **9**, 197-199.

Della Porta, A. J. (1985). Classification of orbiviruses: a need for supergroups of genera. *Prog Clin Biol Res* **178**, 267-274.

Delling, U., Reid, L. S., Barnett, R. W., Ma, M. Y., Climie, S., Sumner Smith, M. & Sonenberg, N. (1992). Conserved nucleotides in the TAR RNA stem of human immunodeficiency virus type 1 are critical for Tat binding and trans activation: model for TAR RNA tertiary structure. *J Virol* **66**, 3018-3025.

Devaney, M. A., Kendall, J. & Grubman, M. J. (1988). Characterization of a nonstructural phosphoprotein of two orbiviruses. *Virus Res* **11**, 151-164.

Dong, Y., Zeng, C. Q., Ball, J. M., Estes, M. K. & Morris, A. P. (1997). The rotavirus enterotoxin NSP4 mobilizes intracellular calcium in human intestinal cells by stimulating phospholipase C-mediated inositol 1,4,5-trisphosphate production. *Proc Natl Acad Sci U S A* **94**, 3960-3965.

Draper, D. E. (1995). Protein-RNA recognition. *Annual Review of Biochemistry* **64**, 593-620.

Dryden, K. A., Wang, G., Yeager, M., Nibert, M. L., Coombs, K. M., Furlong, D. B., Fields, B. N. & Baker, T. S. (1993). Early steps in reovirus infection are associated with dramatic changes in supramolecular structure and protein conformation: analysis of virions and subviral particles by cryoelectron microscopy and image reconstruction. *Journal of Cell Biology* **122**, 1023-1041.

Du Toit, R. M. (1944). The transmission of blue-tongue and horse-sickness by *Culicodes*. *Onderspoort J Vet Sci Anim Ind* **19**, 7-16.

Duncan, R. F. (1990). Protein synthesis initiation factor modifications during viral infections: implications for translational control. *Electrophoresis* **11**, 219-227.

Eaton, B. T., Hyatt, A. D. & Brookes, S. M. (1990). The replication of bluetongue virus. *Curr Top Microbiol Immunol* **162**, 89-118.

Eaton, B. T., Hyatt, A. D. & White, J. R. (1987). Association of bluetongue virus with the cytoskeleton. *Virology* **157**, 107-116.

Eaton, B. T., Hyatt, A. D. & White, J. R. (1988). Localization of the nonstructural protein NS1 in bluetongue virus-infected cells and its presence in virus particles. *Virology* **163**, 527-537.

Erasmus, B. J. (1975). Bluetongue in sheep and goats. *Aust Vet J* **51**, 165-170.

Ericson, B. L., Graham, D. Y., Mason, B. B. & Estes, M. K. (1982). Identification, synthesis, and modifications of simian rotavirus SA11 polypeptides in infected cells. *J Virol* **42**, 825-839.

Ericson, B. L., Graham, D. Y., Mason, B. B., Hanssen, H. H. & Estes, M. K. (1983). Two types of glycoprotein precursors are produced by the simian rotavirus SA11. *Virology* **127**, 320-332.

Estes, M. K. & Cohen, J. (1989). Rotavirus gene structure and function. *Microbiol Rev* **53**, 410-449.

Estes, M. K., Graham, D. Y. & Mason, B. B. (1981). Proteolytic enhancement of rotavirus infectivity: molecular mechanisms. *J Virol* **39**, 879-888.

Falconer, M. M., Gilbert, J. M., Roper, A. M., Greenberg, H. B. & Gavora, J. S. (1995). Rotavirus-induced fusion from without in tissue culture cells. *J Virol* **69**, 5582-5591.

Fenner, F. (1976). The classification and nomenclature of viruses. *Intervirology* **6**, 1-12.

Fodor, E., Pritlove, D. C. & Brownlee, G. G. (1994). The influenza virus panhandle is involved in the initiation of transcription. *J Virol* **68**, 4092-4096.

Fodor, E., Pritlove, D. C. & Brownlee, G. G. (1995). Characterization of the RNA-fork model of virion RNA in the initiation of transcription in influenza A virus. *J Virol* **69**, 4012-4019.

Frankel, A. D. (1992). Peptide models of the Tat-TAR protein-RNA interaction. *Protein Sci* **1**, 1539-1542.

French, T. J., Inumaru, S. & Roy, P. (1989). Expression of two related nonstructural proteins of bluetongue virus (BTV) type 10 in insect cells by a recombinant baculovirus: production of polyclonal ascitic fluid and characterization of the gene product in BTV-infected BHK cells. *J Virol* **63**, 3270-3278.

French, T. J., Marshall, J. J. & Roy, P. (1990). Assembly of double-shelled, viruslike particles of bluetongue virus by the simultaneous expression of four structural proteins. *J Virol* **64**, 5695-5700.

French, T. J. & Roy, P. (1990). Synthesis of bluetongue virus (BTV) corelike particles by a recombinant baculovirus expressing the two major structural core proteins of BTV. *J Virol* **64**, 1530-1536.

Fukuhara, N., Nishikawa, K., Gorziglia, M. & Kapikian, A. Z. (1989). Nucleotide sequence of gene segment 1 of a porcine rotavirus strain. *Virology* **173**, 743-749.

Fukuhara, N., Yoshie, O., Kitaoka, S. & Konno, T. (1988). Role of VP3 in human rotavirus internalization after target cell attachment via VP7. *J Virol* **62**, 2209-2218.

Furuichi, Y., Morgan, M., Muthukrishnan, S. & Shatkin, A. J. (1975a). Reovirus messenger RNA contains a methylated, blocked 5'-terminal structure: m-7G(5')ppp(5')G-MpCp-. *Proc Natl Acad Sci U S A* **72**, 362-366.

Furuichi, Y., Muthukrishnan, S. & Shatkin, A. J. (1975b). 5'-Terminal m-7G(5')ppp(5')G-m-p in vivo: identification in reovirus genome RNA. *Proc Natl Acad Sci U S A* **72**, 742-745.

Gallegos, C. O. & Patton, J. T. (1989). Characterization of rotavirus replication intermediates: a model for the assembly of single-shelled particles. *Virology* **172**, 616-627.

Gao, Y. & Lenard, J. (1995a). Cooperative binding of multimeric phosphoprotein (P) of vesicular stomatitis virus to polymerase (L) and template: pathways of assembly. *J Virol* **69**, 7718-7723.

Gao, Y. & Lenard, J. (1995b). Multimerization and transcriptional activation of the phosphoprotein (P) of vesicular stomatitis virus by casein kinase-II. *Embo J* **14**, 1240-1247.

Geisow, M. J., Fritsche, U., Hexham, J. M., Dash, B. & Johnson, T. (1986). A consensus amino-acid sequence repeat in Torpedo and mammalian Ca2+-dependent membrane-binding proteins. *Nature* **320**, 636-638.

Gerke, V. & Weber, K. (1985). Calcium-dependent conformational changes in the 36-kDa subunit of intestinal protein I related to the cellular 36-kDa target of Rous sarcoma virus tyrosine kinase. *J Biol Chem* **260**, 1688-1695.

Gibson, W. (1996). Structure and assembly of the virion. *Intervirology* **39**, 389-400.

Giege, R. & Ducruix, D. (1992). An introduction to the crystallogenesis of biological macromolecules. In *Crystallization of nucleic acids and proteins*, pp. 1-18. Edited by D. Ducruix & R. Giege. Oxford: Oxford University Press.

Gillian, A. L. & Nibert, M. L. (1997). The extreme N terminus of reovirus protein σNS is important for both RNA binding and maintenance of 16S complexes. In *16th Annual Meeting of the American Society for Virology*. Bozeman, Montana, USA.

Glenney, J. (1986). Two related but distinct forms of the Mr 36,000 tyrosine kinase substrate (calpactin) that interact with phospholipid and actin in a Ca2+-dependent manner. *Proc Natl Acad Sci U S A* **83**, 4258-4262.

Gombold, J. L., Estes, M. K. & Ramig, R. F. (1985). Assignment of simian rotavirus SA11 temperature-sensitive mutant groups B and E to genome segments. *Virology* **143**, 309-320.

Gonzalez, S. A. & Burrone, O. R. (1991). Rotavirus NS26 is modified by addition of single O-linked residues of N-acetylglucosamine. *Virology* **182**, 8-16.

Gorman, B. M. (1990). The bluetongue viruses. *Curr Top Microbiol Immunol* **162**, 1-19.

Gottlieb, P., Strassman, J. & Mindich, L. (1992). Protein P4 of the bacteriophage phi 6 procapsid has a nucleoside triphosphate-binding site with associated nucleoside triphosphate phosphohydrolase activity. *J Virol* **66**, 6220-6222.

Gould, A. R. (1988). Nucleotide sequence of the Australian bluetongue virus serotype 1 RNA segment 10. *J Gen Virol* **69**, 945-949.

Green, P. L., Yip, M. T., Xie, Y. & Chen, I. S. (1992). Phosphorylation regulates RNA binding by the human T-cell leukemia virus Rex protein. *J Virol* **66**, 4325-4330.

Greenberg, H. B., Valdesuso, J., van Wyke, K., Midthun, K., Walsh, M., McAuliffe, V., Wyatt, R. G., Kalica, A. R., Flores, J. & Hoshino, Y. (1983). Production and preliminary characterization of monoclonal antibodies directed at two surface proteins of rhesus rotavirus. *J Virol* **47**, 267-275.

Grimes, J., Basak, A. K., Roy, P. & Stuart, D. (1995). The crystal structure of bluetongue virus VP7. *Nature* **373**, 167-170.

Grubman, M. J., Appleton, J. A. & Letchworth, G. J. d. (1983). Identification of bluetongue virus type 17 genome segments coding for polypeptides associated with virus neutralization and intergroup reactivity. *Virology* **131**, 355-366.

Haig, D. A., McKercher, D. G. & Alexander, R. A. (1956). The cytopathogenic action of bluetongue virus on tissue cultures and its application to the detection of antibodies in the serum of sheep. *Onderspoort J Vet Res* **27**, 171-175.

Hanks, S. K. & Quinn, A. M. (1991). Protein kinase catalytic domain sequence database: identification of conserved features of primary structure and classification of family members. *Methods Enzymol* **200**, 38-62.

Hardy, W. T. & Price, D. A. (1952). Soremuzzle of sheep. *J Am Vet Med Assoc* **120**, 23-25.

Heaphy, S., Dingwall, C., Ernberg, I., Gait, M. J., Green, S. M., Karn, J., Lowe, A. D., Singh, M. & Skinner, M. A. (1990). HIV-1 regulator of virion expression (Rev) protein binds to an RNA stem-loop structure located within the Rev response element region. *Cell* **60**, 685-693.

Hewat, E. A., Booth, T. F., Loudon, P. T. & Roy, P. (1992a). Three-dimensional reconstruction of baculovirus expressed bluetongue virus core-like particles by cryo-electron microscopy. *Virology* **189**, 10-20.

Hewat, E. A., Booth, T. F. & Roy, P. (1992b). Structure of bluetongue virus particles by cryoelectron microscopy. *J Struct Biol* **109**, 61-69.

Hewat, E. A., Booth, T. F., Wade, R. H. & Roy, P. (1992c). 3-D reconstruction of bluetongue virus tubules using cryoelectron microscopy. *J Struct Biol* **108**, 35-48.

Hidaka, H. & Kobayashi, R. (1993). Use of protein (serine/threoinine) kinase activators and inhibitors to study protein phosphorylation in intact cells. In

Protein phosphorylation: a practical approach, pp. 87-107. Edited by D. G. Hardie. Oxford: Oxford University Press.

Hooke, S. D., Radford, S. E. & Dobson, C. M. (1994). The refolding of human lysozyme: a comparison with the structurally homologous hen lysozyme. *Biochemistry* **33**, 5867-5876.

Horscroft, N. J. & Roy, P. (1997). Thermal denaturation of proteins for SDS-PAGE analysis by microwave irradiation. *Biotechniques* **22**, 224-226.

Howell, P. G. (1960). Bluetongue. In *Emerging diseases of animals. FAO Agricultural Studies No. 61*, pp. 109-153. Rome: FAO.

Hsu, M. T., Parvin, J. D., Gupta, S., Krystal, M. & Palese, P. (1987). Genomic RNAs of influenza viruses are held in a circular conformation in virions and in infected cells by a terminal panhandle. *Proc Natl Acad Sci U S A* **84**, 8140-8144.

Hua, J., Chen, X. & Patton, J. T. (1994). Deletion mapping of the rotavirus metalloprotein NS53 (NSP1): the conserved cysteine-rich region is essential for virus-specific RNA binding. *J Virol* **68**, 3990-4000.

Hua, J., Mansell, E. A. & Patton, J. T. (1993). Comparative analysis of the rotavirus NS53 gene: conservation of basic and cysteine-rich regions in the protein and possible stem-loop structures in the RNA. *Virology* **196**, 372-378.

Hua, J. & Patton, J. T. (1994). The carboxyl-half of the rotavirus nonstructural protein NS53 (NSP1) is not required for virus replication. *Virology* **198**, 567-576.

Huang, I. J., Hwang, G. Y., Yang, Y. Y., Hayama, E. & Li, J. K. (1995). Sequence analyses and antigenic epitope mapping of the putative RNA-directed RNA polymerase of five U.S. bluetongue viruses. *Virology* **214**, 280-288.

Huismans, H. (1970). Macromolecular synthesis in bluetongue virus infected cells. II. Host cell metabolism. *Onderstepoort J Vet Res* **37**, 199-209.

Huismans, H. (1971). Host cell protein synthesis after infection with bluetongue virus and reovirus. *Virology* **46**, 500-503.

Huismans, H. (1979). Protein synthesis in bluetongue virus-infected cells. *Virology* **92**, 385-396.

Huismans, H. & Els, H. J. (1979). Characterization of the tubules associated with the replication of three different orbiviruses. *Virology* **92**, 397-406.

Huismans, H. & Erasmus, B. J. (1981). Identification of the serotype-specific and group-specific antigens of bluetongue virus. *Onderstepoort J Vet Res* **48**, 51-58.

Huismans, H. & Van Dijk, A. A. (1990). Bluetongue virus structural components. *Curr Top Microbiol Immunol* **162**, 21-41.

Huismans, H., van Dijk, A. A. & Bauskin, A. R. (1987a). In vitro phosphorylation and purification of a nonstructural protein of bluetongue virus with affinity for single-stranded RNA. *J Virol* **61**, 3589-3595.

Huismans, H., van Dijk, A. A. & Els, H. J. (1987b). Uncoating of parental bluetongue virus to core and subcore particles in infected L cells. *Virology* **157**, 180-188.

Huismans, H. & Verwoerd, D. W. (1973). Control of transcription during the expression of the bluetongue virus genome. *Virology* **52**, 81-88.

Hwang, G. Y., Yang, Y. Y., Chiou, J. F. & Li, J. K. (1992). Sequence conservation among the cognate nonstructural NS3/3A protein genes of six bluetongue viruses. *Virus Res* **23**, 151-161.

Hyatt, A. D. & Eaton, B. T. (1988). Ultrastructural distribution of the major capsid proteins within bluetongue virus and infected cells. *J Gen Virol* **69**, 805-815.

Hyatt, A. D., Eaton, B. T. & Brookes, S. M. (1989). The release of bluetongue virus from infected cells and their superinfection by progeny virus. *Virology* **173**, 21-34.

Hyatt, A. D., Gould, A. R., Coupar, B. & Eaton, B. T. (1991). Localization of the non-structural protein NS3 in bluetongue virus-infected cells. *J Gen Virol* **72**, 2263-2267.

Hyatt, A. D., Zhao, Y. & Roy, P. (1993). Release of bluetongue virus-like particles from insect cells is mediated by BTV nonstructural protein NS3/NS3A. *Virology* **193**, 592-603.

Imai, M., Akatani, K., Ikegami, N. & Furuichi, Y. (1983). Capped and conserved terminal structures in human rotavirus genome double-stranded RNA segments. *J Virol* **47**, 125-136.

Iwata, H., Chuma, T. & Roy, P. (1992a). Characterization of the genes encoding two of the major capsid proteins of epizootic haemorrhagic disease virus indicates a close genetic relationship to bluetongue virus. *J Gen Virol* **73**, 915-924.

Iwata, H., Yamagawa, M. & Roy, P. (1992b). Evolutionary relationships among the gnat-transmitted orbiviruses that cause African horse sickness, bluetongue, and epizootic hemorrhagic disease as evidenced by their capsid protein sequences. *Virology* **191**, 251-261.

Jain, C. & Belasco, J. G. (1996). A structural model for the HIV-1 Rev-RRE complex deduced from altered-specificity rev variants isolated by a rapid genetic strategy. *Cell* **87**, 115-125.

Johnson, J. E. (1996). Functional implications of protein-protein interactions in icosahedral viruses. *Proc Natl Acad Sci U S A* **93**, 27-33.

Johnson Jr., W. C. (1990). Protein secondary and circular dichroism: A practical guide. *Proteins: Structure, Function and Genetics* **7**, 205-214.

Johnston, S. D., Yu, X. M. & Mertz, J. E. (1996). The major transcriptional transactivation domain of simian virus 40 large T antigen associates nonconcurrently with multiple components of the transcriptional preinitiation complex. *J Virol* **70**, 1191-1202.

Joklik, W. K. (1981). Structure and function of the reovirus genome. *Microbiol Rev* **45**, 483-501.

Kabcenell, A. K. & Atkinson, P. H. (1985). Processing of the rough endoplasmic reticulum membrane glycoproteins of rotavirus SA11. *Journal of Cell Biology* **101**, 1270-1280.

Kahlon, J., Sugiyama, K. & Roy, P. (1983). Molecular basis of bluetongue virus neutralization. *J Virol* **48**, 627-632.

Kalica, A. R., Flores, J. & Greenberg, H. B. (1983). Identification of the rotaviral gene that codes for hemagglutination and protease-enhanced plaque formation. *Virology* **125**, 194-205.

Kaljot, K. T., Shaw, R. D., Rubin, D. H. & Greenberg, H. B. (1988). Infectious rotavirus enters cells by direct cell membrane penetration, not by endocytosis. *J Virol* **62**, 1136-1144.

Kattoura, M. D., Chen, X. & Patton, J. T. (1994). The rotavirus RNA-binding protein NS35 (NSP2) forms 10S multimers and interacts with the viral RNA polymerase. *Virology* **202**, 803-813.

Kattoura, M. D., Clapp, L. L. & Patton, J. T. (1992). The rotavirus nonstructural protein, NS35, possesses RNA-binding activity in vitro and in vivo. *Virology* **191**, 698-708.

Kay, L. E. & Gardner, K. H. (1997). Solution NMR spectroscopy beyond 25 kDa. *Current Opinion in Structural Biology* **7**, 722-731.

King, L. A. & Possee, R. D. (1992). The baculovirus expresssion system, a laboratory guide, pp. 229. London: Chapman & Hall.

Kim, H. J., Fodor, E., Brownlee, G. G. & Seong, B. L. (1997). Mutational analysis of the RNA-fork model of the influenza A virus vRNA promoter in vivo. *J Gen Virol* **78**, 353-357.

Knudson, D. L. & Shope, R. E. (1985). Overview of the orbiviruses. *Prog Clin Biol Res* **178**, 255-266.

Kumar, A., Charpilienne, A. & Cohen, J. (1989). Nucleotide sequence of the gene encoding for the RNA binding protein (VP2) of RF bovine rotavirus. *Nucleic Acids Res* **17**, 2126.

Kurg, A., Sommer, G. & Metspalu, A. (1995). An RNA stem-loop structure involved in the packaging of bovine leukemia virus genomic RNA in vivo. *Virology* **211**, 434-442.

Labbe, M., Baudoux, P., Charpilienne, A., Poncet, D. & Cohen, J. (1994). Identification of the nucleic acid binding domain of the rotavirus VP2 protein. *J Gen Virol* **75**, 3423-3430.

Labbe, M., Charpilienne, A., Crawford, S. E., Estes, M. K. & Cohen, J. (1991). Expression of rotavirus VP2 produces empty corelike particles. *J Virol* **65**, 2946-2952.

Laemmli, U. K. (1970). Cleavage of structural proteins during assembly of the head of bacteriophage T4. *Nature* **277**, 660-685.

Lai, M. M., Liao, C. L., Lin, Y. J. & Zhang, X. (1994). Coronavirus: how a large RNA viral genome is replicated and transcribed. *Infect Agents Dis* **3**, 98-105.

Langland, J. O., Pettiford, S., Jiang, B. & Jacobs, B. L. (1994). Products of the porcine group C rotavirus NSP3 gene bind specifically to double-stranded RNA and inhibit activation of the interferon-induced protein kinase PKR. *J Virol* **68**, 3821-3829.

Le Blois, H., French, T., Mertens, P. P., Burroughs, J. N. & Roy, P. (1992). The expressed VP4 protein of bluetongue virus binds GTP and is the candidate guanylyl transferase of the virus. *Virology* **189**, 757-761.

Leader, D. P. & Katan, M. (1988). Viral aspects of protein phosphorylation. *J Gen Virol* **69**, 1441-1464.

LeCuyer, K. A., Behlen, L. S. & Uhlenbeck, O. C. (1995). Mutants of the bacteriophage MS2 coat protein that alter its cooperative binding to RNA. *Biochemistry* **34**, 10600-10606.

Lee, J. W. & Roy, P. (1986). Nucleotide sequence of a cDNA clone of RNA segment 10 of bluetongue virus (serotype 10). *J Gen Virol* **67**, 2833-2837.

Liu, M., Mattion, N. M. & Estes, M. K. (1992). Rotavirus VP3 expressed in insect cells possesses guanylyltransferase activity. *Virology* **188**, 77-84.

Loudon, P. T. & Roy, P. (1991). Assembly of five bluetongue virus proteins expressed by recombinant baculoviruses: inclusion of the largest protein VP1 in the core and virus-like proteins. *Virology* **180**, 798-802.

Loudon, P. T. & Roy, P. (1992). Interaction of nucleic acids with core-like and subcore-like particles of bluetongue virus. *Virology* **191**, 231-236.

Lowery, C. & Richardson, J. P. (1977a). Characterization of the nucleoside triphosphate phosphohydrolase (ATPase) activity of RNA synthesis termination factor p. I. Enzymatic properties and effects of inhibitors. *J Biol Chem* **252**, 1375-1380.

Lowery, C. & Richardson, J. P. (1977b). Characterization of the nucleoside triphosphate phosphohydrolase (ATPase) activity of RNA synthesis termination factor p. II. Influence of synthetic RNA homopolymers and random copolymers on the reaction. *J Biol Chem* **252**, 1381-1385.

Lu, H., Buck, M., Radford, S. E. & Dobson, C. M. (1997). Acceleration of the folding of hen lysozyme by trifluoroethanol. *J Mol Biol* **265**, 112-117.

Ludert, J. E., Feng, N., Yu, J. H., Broome, R. L., Hoshino, Y. & Greenberg, H. B. (1996). Genetic mapping indicates that VP4 is the rotavirus cell attachment protein in vitro and in vivo. *J Virol* **70**, 487-493.

Maass, D. R. & Atkinson, P. H. (1990). Rotavirus proteins VP7, NS28, and VP4 form oligomeric structures. *J Virol* **64**, 2632-2641.

Maniatis, T., Fritsch, E. F. & Sambrook, J. (1982). Molecular Cloning, a laboratory manual, 1st edn: Cold Spring Harbor.

Mansell, E. A. & Patton, J. T. (1990). Rotavirus RNA replication: VP2, but not VP6, is necessary for viral replicase activity. *J Virol* **64**, 4988-4996.

Mansell, E. A., Ramig, R. F. & Patton, J. T. (1994). Temperature-sensitive lesions in the capsid proteins of the rotavirus mutants tsF and tsG that affect virion assembly. *Virology* **204**, 69-81.

Marello, K., LaRovere, J. & Sommerville, J. (1992). Binding of Xenopus oocyte masking proteins to mRNA sequences. *Nucleic Acids Res* **20**, 5593-5600.

Marshall, J. J. & Roy, P. (1990). High level expression of the two outer capsid proteins of bluetongue virus serotype 10: their relationship with the neutralization of virus infection. *Virus Res* **15**, 189-195.

Martin, S. A. & Zweerink, H. J. (1972). Isolation and characterization of two types of bluetongue virus particles. *Virology* **50**, 495-506.

Martinez-Costas, J., Sutton, G., Willis, A. & Roy, P. (1997). Guanylyltransferase and RNA 5' triphosphatase activities of the purified expressed VP4 protein of Bluetongue virus: Identification of the active nucleotide-binding site. *Submitted.*

Mason, J. H. & Neitz, W. O. (1940). The susceptibility of cattle to the virus of bluetongue. *Onderstepoort J Vet Sci Anim Ind* **15**, 149-157.

Massiah, M. A., Worthylake, D., Christensen, A. M., Sundquist, W. I., Hill, C. P. & Summers, M. F. (1996). Comparison of the NMR and X-ray structures of the HIV-1 matrix protein: evidence for conformational changes during viral assembly. *Protein Sci* **5**, 2391-2398.

Mattion, N. M., Cohen, J., Aponte, C. & Estes, M. K. (1992). Characterization of an oligomerization domain and RNA-binding properties on rotavirus nonstructural protein NS34. *Virology* **190**, 68-83.

Mattion, N. M., Cohen, J. & Estes, M. K. (1994). Rotavirus proteins. In *Viral infections of the gastrointestinal tract*, pp. 169-249. Edited by A. Kapikian. New York: Marcel Dekker, Inc.

Mattion, N. M., Mitchell, D. B., Both, G. W. & Estes, M. K. (1991). Expression of rotavirus proteins encoded by alternative open reading frames of genome segment 11. *Virology* **181**, 295-304.

Mattson, G., Conklin, E., Desai, S., Nielander, G., Savage, M. D. & Morgensen, S. (1993). A practical approach to crosslinking. *Molecular Biology reports* **17**, 167-183.

McCrae, M. A. & McCorquodale, J. G. (1983). Molecular biology of rotaviruses. V. Terminal structure of viral RNA species. *Virology* **126**, 204-212.

Meggio, F., DM, D. A., Ciminale, V., Chieco Bianchi, L. & Pinna, L. A. (1996). Phosphorylation of HIV-1 Rev protein: implication of protein kinase CK2 and pro-directed kinases. *Biochem Biophys Res Commun* **226**, 547-554.

Mertens, P. P., Brown, F. & Sangar, D. V. (1984). Assignment of the genome segments of bluetongue virus type 1 to the proteins which they encode. *Virology* **135**, 207-217.

Mertens, P. P., Burroughs, J. N. & Anderson, J. (1987). Purification and properties of virus particles, infectious subviral particles, and cores of bluetongue virus serotypes 1 and 4. *Virology* **157**, 375-386.

Mertens, P. P., Burroughs, J. N., Wade-Evans, A. M., Le Blois, H., Oldfield, S., Basak, A., Loudon, P. & Roy, P. (1991). Analysis of guanylyltransferase and

transmethylase activities associated with bluetongue virus cores and recombinant baculovirus-expressed core-like particles. In *Bluetongue, African Horse-Sickness, and related Orbiviruses*, pp. 404-415. Edited by T. E. Walton & B. I. Osburn. Paris, France: CRC Press.

Mertens, P. P., Pedley, S., Cowley, J., Burroughs, J. N., Corteyn, A. H., Jeggo, M. H., Jennings, D. M. & Gorman, B. M. (1989). Analysis of the roles of bluetongue virus outer capsid proteins VP2 and VP5 in determination of virus serotype. *Virology* **170**, 561-565.

Mertens, P. P. & Sangar, D. V. (1985). Analysis of the terminal sequences of the genome segments of four orbiviruses. *Prog Clin Biol Res* **178**, 371-387.

Mertens, P. P. C. & Roy, P. (1994). Orbiviruses and Coltiviruses. In *Encyclopedia of Virology*, pp. 941-964. Edited by R. G. Webster & A. Granoff. London: Academic Press.

Metcalf, P., Cyrklaff, M. & Adrian, M. (1991). The three-dimensional structure of reovirus obtained by cryo-electron microscopy. *Embo J* **10**, 3129-3136.

Mitchell, C., Blaho, J. A. & Roizman, B. (1994). Casein kinase II specifically nucleotidylylates in vitro the amino acid sequence of the protein encoded by the alpha 22 gene of herpes simplex virus 1. *Proc Natl Acad Sci U S A* **91**, 11864-11868.

Mitchell, D. B. & Both, G. W. (1990a). Completion of the genomic sequence of the simian rotavirus SA11: nucleotide sequences of segments 1, 2, and 3. *Virology* **177**, 324-331.

Mitchell, D. B. & Both, G. W. (1990b). Conservation of a potential metal binding motif despite extensive sequence diversity in the rotavirus nonstructural protein NS53. *Virology* **174**, 618-621.

Monastyrskaya, K., Booth, T., Nel, L. & Roy, P. (1994). Mutation of either of two cysteine residues or deletion of the amino or carboxy terminus of nonstructural protein NS1 of bluetongue virus abrogates virus-specified tubule formation in insect cells. *J Virol* **68**, 2169-2178.

Montenarh, M. & Muller, D. (1987). The phosphorylation at Thr 124 of simian virus 40 large T antigen is crucial for its oligomerization. *FEBS Lett* **221**, 199-204.

Musalem, C. & Espejo, R. T. (1985). Release of progeny virus from cells infected with simian rotavirus SA11. *J Gen Virol* **66**, 2715-2724.

Nagai, K. (1996). RNA-protein complexes. *Curr Opin Struct Biol* **6**, 53-61.

Nakata, T., Sobue, K. & Hirokawa, N. (1990). Conformational change and localization of calpactin I complex involved in exocytosis as revealed by quick-

freeze, deep-etch electron microscopy and immunocytochemistry. *Journal of Cell Biology* **110**, 13-25.

Nandi, P., Charpilienne, A. & Cohen, J. (1992). Interaction of rotavirus particles with liposomes. *J Virol* **66**, 3363-3367.

Ni, C. Z., Syed, R., Kodandapani, R., Wickersham, J., Peabody, D. S. & Ely, K. R. (1995). Crystal structure of the MS2 coat protein dimer: implications for RNA binding and virus assembly. *Structure* **3**, 255-263.

Noble, S. & Nibert, M. L. (1997a). Characterization of an ATPase activity in reovirus cores and its genetic association with core-shell protein lambda1. *J Virol* **71**, 2182-2191.

Noble, S. & Nibert, M. L. (1997b). Core protein μ2 is a second determinant of nucleoside triphosphatase activities by reovirus cores. *J Virol* **71**, 7728-7735.

Ojala, P. M., Paatero, A. O. & Bamford, D. H. (1994). NTP binding induces conformational changes in the double-stranded RNA bacteriophage o6 subviral particles. *Virology* **205**, 170-178.

Owen, N. C. & Munz, E. K. (1966). Observations on a strain of bluetongue virus by electron microscopy. *Onderstepoort J Vet Res* **33**, 9-14.

Paatero, A. O., Syvaoja, J. E. & Bamford, D. H. (1995). Double-stranded RNA bacteriophage phi 6 protein P4 is an unspecific nucleoside triphosphatase activated by calcium ions. *J Virol* **69**, 6729-6734.

Palacios, I., Weis, K., Klebe, C., Mattaj, I. W. & Dingwall, C. (1996). RAN/TC4 mutants identify a common requirement for snRNP and protein import into the nucleus. *Journal of Cell Biology* **133**, 485-494.

Parsonson, I. M. (1991). Overview of bluetongue virus infection of sheep. In *Bluetongue, African Horse-Sickness, and related Orbiviruses*, pp. 713-724. Edited by T. E. Walton & B. I. Osburn. Paris, France: CRC Press.

Pashev, I. G., Dimitrov, S. I. & Angelov, D. (1991). Crosslinking proteins to nucleic acids by ultraviolet laser irradiation. *Trends Biochem Sci* **16**, 323-326.

Paterson, R. G. & Lamb, R. A. (1993). The molecular biology of influenza viruses and paramyxoviruses. In *Molecular virology: a practical approach*, pp. 35-73. Edited by A. J. Davison & R. M. Elliott. Oxford: Oxford University Press.

Patton, J. T. (1986). Synthesis of simian rotavirus SA11 double-stranded RNA in a cell-free system. *Virus Res* **6**, 217-233.

Patton, J. T. (1990). Evidence for equimolar synthesis of double-strand RNA and minus-strand RNA in rotavirus-infected cells. *Virus Res* **17**, 199-208.

Patton, J. T. (1995). Structure and function of the rotavirus RNA-binding proteins. *J Gen Virol* **76**, 2633-2644.

Patton, J. T. (1996). Rotavirus VP1 alone specifically binds to the 3' end of viral mRNA, but the interaction is not sufficient to initiate minus-strand synthesis. *J Virol* **70**, 7940-7947.

Patton, J. T. & Gallegos, C. O. (1988). Structure and protein composition of the rotavirus replicase particle. *Virology* **166**, 358-365.

Patton, J. T. & Gallegos, C. O. (1990). Rotavirus RNA replication: single-stranded RNA extends from the replicase particle. *J Gen Virol* **71**, 1087-1094.

Patton, J. T., Salter Cid, L., Kalbach, A., Mansell, E. A. & Kattoura, M. (1993). Nucleotide and amino acid sequence analysis of the rotavirus nonstructural RNA-binding protein NS35. *Virology* **192**, 438-446.

Pearson, R. B., Mitchelhill, K. I. & Kemp, B. E. (1993). Studies of protein kinase/phosphatse specificity using synthetic peptides. In *Protein phosphorylation: a practical approach*, pp. 265-291. Edited by D. G. Hardie. Oxford: Oxford University Press.

Pedley, S., Mohamed, M. E. & Mertens, P. P. (1988). Analysis of genome segments from six different isolates of bluetongue virus using RNA-RNA hybridisation: a generalised coding assignment for bluetongue viruses. *Virus Res* **10**, 381-390.

Perczel, A., Park, K. & Fasman, G. D. (1992). Analysis of the circular dichroism spectrum of proteins using the convex constraint algorithm: a practical guide. *Anal Biochem* **203**, 83-93.

Petrie, B. L., Graham, D. Y., Hanssen, H. & Estes, M. K. (1982). Localization of rotavirus antigens in infected cells by ultrastructural immunocytochemistry. *J Gen Virol* **63**, 457-467.

Petrie, B. L., Greenberg, H. B., Graham, D. Y. & Estes, M. K. (1984). Ultrastructural localization of rotavirus antigens using colloidal gold. *Virus Res* **1**, 133-152.

Pickett, G. G. & Peabody, D. S. (1993). Encapsidation of heterologous RNAs by bacteriophage MS2 coat protein. *Nucleic Acids Res* **21**, 4621-4626.

Pinna, L. A. (1990). Casein kinase 2: an 'eminence grise' in cellular regulation? *Biochim Biophys Acta* **1054**, 267-284.

Pinna, L. A. & Ruzzene, M. (1996). How do protein kinases recognize their substrates? *Biochim Biophys Acta* **1314**, 191-225.

Pizarro, J. L., Sandino, A. M., Pizarro, J. M., Fernandez, J. & Spencer, E. (1991). Characterization of rotavirus guanylyltransferase activity associated with polypeptide VP3. *J Gen Virol* **72**, 325-332.

Pollack, J. R. & Ganem, D. (1994). Site-specific RNA binding by a hepatitis B virus reverse transcriptase initiates two distinct reactions: RNA packaging and DNA synthesis. *J Virol* **68**, 5579-5587.

Poncet, D., Aponte, C. & Cohen, J. (1993). Rotavirus protein NSP3 (NS34) is bound to the 3' end consensus sequence of viral mRNAs in infected cells. *J Virol* **67**, 3159-3165.

Poncet, D., Laurent, S. & Cohen, J. (1994). Four nucleotides are the minimal requirement for RNA recognition by rotavirus non-structural protein NSP3. *Embo J* **13**, 4165-4173.

Poncet, D., Lindenbaum, P., R, L. H. & Cohen, J. (1997a). In vivo and in vitro phosphorylation of rotavirus NSP5 correlates with its localization in viroplasms. *J Virol* **71**, 34-41.

Poncet, D., Vende, P., Piron, M. & Cohen, J. (1997b). Interaction of rotavirus NSP3 with the translation initiation factor eIF4G. In *6th International Symposium on Double Stranded RNA Viruses*. Mexico.

Poruchynsky, M. S. & Atkinson, P. H. (1988). Primary sequence domains required for the retention of rotavirus VP7 in the endoplasmic reticulum. *Journal of Cell Biology* **107**, 1697-1706.

Poruchynsky, M. S. & Atkinson, P. H. (1991). Rotavirus protein rearrangements in purified membrane-enveloped intermediate particles. *J Virol* **65**, 4720-4727.

Poruchynsky, M. S., Maass, D. R. & Atkinson, P. H. (1991). Calcium depletion blocks the maturation of rotavirus by altering the oligomerization of virus-encoded proteins in the ER. *Journal of Cell Biology* **114**, 651-656.

Prasad, B. V., Burns, J. W., Marietta, E., Estes, M. K. & Chiu, W. (1990). Localization of VP4 neutralization sites in rotavirus by three-dimensional cryo-electron microscopy. *Nature* **343**, 476-479.

Prasad, B. V., Rothnagel, R., Zeng, C. Q., Jakana, J., Lawton, J. A., Chiu, W. & Estes, M. K. (1996). Visualization of ordered genomic RNA and localization of transcriptional complexes in rotavirus. *Nature* **382**, 471-473.

Prasad, B. V., Wang, G. J., Clerx, J. P. & Chiu, W. (1988). Three-dimensional structure of rotavirus. *J Mol Biol* **199**, 269-275.

Prasad, B. V., Yamaguchi, S. & Roy, P. (1992). Three-dimensional structure of single-shelled bluetongue virus. *J Virol* **66**, 2135-2142.

Pritlove, D. C., Fodor, E., Seong, B. L. & Brownlee, G. G. (1995). In vitro transcription and polymerase binding studies of the termini of influenza A virus cRNA: evidence for a cRNA panhandle. *J Gen Virol* **76**, 2205-2213.

Qiao, X., Qiao, J. & Mindich, L. (1997). Stoichiometric packaging of the three genomic segments of double-stranded RNA bacteriophage phi6. *Proc Natl Acad Sci U S A* **94**, 4074-4079.

Ramadevi, N., Rodriguez, J. & Roy, P. (1997). Leucine zipper-like domain is essential for dimerization and encapsidation of bluetongue virus nucleocapsid protein VP4. *J Virol* **In Press**.

Ramig, R. F. (1982). Isolation and genetic characterization of temperature-sensitive mutants of simian rotavirus SA11. *Virology* **120**, 93-105.

Ramig, R. F. & Petrie, B. L. (1984). Characterization of temperature-sensitive mutants of simian rotavirus SA11: protein synthesis and morphogenesis. *J Virol* **49**, 665-673.

Ranjan, M., Tafuri, S. R. & Wolffe, A. P. (1993). Masking mRNA from translation in somatic cells. *Genes Dev* **7**, 1725-1736.

Rao, C. D., Das, M., Ilango, P., Lalwani, R., Rao, B. S. & Gowda, K. (1995). Comparative nucleotide and amino acid sequence analysis of the sequence-specific RNA-binding rotavirus nonstructural protein NSP3. *Virology* **207**, 327-333.

Rao, C. D., Kiuchi, A. & Roy, P. (1983). Homologous terminal sequences of the genome double-stranded RNAs of bluetongue virus. *J Virol* **46**, 378-383.

Richter, J. D. & Smith, L. D. (1984). Reversible inhibition of translation by Xenopus oocyte-specific proteins. *Nature* **309**, 378-380.

Rodnina, M. V., Savelsbergh, A., Katunin, V. I. & Wintermeyer, W. (1997). Hydrolysis of GTP by elongation factor G drives tRNA movement on the ribosome. *Nature* **385**, 37-41.

Rossmann, M. G., Abad Zapatero, C., Erickson, J. W. & Savithri, H. S. (1983). RNA-protein interactions in some small plant viruses. *J Biomol Struct Dyn* **1**, 565-579.

Rossmann, M. G., Olson, N. H., Kolatkar, P. R., Oliveira, M. A., Cheng, R. H., Greve, J. M., McClelland, A. & Baker, T. S. (1994). Crystallographic and cryo EM analysis of virion-receptor interactions. *Arch Virol Suppl* **9**, 531-541.

Rost, B. & Sander, C. (1993). Prediction of protein secondary structure at better than 70% accuracy. *J Mol Biol* **232**, 584-599.

Rost, B. & Sander, C. (1994). Combining evolutionary information and neural networks to predict protein secondary structure. *Proteins* **19**, 55-72.

Rost, B., Sander, C. & Schneider, R. (1994). PHD--an automatic mail server for protein secondary structure prediction. *Comput Appl Biosci* **10**, 53-60.

Roy, P. (1991). Towards the control of emerging bluetongue disease, 1 edn, pp. 71. London: Oxford Virology Publications.

Roy, P. (1993). Dissecting the assembly of orbiviruses. *Trends Microbiol* **1**, 299-305.

Roy, P. (1996a). Orbivirus structure and assembly. *Virology* **216**, 1-11.

Roy, P. (1996b). Orbiviruses and their replication. In *Field's Virology*, 3rd edn, pp. 1709-1734. Edited by B. N. Fields. Philadelphia: Lippincott-Raven.

Roy, P., Adachi, A., Urakawa, T., Booth, T. F. & Thomas, C. P. (1990a). Identification of bluetongue virus VP6 protein as a nucleic acid-binding protein and the localization of VP6 in virus-infected vertebrate cells. *J Virol* **64**, 1-8.

Roy, P., Fukusho, A., Ritter, G. D. & Lyon, D. (1988). Evidence for genetic relationship between RNA and DNA viruses from the sequence homology of a putative polymerase gene of bluetongue virus with that of vaccinia virus: conservation of RNA polymerase genes from diverse species. *Nucleic Acids Res* **16**, 11759-11767.

Roy, P., Marshall, J. J. & French, T. J. (1990b). Structure of the bluetongue virus genome and its encoded proteins. *Curr Top Microbiol Immunol* **162**, 43-87.

Rumenapf, T., Brown, D. T., Strauss, E. G., Konig, M., Rameriz Mitchel, R. & Strauss, J. H. (1995). Aura alphavirus subgenomic RNA is packaged into virions of two sizes. *J Virol* **69**, 1741-1746.

Rychlik, W. (1992). Oligo 4.1: primer analysis software. Plymouth: Natinal Biosciences Inc.,.

Sandino, A. M., Jashes, M., Faundez, G. & Spencer, E. (1986). Role of the inner protein capsid on in vitro human rotavirus transcription. *J Virol* **60**, 797-802.

Schmid, F. X. (1997). Optical spectroscopy to characterise protein conformation and conformational changes. In *Protein structure: a pratical approach*, 2nd edn, pp. 261-297. Edited by T. E. Creighton. Oxford: Oxford University Press.

Schoehn, G., Moss, S. R., Nuttall, P. A. & Hewat, E. A. (1997). Structure of Broadhaven virus by cryoelectron microscopy: correlation of structural and antigenic properties of Broadhaven virus and Bluetongue virus outer capsid proteins. *Virology* **235**, 191-200.

Schubert, U., Schneider, T., Henklein, P., Hoffmann, K., Berthold, E., Hauser, H., Pauli, G. & Porstmann, T. (1992). Human-immunodeficiency-virus-type-1-encoded Vpu protein is phosphorylated by casein kinase II. *Eur J Biochem* **204**, 875-883.

Schultz, D. E., Hardin, C. C. & Lemon, S. M. (1996). Specific interaction of glyceraldehyde 3-phosphate dehydrogenase with the 5'-nontranslated RNA of hepatitis A virus. *J Biol Chem* **271**, 14134-14142.

Schwemmle, M., De, B., Shi, L., Banerjee, A. & Lipkin, W. I. (1997). Borna disease virus P-protein is phosphorylated by protein kinase Cε and casein kinase II. *J Biol Chem* **In Press**.

Schwer, B. & Guthrie, C. (1992a). A conformational rearrangement in the spliceosome is dependent on PRP16 and ATP hydrolysis. *Embo J* **11**, 5033-5039.

Schwer, B. & Guthrie, C. (1992b). A dominant negative mutation in a spliceosomal ATPase affects ATP hydrolysis but not binding to the spliceosome. *Mol Cell Biol* **12**, 3540-3547.

Sellers, R. F. (1975). Bluetongue in Cyprus. *Aust Vet J* **51**, 198-203.

Shatkin, A. J., Both, G. W., Furuichi, Y., Kozak, M. & Muthukrishnan, S. (1976). 5'-terminal 7-methylguanosine in viral mRNA's and its role in translation. In *Animal virology*, pp. 659-676. Edited by e. a. Baltimore D. New York: Academic Press.

Shaw, A. L., Rothnagel, R., Chen, D., Ramig, R. F., Chiu, W. & Prasad, B. V. (1993). Three-dimensional visualization of the rotavirus hemagglutinin structure. *Cell* **74**, 693-701.

Shaw, A. L., Samal, S. K., Subramanian, K. & Prasad, B. V. (1996). The structure of aquareovirus shows how the different geometries of the two layers of the capsid are reconciled to provide symmetrical interactions and stabilization. *Structure* **4**, 957-967.

Shen, S., Burke, B. & Desselberger, U. (1994). Rearrangement of the VP6 gene of a group A rotavirus in combination with a point mutation affecting trimer stability. *J Virol* **68**, 1682-1688.

Shimshony, A., Barzilai, E., Savir, D. & Davidson, M. (1988). Epidemiology and control of bluetongue disease in Israel. *Rev. Sci. Tech. Off. Int. Epiz.* **7**, 311.

Simmons, D. T., Chou, W. & Rodgers, K. (1986). Phosphorylation downregulates the DNA-binding activity of simian virus 40 T antigen. *J Virol* **60**, 888-894.

Sommerville, J. & Ladomery, M. (1996a). Masking of mRNA by Y-box proteins. *Faseb J* **10**, 435-443.

Sommerville, J. & Ladomery, M. (1996b). Transcription and masking of mRNA in germ cells: involvement of Y-box proteins. *Chromosoma* **104**, 469-478.

Spadafora, D., Canter, D. M., Jackson, R. L. & Perrault, J. (1996). Constitutive phosphorylation of the vesicular stomatitis virus P protein modulates polymerase complex formation but is not essential for transcription or replication. *J Virol* **70**, 4538-4548.

Spencer, E. & Garcia, B. I. (1984). Effect of S-adenosylmethionine on human rotavirus RNA synthesis. *J Virol* **52**, 188-197.

Spreull, J. (1905). Malarial catarrhal fever (bluetongue) of sheep in South Africa. *J. Comp. Pathol. Thera.* **18**, 321.

Stacy Phipps, S. & Patton, J. T. (1987). Synthesis of plus- and minus-strand RNA in rotavirus-infected cells. *J Virol* **61**, 3479-3484.

Staeuber, N., Martinez-Costas, J., Sutton, G., Monastyrskaya, K. & Roy, P. (1997). Bluetongue virus VP6 binds ATP, exhibits an RNA-dependent adenosine nucleoside triphosphatase (ATPase) function and a helicase activity that catalyses the unwinding of double-stranded RNA substrates. *Journal of Virology* **71**, 7220-7226.

Standart, N. & Jackson, R. (1994). Translational regulation. Y the message is masked? *Curr Biol* **4**, 939-941.

Stefano, J. E. (1984). Purified lupus antigen La recognizes an oligouridylate stretch common to the 3' termini of RNA polymerase III transcripts. *Cell* **36**, 145-154.

Stoeckle, M. Y., Shaw, M. W. & Choppin, P. W. (1987). Segment-specific and common nucleotide sequences in the noncoding regions of influenza B virus genome RNAs. *Proc Natl Acad Sci U S A* **84**, 2703-2707.

Studdert, M. J., Pangborn, J. & Addison, R. B. (1966). Bluetongue virus structure. *Virology* **29**, 509-511.

Tabernero, C., Zolotukhin, A. S., Valentin, A., Pavlakis, G. N. & Felber, B. K. (1996). The posttranscriptional control element of the simian retrovirus type 1 forms an extensive RNA secondary structure necessary for its function. *J Virol* **70**, 5998-6011.

Tan, R. & Frankel, A. D. (1994). Costabilization of peptide and RNA structure in an HIV Rev peptide-RRE complex. *Biochemistry* **33**, 14579-14585.

Taniguchi, K., Kojima, K. & Urasawa, S. (1996). Nondefective rotavirus mutants with an NSP1 gene which has a deletion of 500 nucleotides, including a cysteine-rich zinc finger motif-encoding region (nucleotides 156 to 248), or which has a nonsense codon at nucleotides 153-155. *J Virol* **70**, 4125-4130.

Taylor, J. A., JA, O. B. & Yeager, M. (1996). The cytoplasmic tail of NSP4, the endoplasmic reticulum-localized non-structural glycoprotein of rotavirus, contains distinct virus binding and coiled coil domains. *Embo J* **15**, 4469-4476.

Theiler, A. (1908). Inoculation of sheep against bluetongue and results in practice. *Vet J* **64**, 600-607.

Theron, J., Huismans, H. & Nel, L. H. (1996). Identification of a short domain within the non-structural protein NS2 of epizootic haemorrhagic disease virus that is important for single strand RNA-binding activity. *J Gen Virol* **77**, 129-137.

Theron, J. & Nel, L. H. (1997). Stable protein-RNA interaction involves the terminal domains of bluetongue virus mRNA, but not the terminally conserved sequences. *Virology* **229**, 134-142.

Theron, J., Uitenweerde, J. M., Huismans, H. & Nel, L. H. (1994). Comparison of the expression and phosphorylation of the non-structural protein NS2 of three different orbiviruses: evidence for the involvement of an ubiquitous cellular kinase. *J Gen Virol* **75**, 3401-3411.

Thomas, C. P. (1990). The expression of bluetongue virus non-structural protein NS2 and its structure function relationship. *D.Phil Thesis.* University of Oxford.

Thomas, C. P., Booth, T. F. & Roy, P. (1990). Synthesis of bluetongue virus-encoded phosphoprotein and formation of inclusion bodies by recombinant baculovirus in insect cells: it binds the single-stranded RNA species. *J Gen Virol* **71**, 2073-2083.

Tian, P., Ball, J. M., Zeng, C. Q. & Estes, M. K. (1996). The rotavirus nonstructural glycoprotein NSP4 possesses membrane destabilization activity. *J Virol* **70**, 6973-6981.

Tian, P., Estes, M. K., Hu, Y., Ball, J. M., Zeng, C. Q. & Schilling, W. P. (1995). The rotavirus nonstructural glycoprotein NSP4 mobilizes Ca2+ from the endoplasmic reticulum. *J Virol* **69**, 5763-5772.

Tian, P., Hu, Y., Schilling, W. P., Lindsay, D. A., Eiden, J. & Estes, M. K. (1994). The nonstructural glycoprotein of rotavirus affects intracellular calcium levels. *J Virol* **68**, 251-257.

Tian, Y., Tarlow, O., Ballard, A., Desselberger, U. & McCrae, M. A. (1993). Genomic concatemerization/deletion in rotaviruses: a new mechanism for

generating rapid genetic change of potential epidemiological importance. *J Virol* **67**, 6625-6632.

Timmins, P. A., Wild, D. & Witz, J. (1994). The three-dimensional distribution of RNA and protein in the interior of tomato bushy stunt virus: a neutron low-resolution single-crystal diffraction study. *Structure* **2**, 1191-1201.

Tucker, S. P., Penn, C. R. & McCauley, J. W. (1991). Characterisation of the influenza virus associated protein kinase and its resemblance to casein kinase II. *Virus Res* **18**, 243-261.

Uitenweerde, J. M., Theron, J., Stoltz, M. A. & Huismans, H. (1995). The multimeric nonstructural NS2 proteins of bluetongue virus, African horsesickness virus, and epizootic hemorrhagic disease virus differ in their single-stranded RNA-binding ability. *Virology* **209**, 624-632.

Urakawa, T., Ritter, D. G. & Roy, P. (1989). Expression of largest RNA segment and synthesis of VP1 protein of bluetongue virus in insect cells by recombinant baculovirus: association of VP1 protein with RNA polymerase activity. *Nucleic Acids Res* **17**, 7395-7401.

Urakawa, T. & Roy, P. (1988). Bluetongue virus tubules made in insect cells by recombinant baculoviruses: expression of the NS1 gene of bluetongue virus serotype 10. *J Virol* **62**, 3919-3927.

Valenzuela, S., Pizarro, J., Sandino, A. M., Vasquez, M., Fernandez, J., Hernandez, O., Patton, J. & Spencer, E. (1991). Photoaffinity labeling of rotavirus VP1 with 8-azido-ATP: identification of the viral RNA polymerase. *J Virol* **65**, 3964-3967.

van der Graaf, M. & Hemminga, M. A. (1991). Conformational studies on a peptide fragment representing the RNA-binding N-terminus of a viral coat protein using circular dichroism and NMR spectroscopy. *Eur J Biochem* **201**, 489-494.

Van Dijk, A. A. & Huismans, H. (1980). The in vitro activation and further characterization of the bluetongue virus-associated transcriptase. *Virology* **104**, 347-356.

Van Dijk, A. A. & Huismans, H. (1982). The effect of temperature on the in vitro transcriptase reaction of bluetongue virus, epizootic haemorrhagic disease virus and African horsesickness virus. *Onderstepoort J Vet Res* **49**, 227-232.

Van Dijk, A. A. & Huismans, H. (1988). In vitro transcription and translation of bluetongue virus mRNA. *J Gen Virol* **69**, 573-581.

van Staden, V., Theron, J., Greyling, B. J., Huismans, H. & Nel, L. H. (1991). A comparison of the nucleotide sequences of cognate NS2 genes of three different orbiviruses. *Virology* **185**, 500-504.

Vasquez, M., Sandino, A. M., Pizarro, J. M., Fernandez, J., Valenzuela, S. & Spencer, E. (1993). Function of rotavirus VP3 polypeptide in viral morphogenesis. *J Gen Virol* **74**, 937-941.

Verwoerd, D. W. (1969). Purification and characterization of bluetongue virus. *Virology* **38**, 203-212.

Verwoerd, D. W., Els, H. J., De Villiers, E. M. & Huismans, H. (1972). Structure of the bluetongue virus capsid. *J Virol* **10**, 783-794.

Verwoerd, D. W. & Huismans, H. (1972). Studies on the in vitro and the in vivo transcription of the bluetongue virus genome. *Onderstepoort J Vet Res* **39**, 185-191.

Veschambre, P., Roisin, A. & Jalinot, P. (1997). Biochemical and functional interaction of the human immunodeficiency virus type 1 Tat transactivator with the general transcription factor TFIIB. *J Gen Virol* **78**, 2235-2245.

Wade Evans, A. M. (1990). Complete sequence of genome segment 10, encoding the NS3 protein, of bluetongue virus, serotype 1 from South Africa. *Nucleic Acids Res* **18**, 4920.

Wade, R. H. & Hewat, E. A. (1994). Cryoelectron microscopy of macromolecular complexes. *Biol Cell* **80**, 211-220.

Wang, H. W., Chen, P. J., Lee, C. Z., Wu, H. L. & Chen, D. S. (1994). Packaging of hepatitis delta virus RNA via the RNA-binding domain of hepatitis delta antigens: different roles for the small and large delta antigens. *J Virol* **68**, 6363-6371.

Welch, S. K., Crawford, S. E. & Estes, M. K. (1989). Rotavirus SA11 genome segment 11 protein is a nonstructural phosphoprotein. *J Virol* **63**, 3974-3982.

Wemmer, D. E. (1996). New features in RNA recognition: a Tat-TAR complex. *Chem Biol* **3**, 17-19.

Whetter, L. E., Gebhard, D. H. & MacLachlan, N. J. (1990). Temporal appearance of structural and nonstructural bluetongue viral proteins in infected cells, as determined by immunofluorescence staining and flow cytometry. *Am J Vet Res* **51**, 1174-1179.

Wiener, J. R. & Joklik, W. K. (1987). Comparison of the reovirus serotype 1, 2, and 3 S3 genome segments encoding the nonstructural protein sigma NS. *Virology* **161**, 332-339.

Wikoff, W. R., Tsai, C. J., Wang, G., Baker, T. S. & Johnson, J. E. (1997). The structure of cucumber mosaic virus: cryoelectron microscopy, X-ray crystallography, and sequence analysis. *Virology* **232**, 91-97.

Will, C. L., Kastner, B. & Luhrmann, R. (1994). Analysis of ribonucleoprotein interactions. In *RNA processing: a practical approach*, pp. 141-177. Edited by S. J. Higgins & B. D. Hames. Oxford: Oxford University Press.

Williamson, J. R., Battiste, J. L., Mao, H. & Frankel, A. D. (1995). Interaction of HIV Rev peptides with the Rev response element RNA. *Nucleic Acids Symp Ser* **33**, 46-48.

Wolffe, A. P. (1994). Structural and functional properties of the evolutionarily ancient Y-box family of nucleic acid binding proteins. *Bioessays* **16**, 245-251.

Woody, R. W. (1985). Circular dichroism of peptides. In *The Peptides*, pp. 15-114. Edited by V. J. Hruby. New York: Academic Press.

Wu, X., Chen, S. Y., Iwata, H., Compans, R. W. & Roy, P. (1992). Multiple glycoproteins synthesized by the smallest RNA segment (S10) of bluetongue virus. *J Virol* **66**, 7104-7112.

Yang, J. T., Wu, C. S. & Martinez, H. M. (1986). Calculation of protein conformation from circular dichroism. *Methods Enzymol.* **130**, 208-269.

Yang, Y. Y. & Li, J. K. (1993). Glycosylation of the major outer capsid protein of bluetongue viruses. *Virology* **194**, 350-354.

Yeager, M., Berriman, J. A., Baker, T. S. & Bellamy, A. R. (1994). Three-dimensional structure of the rotavirus haemagglutinin VP4 by cryo-electron microscopy and difference map analysis. *Embo J* **13**, 1011-1018.

Yeager, M., Dryden, K. A., Olson, N. H., Greenberg, H. B. & Baker, T. S. (1990). Three-dimensional structure of rhesus rotavirus by cryoelectron microscopy and image reconstruction. *Journal of Cell Biology* **110**, 2133-2144.

Zeng, C. Q., Labbe, M., Cohen, J., Prasad, B. V., Chen, D., Ramig, R. F. & Estes, M. K. (1994). Characterization of rotavirus VP2 particles. *Virology* **201**, 55-65.

Zeng, C. Q., Wentz, M. J., Cohen, J., Estes, M. K. & Ramig, R. F. (1996). Characterization and replicase activity of double-layered and single-layered rotavirus-like particles expressed from baculovirus recombinants. *J Virol* **70**, 2736-2742.

Zhang, Y., Feigenblum, D. & Schneider, R. J. (1994). A late adenovirus factor induces eIF-4E dephosphorylation and inhibition of cell protein synthesis. *J Virol* **68**, 7040-7050.

Zhao, Y., Thomas, C., Bremer, C. & Roy, P. (1994). Deletion and mutational analyses of bluetongue virus NS2 protein indicate that the amino but not the carboxy terminus of the protein is critical for RNA-protein interactions. *J Virol* **68**, 2179-2185.

Zoll, J., Galama, J. M., van Kuppeveld, F. J. & Melchers, W. J. (1996). Mengovirus leader is involved in the inhibition of host cell protein synthesis. *J Virol* **70**, 4948-4952.

APPENDIX

Secondary structure predictions for orbivirus NS2, reovirus σNS and rotavirus NSP2 and NSP5. Predictions were made by the PHD server (http://www.embl-heidelberg.de/predictprotein/phd_pred.html) at EMBL (Rost & Sander, 1993, Rost & Sander, 1994, Rost *et al.*, 1994).

BTV NS2 alignments and structure prediction

The green underlined region shows the amino acids shown to be important for RNA-binding by Zhao *et al.*, (1994). The stars correspond to the region identified by van Staden *et al.*, (1991) in orbivirus NS2 as well as reovirus σNS and rotavirus NSP3. Mutations in this region of EHDV were shown to have an effect on RNA-binding (Theron *et al.*, 1996). The red balls indicate the serine residues found in CKII consensus phosphorylation sites in BTV-10.

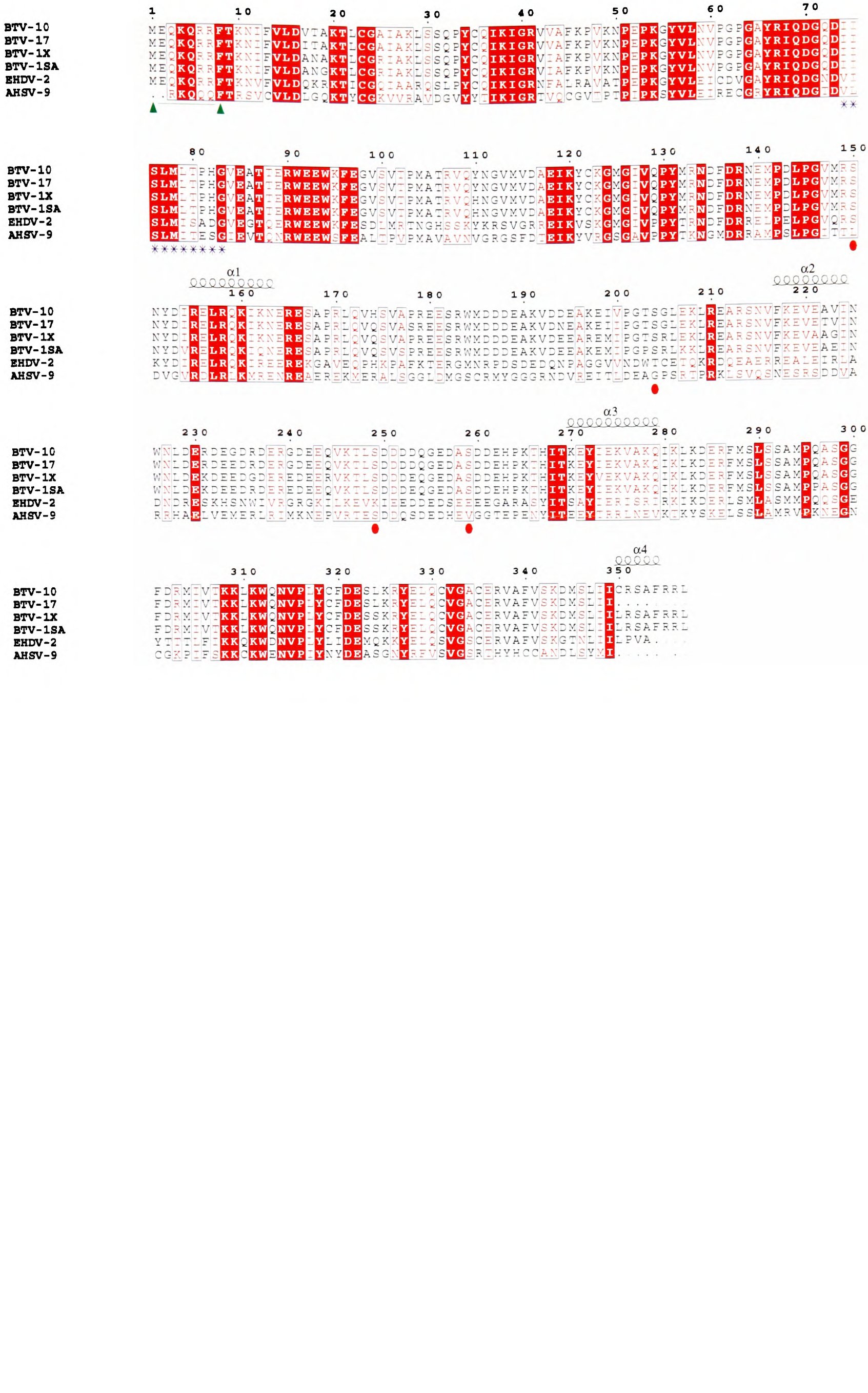
BTV-10
BTV-17
BTV-1X
BTV-1SA
EHDV-2
AHSV-9
α1
α2
α3
α4

Reovirus σNS alignments and structure predictions

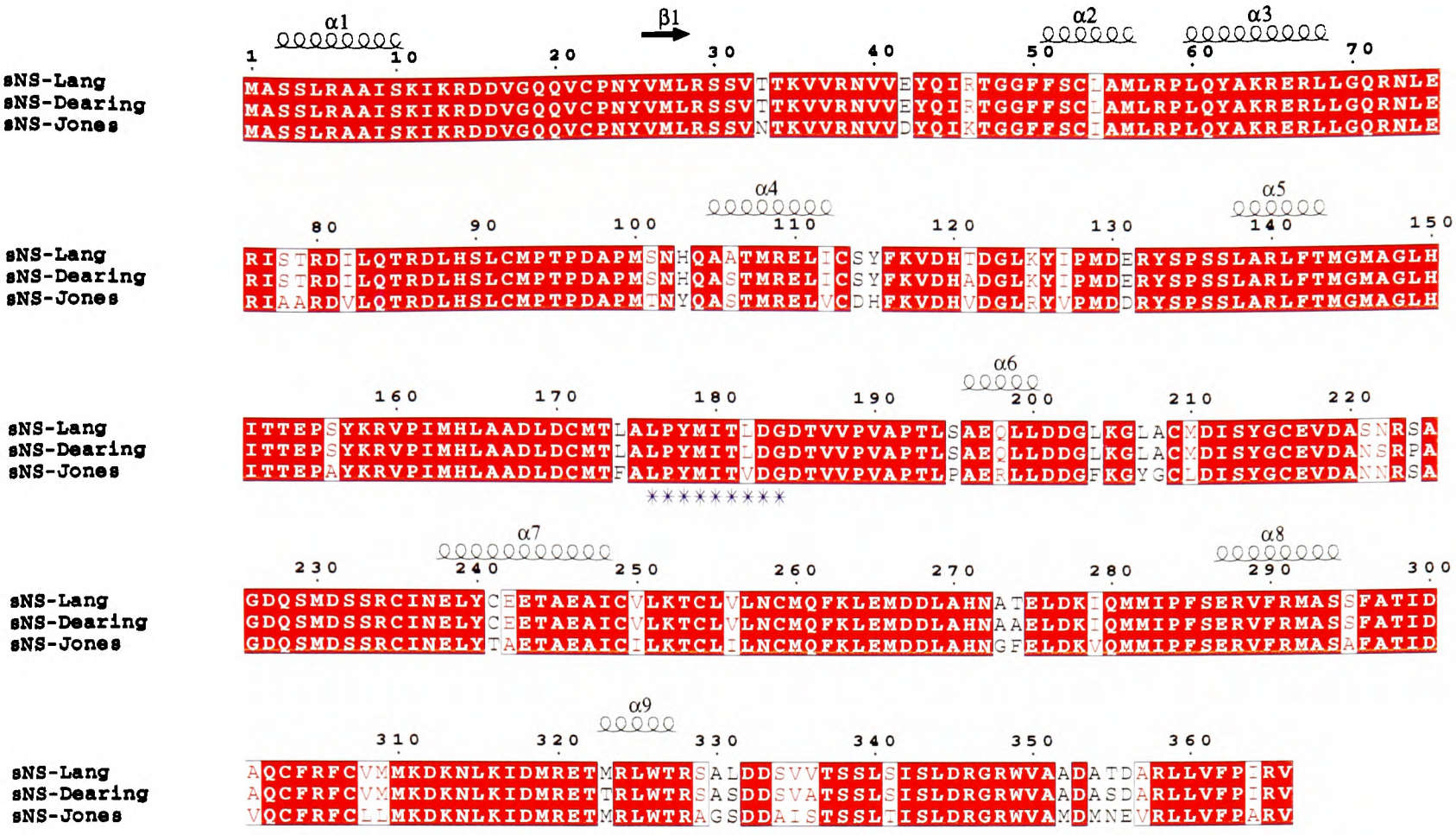
α1
β1
α2
α3
1
10
20
30
40
50
60
70
sNS-Lang MASSLRAAISKIKRDDVGQQVCPNYVMLRSSVTTKVVRNVVEYQIRTGGFFSCIAMLRPLQYAKRERLLGQRNLE
sNS-Dearing MASSLRAAISKIKRDDVGQQVCPNYVMLRSSVTTKVVRNVVEYQIRTGGFFSCIAMLRPLQYAKRERLLGQRNLE
sNS-Jones MASSLRAAISKIKRDDVGQQVCPNYVMLRSSVNTKVVRNVVDYQIKTGGFFSCIAMLRPLQYAKRERLLGQRNLE
α4
α5
80
90
100
110
120
130
140
150
sNS-Lang RISTRDILQTRDLHSLCMPTPDAPMSNHQAATMRELICSYFKVDHTDGLKYIPMDERYSPSSLARLFTMGMAGLH
sNS-Dearing RISTRDILQTRDLHSLCMPTPDAPMSNHQASTMRELICSYFKVDHADGLKYIPMDERYSPSSLARLFTMGMAGLH
sNS-Jones RIAARDVLQTRDLHSLCMPTPDAPMINYQASTMRELVCDHFKVDHVDGLRYVPMDDRYSPSSLARLFTMGMAGLH
α6
160
170
180
190
200
210
220
sNS-Lang ITTEPSYKRVPIMHLAADLDCMTLALPYMITLDGDTVVPVAPTLSAEQLLDDGLKGLACMDISYGCEVDASNRSA
sNS-Dearing ITTEPSYKRVPIMHLAADLDCMTLALPYMITLDGDTVVPVAPTLSAEQLLDDGLKGLACMDISYGCEVDANSRPA
sNS-Jones ITTEPAYKRVPIMHLAADLDCMTFALPYMITVDGDTVVPVAPTLPAERLLDDGFKGYGCLDISYGCEVDANNRSA
α7
α8
230
240
250
260
270
280
290
300
sNS-Lang GDQSMDSSRCINELYCEETAEAICVLKTCLVLNCMQFKLEMDDLAHNATELDKIQMMIPFSERVFRMASSFATID
sNS-Dearing GDQSMDSSRCINELYCEETAEAICVLKTCLVLNCMQFKLEMDDLAHNAAELDKIQMMIPFSERVFRMASSFATID
sNS-Jones GDQSMDSSRCINELYTAETAEAICILKTCLILNCMQFKLEMDDLAHNGFELDKVQMMIPFSERVFRMASAFATID
α9
310
320
330
340
350
360
sNS-Lang AQCFRFCVMMKDKNLKIDMRETMRLWTRSALDDSVVTSSLSISLDRGRWVAADATDARLLVFPIRV
sNS-Dearing AQCFRFCVMMKDKNLKIDMRETTRLWTRSASDDSVATSSLSISLDRGRWVAADASDARLLVFPIRV
sNS-Jones VQCFRFCLLMKDKNLKIDMRETMRLWTRAGSDDAISTSSLTISLDRGRWVAMDMNEVRLLVFPARV

Rotavirus NSP2 alignments and structure prediction

```
                                  α1
                                 ooooo                                                                                  ς
                  1                 10                  20                  30                  40                  50                  60                  70
vn35_rothd        MAELACFCYPHLENDSYKFIPFNNLAIKCMLIAKVDKKDQDKFYNSIIYGIAPPPQFKKRYNTNDNSRGMNYETS
vn35_rotbu        MAELACFCYPHLENDSYKFIPFNNLAIKCMLIAKVDRKDQDKFYNSIIYGIAPPPQFKKRYNTNDNSRGMNYETS
vn35_rots1        MAELACFCYPHLENDSYRFIPFNSLAIKCMLIAKVDKKDQDKFYNSIIYGIAPPPQFKKRYNTSDNSRGMNYETS
vn35_rotbn        MAELACFCYPHLENDSYRFIPFNSLAIKCMLIAKVDKKDQDKFYNSIIYGIAPPPQFKKRYNTNDNSRGMNYETP
vn35_rothw        MAELACFCYPHLENDSYKFIPFNNLAIKCMLIAKVEKKDQDKFYNSIVYGIAPPPQFKKRYNTSDNSRGMNYETT
vn35_rotp5        MAELACFCYPHLEKDSYKFIPFNSLAIKCMLIAKVDKKDQDKFYNSIVYGIAPPPQFKKRYNTNDNSRGMNFETS
vn35_rotsr        MAELACFCYPHLENDSYKFIPFNNLAIKAMLIAKVDKKDMDKFYDSIIYGIAPPPQFKKRYNTNDNSRGMNFETT
vn35_rotsp        MAELACFCYPHLENDSYKFIPFNNLAIKAMLIAKVDKKDMDKFYDSIIYGIAPPPQFKKRYNTNDNSRGMNFETT
vn35_rott1        MAELACFCYPCDREGA.SVARYSRSAIKCMLSAKIDKSHSSQPYDTQVYGIAPPPVYKKRFNDGNNSRGMNFDTD

                       α2                                                α3
                     ooooooooooooo                                     ooooo
                          80                  90                  100                 110                 120                 130                 140                 150
vn35_rothd        MFNKVAALICEALNSTKVTQSDIASVLSRVVSVRHLENLVLRRENHQDVLFHSKELLLKSVLIAIGHSKEIETTA
vn35_rotbu        MFNKVAVLICEALNSIKVTQSDVANVLSRVVSVRHLENLVLRRENHQDVLFHSKELLLKSVLIAIGHSKEIETTA
vn35_rots1        MFNKVAALICEALNSIKVTQSDVASVLSKIVSVRHLENLVLRRENHQDVLFHSKELLLKSVLIAIGHSKEIETTA
vn35_rotbn        MFNKVAVLICEALNSIKVTQSDVASVLSKVISVRHLENLVLRRENHQDVLFHSKELLLRSVLIAIGHSKEIETTA
vn35_rothw        MFNKVAVLICEALNSIKITQSDVANVLSRVVSVRHLENLVLRKENHQDVLFHSKELLLKSVLIAIGQSKEIETTA
vn35_rotp5        MFNKVAILICEALNSIKVTQSDVANVLSRVVSVRHLENLVLRKENHQDVLFHSKELLLKAVLIAIGQSKEIETTA
vn35_rotsr        MFTKVAMLICEALNSLKVTQANVSNVLSRVVSIRHLENLVIRKENPQDILFHSKDLLLKSTLIAIGQSKEIETTI
vn35_rotsp        MFTKVAMLICEALNSIKVTQANVSNVLSRVVSIRHLENLVIRKENPQDILFHSKDLLLKSTLIAIGQSKEIETTI
vn35_rott1        MVDKVADLLVQILNGIKIGKDKAAEIMAVPISVRHLENLIVRIENKDDILSADPNLITKSVLIAMGLIKDCEITT

                                                  β1                                  α4
                                                 ->                                ooooooooooooo
                          160                 170                 180                 190                 200                 210                 220
vn35_rothd        TAEGGEIVFQNTAFTMWRLTYLEHKLMPILDPNFIEYKITVNEGKPISESHIKELIAELRWQYNKFAVITHGKGH
vn35_rotbu        TAEGGEIVFQNAAFTMWKLTYLEHKLMPILDQNFIEYKITVNEDKPISESHVKELIAELRWQYNKFAVITHGKGH
vn35_rots1        TAEGGEIVFQNAAFTMWKLTYLEHKLMPILDQNFIEYKITLNEDKPISESHVKELIAELRWQYNKFAVITHGKGH
vn35_rotbn        TAEGGEVVFQNAAFTMWKLTYLEHRLMPILDQNFIEYKITVNEDKPISESHVRELIAELRWQYNKFAVITHGKGH
vn35_rothw        TAEGGEIVFQNAAFTMWKLTYLDHKLMPILDQNFIEYKITLNEDKPISDVCIKELVAELRWQYNRFAVITHGKGH
vn35_rotp5        TAEGGEIVFQNAAFTMWKLTYLDHKLMPILDQNFIEYKITLNEDKPISDACVKELVAELRWQYNRFAVITHGKGH
vn35_rotsr        TAEGGEIVFQNAAFTMWKLTYLEHQLMPILDQNFIEYKVTLNEDKPISDVHVKELVAELRWQYNKFAVITHGKGH
vn35_rotsp        TAEGGEIVFQNAAFTMWKLTYLEHQLMPILDQNFIEYKVTLNEDKPISDVHVKELVAELRWQYNKFAVITHGKGH
vn35_rott1        TAEGGDIVFQNQGFTMWRLDYKSHVLMPITDPNFVEYKITLNHTNPIDDKIVKELVAELRWQYNKFAVITHGKGH

                  β2                                                α5                                  α6
                 ->                                               ooooooooooo                        ooooooooo
                          230                 240                 250                 260                 270                 280                 290                 300
vn35_rothd        YRVVKYSSVANHADRVYATYKSNNKNGNMLEFNLLDQRIIWQNWYAFTSSMKQGNTLDTQKKLLFQKIKRESNPF
vn35_rotbu        YRVVKYSSVANHADRVYATFKSNNKNGNVLEFNLLDQRIIWQNWYAFTSSMKQGNTLDIQKKLLFQKMKRESNPF
vn35_rots1        YRVVKYSSVANHADRVYATFKSNNKNGNMIEFNLLDQRIIWQNWYAFTSSMKQGNTLEIQKKLLFQKMKRESNPF
vn35_rotbn        YRVVKYSSVANHADRVYATFKSNNKNGNVIEFNLLDQRIIWQNWYAFTSSMKQGNTLEIQKKLLFQKMKRESNPF
vn35_rothw        YRVVKYSSVANHADRVFATYKNSAKSGNVIDFNLLDQRIIWQNWYAFTSSMKQGNTLDVQKKLLFQKMKQEKNPF
vn35_rotp5        YRVVKYSSVANHADRVFATYKNNAKSGNVTDFNLLDQRIIWQNWYAFTSSMKQGNTLDVQKKLLFQKMKQEKNPF
vn35_rotsr        YRIVKYSSVANHADRVYATFKSNVKTGVNNDFNLLDQRIIWQNWYAFTSSMKQGNTLDVQKRLLFQKMKPEKNPF
vn35_rotsp        YRIVKYSSVANHADRVYATFKSNVKTGVNNDFNLLDQRIIWQNWYAFTSTMKQGNTLDVQKRLLFQKMKPEKNPF
vn35_rott1        YRVVRYSTVANHADRVYSTFKSIQKRNPSYKFNELDTRVIWINWAAFVKSMLNGMKLDDSKRLLFTKMKPNESSF

                                  310
                                  .
vn35_rothd        KGLSTDRKMDEVSQIGI
vn35_rotbu        KGLSTDRKMDEVSQIGI
vn35_rots1        KGLSTDRKMDEVSQIGI
vn35_rotbn        KGLSTDRKMDEVSQIGI
vn35_rothw        KGLSTDRKMDEVSHVGI
vn35_rotp5        KGLSTDRKMDEVSHVGI
vn35_rotsr        KGLSTDRKMDEVSQVGV
vn35_rotsp        KGLSTDRKMDEVSQVGV
vn35_rott1        KGVITERKLDEVSLLG.
```

Rotavirus NSP5 alignments and structure prediction

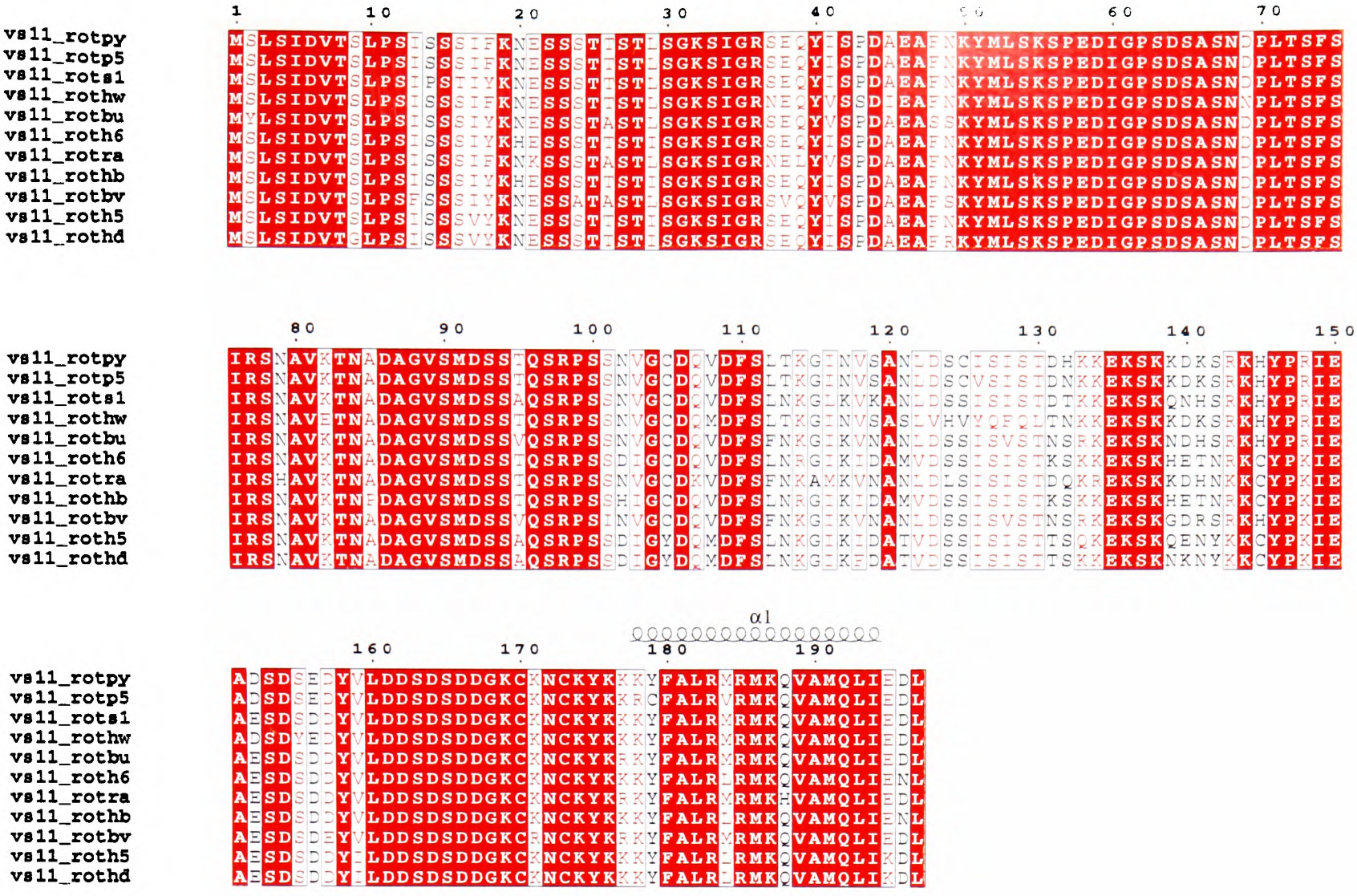
vs11_rotpy
vs11_rotp5
vs11_rots1
vs11_rothw
vs11_rotbu
vs11_roth6
vs11_rotra
vs11_rothb
vs11_rotbv
vs11_roth5
vs11_rothd
α1